

BOSTON UNIVERSITY
COLLEGE OF ENGINEERING

Dissertation

**DISTRIBUTION POWER MARKETS: DETAILED
MODELING AND TRACTABLE ALGORITHMS**

by

ELLI NTAKOU

Diploma, National Technical University of Athens, 2011
M.S., Boston University, 2014

Submitted in partial fulfillment of the
requirements for the degree of
Doctor of Philosophy

2017

© 2017 by
ELLI NTAKOU
All rights reserved

Approved by

First Reader

Michael Caramanis, Ph.D.
Professor of Mechanical Engineering
Professor of Systems Engineering

Second Reader

Ali Abur, Ph.D.
Professor of Electrical and Computer Engineering
Northeastern University

Third Reader

Na Li, Ph.D.
Assistant Professor of Electrical Engineering and Applied Mathematics
Harvard University

Fourth Reader

Ioannis Ch. Paschalidis, Ph.D.
Professor of Electrical and Computer Engineering
Professor of Systems Engineering
Professor of Biomedical Engineering

Fifth Reader

Pablo A. Ruiz, Ph.D.
Research Associate Professor of Mechanical Engineering
Senior Associate, The Brattle Group

Acknowledgments

First and foremost, I would like to express my gratitude to Professor Michael Caranias for being my thesis advisor. Thank you for giving a research topic that I really enjoyed working on. The past 5 years have been a great learning experience. One of his quotes that stuck with me was that "you have to be a happy researcher" and I really was one under his supervision.

I am also thankful to Professors Abur, Li, Paschalidis and Ruiz for serving in my committee and for their insightful comments and advice. For the latter, I also thank Dr. Alex Rudkevich and Dr. Richard Tabors.

Many thanks to Professor DeWinter for serving as my committee chair. The highlight of most days was him greeting me with a warm smile and chatting with me even when he was busy.

I will always credit Professor Theodore Moustakas for his kindness and for being the first one to explain to me how research is done and how the education system in the US works. My experience working around him was a main reason in my decision to apply for graduate school in the States. I am sure that without this positive first experience, my academic life would have been much shorter and way less exciting.

I would also like to acknowledge all my co-workers and office mates: Justin Foster, Enes Bilgin, Bowen Zhang, Stefan Gunnsteinson, Na Sun and Hedrigo Batista. Their hard work always inspired me to do my best.

I am undeserving of the truly great friends that I have, whose support, from near or far, helped me make it through: John and Yasaman for their help with the tough adjustment to the PhD life and Boston, Selin and Becky for making the office so much fun, Mina, Sofia, Fulya, Sinem, Ozge and Christiana for the countless laughs we had, and Evi for being a life-long friend. Eyripidis, Sepideh, Effie thank you for everything!

Special thanks are due to Giorgos for he has a special place in my heart. I can only hope that I will be able to return your love and support.

Last but not least, I am beyond grateful to my family for their love and support all my life: my parents, Aphrodite and Thomas, my beloved brother Panagiotis, my grandmothers Penelope and Vaia, and of course my uncle Petro and my aunt Nina, that are really my "second" parents, and my cousins Miranda and Corina, that feel like sisters to me.

DISTRIBUTION POWER MARKETS: DETAILED MODELING AND TRACTABLE ALGORITHMS

ELLI NTAKOU

Boston University, College of Engineering, 2017

Major Professor: Michael Caramanis, PhD
Professor of Mechanical Engineering
Professor of Systems Engineering

ABSTRACT

The increasing integration of renewable generation presents power systems with economic and reliability challenges, mostly due to renewables' volatility, which cannot be effectively addressed with business-as-usual practices. Fortunately, this is concurrent with rising levels of Distributed Energy Resources (DERs), including photovoltaics, microgeneration and flexible loads like HVAC loads and electric vehicles.

DERs are capable of attractive time-shiftable behavior and of transacting reactive power and reserves in addition to real power. If DER capacity is optimally allocated among these three products, distribution network and economic benefits can be realized and renewable-related challenges can be mitigated, enabling increased renewable integration safety limits.

In order to achieve optimal DER scheduling, this thesis proposes the formulation of a spatiotemporal marginal-cost based distribution power market and develops and implements tractable clearing algorithms. First, we formulate a centralized market clearing algorithm whose result is the optimal DER real power, reactive power and reserves schedules and the optimal nodal marginal costs. Our market formulation

develops for the first time detailed and realistic models of the salient distribution network variable costs (transformer degradation, voltage sensitive loads) together with distribution network constraints (voltage bound constraints, that reflect distribution network congestion and AC load flow), and intertemporal DER dynamics and capabilities. However, the centralized algorithm does not scale, motivating the use of distributed algorithms.

We propose two distributed algorithms:

1. A fully distributed algorithm that relies on massively parallel DER and distribution line specific sub-problem solutions, iteratively coordinated by nodal price estimates which promote and eventually enforce nodal balances. Upon convergence, nodal balances hold and optimal marginal costs are discovered. We further existing practices by using local penalty updates and stopping criteria that significantly reduce communication requirements.
2. A novel, partially distributed formulation in which DERs self-schedule in parallel based on centrally calculated price estimates, resulting from a load flow calculation. Nodal balances hold during all iterations.

Finally, we are, to the best of our knowledge, the first to study voltage-constrained distribution market instances cleared with distributed methods. We decrease the deviation of marginal costs from their optimal values using first order optimality conditions and use voltage barrier functions for speedier convergence.

Contents

1	Introduction	1
2	Power System Fundamentals	8
2.1	Electricity Network And Power Fundamentals	8
2.1.1	Voltage and Current	9
2.1.2	Real, Reactive, Apparent and Complex Power	10
2.1.3	Reserves	13
2.1.4	Transmission and Distribution Networks	15
2.2	Calculation of Power Flow	16
2.2.1	Slack (swing) Bus	16
2.2.2	Power Flow Equations	17
2.2.3	Optimal Power Flow	22
3	Power System Components	23
3.1	Electricity Network Resources	23
3.1.1	Lines	23
3.1.2	Transformers	25
3.1.3	Shunt Capacitors	31
3.2	Generators	32
3.3	Traditional Loads	34
3.4	Distributed Energy Resources	35
3.4.1	Distributed Generation Types	36
3.4.2	Flexible Loads	38

4	Electricity Markets	41
4.1	Transmission Power Markets	42
4.2	Distribution Network Operation Today	48
4.3	Problems with today’s practice	50
4.4	Thesis Proposition: Spatiotemporal Distribution Electricity Markets .	53
5	Centralized Algorithm For Distribution Day-Ahead Power Market Clearing	60
5.1	Formulation	60
5.2	Decision and Dependent Variables	64
5.3	Components of the Distribution Locational Marginal Prices	64
5.4	Centralized Solution Feasibility	70
5.4.1	Uniqueness of Solution	70
5.4.2	Existence of Solution	70
5.4.3	Centralized Algorithm modeling Voltage Bound Constraints with a Barrier Function	70
5.5	Numerical Results	72
5.5.1	Un-congested Distribution Network	72
5.5.2	Benefits of Distribution Network Price Granularity	77
5.5.3	Congested Distribution Networks	85
5.6	Computational Effort	87
6	Distributed Algorithms for Distribution Day-Ahead Power Market Clearing	89
6.1	Fully Distributed Algorithm (FDA): Distributed DER Scheduling and Power Flow	98
6.1.1	Problem Formulation with Hard Voltage Bound Constraints .	98
6.1.2	Stopping Criteria	106

6.1.3	Iterative Penalty Change	107
6.1.4	Synchronization of Device Solutions to Nodal Price Updates	109
6.1.5	Enhancements for Voltage Congested Distribution Networks	110
6.1.6	Numerical Results using FDA	115
6.2	Partially Distributed Algorithm (PDA): Distributed DER Scheduling and Centralized Power Flow	130
6.2.1	Problem Formulation with Hard Voltage Bound Constraints	130
6.2.2	DER Subproblems	133
6.2.3	Stepsize Updates	134
6.2.4	PDA modeling Voltage Bound Constraints with a Barrier Func- tion	135
6.2.5	Numerical Results using PDA	137
6.3	Comparison of FDA and PDA results	143
7	Reserves	145
7.1	Reserves in Distribution Power Markets	145
7.1.1	Centralized Day-Ahead Distribution Power Market with Reserves	146
7.1.2	Distribution Locational Marginal Prices with Reserve Consid- erations	150
7.1.3	Fully Distributed Algorithm with Reserves	151
7.1.4	Partially Distributed Algorithm with Reserves	153
7.2	Numerical Results	155
8	Concluding Remarks and Future Work	161
8.1	Contributions	161
8.2	Future Work	167
A	Description of Simulated Distribution Networks	171
A.1	800 bus Distribution Network	171

A.2	47 bus Distribution Network	175
A.3	47 bus Distribution Network with Reserves	177
A.4	253 bus Distribution Network	179
	References	181
	Curriculum Vitae	186

List of Tables

5.1	Dependent and independent variables of Distribution Day Ahead Power Market clearing problem.	64
6.1	Number of iterations required for convergence using Fully Distributed Algorithms with various penalty updates rules.	115
6.2	Average, minimum and maximum deviation of real power prices from P-DLMPs (%) at convergence, with the use of bus specific penalties. .	120
6.3	Average, minimum and maximum deviation of reactive power prices from Q-DLMPs (%) at convergence, with the use of bus specific penalties.	120
6.4	Average, minimum and maximum deviation of real power prices from P-DLMPs (%) at convergence, with the use of bus-and-quantity specific penalties.	121
6.5	Average, minimum and maximum deviation of reactive power prices from Q-DLMPs (%) at convergence, with the use of bus-and-quantity specific penalties.	121
6.6	Ratio of price estimates (reactive over real) and ratio of outputs (reactive over real) for a photovoltaic subproblem in PDA are equal. . . .	137
A.1	Location and capacity of photovoltaics in the 47 bus network.	176
A.2	Location and capacity of shunt capacitors in the 47 bus network. . . .	176
A.3	Location of distribution transformers in the 47 bus network used for simulations including reserves.	177

A.4	Location and capacity of DGs in the 47 bus network used for simulations including reserves.	177
A.5	Location and size of electric vehicles in the 47 bus network used for simulations including reserves.	178
A.6	Location and capacity of photovoltaics in the 253 bus distribution network.	180
A.7	Location and capacity of shunt capacitors in the 253 bus distribution network.	180

List of Figures

2·1	Alternating Current and Voltage over time	9
3·1	Complete transmission/distribution line model.	24
3·2	Transformer’s primary and secondary coils and their ratio.	25
3·3	Autotransformer’s coils.	27
3·4	Generator’s D curve, relating real and reactive power output to capacity.	33
3·5	ZIP model for traditional loads.	34
4·1	Residential demand and rooftop solar generation over a 24 hour period.	51
5·1	Hourly minimum, maximum and substation value of real power DLMP	73
5·2	Hourly minimum, maximum and substation value of reactive power DLMP	74
5·3	Real power DLMP components at selected buses 351 and 689 (see equation 5.26 for explanation of each component)	75
5·4	Reactive power DLMP components at selected buses 351 and 689 (see equations 5.27 for explanation of each component)	75
5·5	Hourly substation voltage versus solar irradiation percentage	77
5·6	Hourly substation voltage and maximum PV voltage	77
5·7	Comparison of the average voltage at load buses under flat prices and DLMPs.	79
5·8	Comparison of Net Cost of Distribution Participants under flat prices and DLMPs.	79

5-9	Comparison of electric vehicle (net) costs under flat prices and DLMPs.	80
5-10	Comparison of space conditioning costs under flat prices and DLMPs.	81
5-11	24-hour trajectory of real power DLMP and smart thermostat consumption at bus 383 under flat prices.	82
5-12	24-hour trajectory of real power DLMP and smart thermostat consumption at bus 383 under DLMPs.	82
5-13	Comparison of inflexible loads costs under flat prices and DLMPs. . .	84
5-14	Comparison of the hourly maximum real power DLMP and the real power ex-post marginal costs under flat prices.	84
5-15	Comparison of the hourly maximum reactive power DLMP and the reactive power ex-post marginal costs under flat prices.	85
5-16	Comparison of Real Power Costs to Curtailable Loads in the presence of hard voltage bound constraints (C-OPT) and soft voltage bound constraints (C-SVC).	86
5-17	Comparison of voltage magnitudes of load buses in the presence of hard voltage bound constraints (C-OPT) and soft voltage bound constraints (C-SVC).	86
6-1	Evolution of centrally adapted penalty across iterations.	116
6-2	Evolution of bus-specific penalty across iterations at a specific distribution bus, starting from different penalty values.	116
6-3	Evolution of bus-specific penalty across iterations at two distribution buses, starting from the same initial penalty value.	117
6-4	Updates of bus-specific penalty of real power, reactive power and voltage consistency across iterations at distribution bus 30.	118
6-5	Updates of bus-specific penalty of real power, reactive power and voltage consistency across iterations at distribution bus 2.	118

6-6	Percent deviation of real power price estimates from optimal reactive power price across iterations.	119
6-7	Percent deviation of reactive power price estimates from optimal reactive power price across iterations.	120
6-8	Average percent deviation of real power price estimates from optimal real power price across iterations, 47-bus network versus 253-bus network.	122
6-9	Maximum percent deviation of real power price estimates from optimal real power price across iterations, 47-bus network versus 253-bus network.	122
6-10	Percent deviation of the sum of the voltage magnitude shadow prices across all buses from the optimal value across iterations.	123
6-11	Minimum, average and maximum percent deviation of real power price estimates across all buses from the optimal value across iterations. . .	124
6-12	Minimum, average and maximum percent deviation of reactive power price estimates across all buses from the optimal value across iterations.	124
6-13	Average percent deviation of the real and reactive power price estimates across all buses from the optimal value long after convergence.	125
6-14	Deviation in satisfying first order optimality conditions of real power DLMPs as a percentage of the benchmark real power DLMP.	126
6-15	Shadow prices of voltage bound constraints, before and after the correction process.	127
6-16	Average percent deviation of real and reactive power price estimates from the optimal values before and after the correction process.	128
6-17	Fully Distributed Algorithms, Average Error in Real power DLMPs across iterations (%)	129
6-18	Fully Distributed Algorithms, Maximum Error in Real power DLMPs across iterations (%)	129

6-19	Partially Distributed Algorithm with Hard Voltage Constraints, Oscillations of Voltage Magnitude results, Bus 689, 690 and 691, Hour 2pm.	138
6-20	Partially Distributed Algorithm with Hard Voltage Constraints, Oscillations of Real power ex-post marginal costs across iterations, Bus 689, 690 and 691, Hour 2pm.	139
6-21	Partially Distributed Algorithm with Soft Voltage Bound Constraints, Maximum deviation of Real power price estimates to real power ex-post marginal costs across buses and iterations, Peak Hour.	140
6-22	Partially Distributed Algorithm with Soft Voltage Bound Constraints, Maximum deviation of Reactive power price estimates to reactive power ex-post marginal costs across buses and iterations, Peak Hour.	140
6-23	Average percent deviation of real power price estimates from the optimal value across all buses and iterations using PDA with SVC.	141
6-24	Average percent deviation of reactive power price estimates from the optimal value across all buses and iterations using PDA with SVC.	142
6-25	Average percent deviation of voltage magnitude iterates from the optimal value across all buses and iterations using PDA with SVC.	142
6-26	Comparison of Average Real power DLMP estimate deviation from the optimal DLMPs during 500 first iterations (%)	144
7-1	Hourly minimum, maximum and substation value of real power DLMP.	155
7-2	Hourly minimum, maximum and substation value of reserve DLMP.	156
7-3	Hourly minimum, maximum and substation value of reactive power DLMP, $y=0$	156
7-4	Flow of real power into the distribution network with small DGs present for the three key values of the regulation signal.	157

7.5	Flow of real power into the distribution network with larger DGs present for the three key values of the regulation signal.	158
7.6	Components of the real power DLMP at Bus 31 during the peak hour.	159
7.7	Components of the reactive power DLMP at Bus 31 during the peak hour, for $y=0$	159
7.8	Components of the reserves DLMP at Bus 31 during the peak hour. .	160
A.1	Topology of the 800-bus distribution network.	172
A.2	Hourly values of the substation real power LMP in \$/MWh.	173
A.3	Hourly values of the solar irradiation as a percentage.	173
A.4	Hourly evolution of the residential and commercial demand as a percentage of the peak demand.	174
A.5	Hourly evolution of the outside temperature in degrees Celcius. . . .	174
A.6	Topology of the 47-bus distribution network.	175
A.7	Hourly values of the substation reserve LMP in \$/MWh.	179
A.8	Topology of the 253-bus distribution network.	179

Nomenclature

The sign convention is positive for consumption (withdrawal from a bus) and negative for generation (injection into a bus). Similarly, for real power flows, a positive value of $P_{b,b'}$ means the flow is from bus b to b' , while negative $P_{b,b'}$ means the flow is from bus b' to b .

Nomenclature

Subscripts and Sets

∞	Subscript denoting the substation bus
(b, b')	Subscript denoting a line or transformer connecting bus b to b' .
(n, n')	Subscripts denoting a transmission line connecting n to n'
b, b', β	Subscripts denoting a typical distribution bus
n, n'	Subscripts denoting a typical transmission bus
α	Subscript denoting a specific device that connects to some network bus b . For example, the notation $\alpha \in G$ means that device α is a generator and that $\alpha \notin D, E, F$
G, D, E, F	Set of all network generators, loads, distributed energy resources and capacitors respectively
G_b, D_b, E_b, F_b	Set of generators, loads, DERs and capacitors respectively connected to bus b
G_n, D_n	Set of generators and loads respectively connected to transmission bus n .
$A_b = G_b \cup D_b \cup E_b \cup F_b$	Set of all devices connected to bus b

up,dn Superscripts referring to different values of the regulation signal y . We use the subscript up for $y = 1$ and dn for $y = -1$.

General Parameters

\rightarrow A symbol used to associate a shadow price to an equality or inequality constraint.

C_α Capacity of device $\alpha \in G \cup D \cup E \cup F$

c_α Marginal cost of device α for real power production

h Hour in the DA market, $h = 1..24$

H_\bullet Heaviside function whose value is $H(\bullet \geq 0) = \infty$ and $H(\bullet \leq 0) = 0$

k Constant

$T^{out}(h)$ Outside Temperature during hour h

Transmission Parameters

$\mathcal{H}(Q_\infty(h))$ Fuel cost of substation generator associated with producing reactive power $Q_\infty(h)$. It is considered to be negligibly small.

$\pi_\infty^P(h)$ Locational Marginal Price of Real Power at the substation bus during hour h .

$\pi_\infty^R(h)$ Locational Marginal Price of Reserves at the substation bus during hour h .

$\pi_{\infty}^{OC}(h)$ Opportunity cost per kW of substation bus auxiliary generator disabled from producing real power or reserves in order to compensate for reactive power $Q_{\infty}(h)$

Distribution Parameters

\check{v} Voltage level at which device $\alpha \in D$ is optimized to work

$|A_b|$ Number of devices connected to bus b

$|H_b|$ Number of lines/ transformers connected to bus b

θ_{α} Voltage and current angle difference of device $\alpha \in D$

c_{∞}^v Coefficient denoting the cost of the square of the difference of the substation voltage from the nominal voltage level

$\cos(\theta_{\alpha})$ Power factor of device $\alpha \in D$

$r_{b,b'}, x_{b,b'}$ Resistance and reactance, respectively, of line or transformer connecting buses b and b'

$u_{\alpha}(P_{\alpha})$ Convex cost function of device $\alpha \in D$ consuming real power P_{α}

w Weight parameter showing the efficiency of transforming real power to useful energy service when $\alpha \in D$ operates at a voltage deviating from \check{v}

Electric Vehicles

h_{arr} Hour of the day that the EV plugs in

h_{dep}	Hour of the day that the EV departs
r_α	Maximum hourly charging rate capacity of EVs
$x_\alpha(h)$	State of discharge (SoD) of EV at beginning of hour h
$u(x_\alpha(h_{dep}))$	Loss of utility (cost) of EV wishing to depart at h_{dep} with SoD x_α . It is zero when $x_\alpha(h_{dep}) = 0$ and positive otherwise.

Transformers

$\Gamma_{b,b'}(h)$	Loss of life of transformer $(b, b') \in tr$ measured in hours of economic life per hour of clock time
$\theta_{b,b'}^{HS}(h)$	Hottest spot temperature in transformer (b, b') during hour h
$c_{b,b'}^{tr}$	Cost of transformer $(b, b') \in tr$ per hour of economic life
$S_{b,b'}^N$	Rating of transformer (b, b')

Smart thermostats

$T_\alpha^{in}(h)$	Inside temperature of building with heat pump α during hour h
--------------------	--

Variables

$P_\alpha(h), Q_\alpha(h), R_\alpha(h)$	Real power, reactive power and reserves respectively of device α during hour h . Negative values denote generation, while positive values denote consumption.
$P_{n,n'}, R_{n,n'}$	Real Power flow and reserves flow respectively on transmission line n, n'

$P_{b,b'}(h), Q_{b,b'}(h), R_{b,b'}(h), S_{b,b'}(h)$	Real power flow, reactive power flow, reserves flow and apparent power flow respectively on line (b, b') during hour h .
$P_\infty(h), Q_\infty(h), R_\infty(h)$	Real power flow, reactive power flow and flow of reserves respectively into the distribution feeder at the substation during hour h .
$v_b(h)$	Voltage magnitude squared of bus b during hour h
$l_{b,b'}(h)$	Current squared on line or transformer connecting buses b and b'
$\check{P}_\alpha(h), \check{Q}_\alpha(h)$	Real and reactive power consumption respectively of device $\alpha \in D$ during hour h , as a function of the corresponding bus voltage
$f_\alpha(P_\alpha(h), Q_\alpha(h))$	Individual costs of device $\alpha, \alpha \in G, D, E, F$ based on its real power $P_\alpha(h)$ and reactive power $Q_\alpha(h)$.
$f_{b,b'}(P_{b,b'}(h), Q_{b,b'}(h), P_{b',b}(h), Q_{b',b}(h))$	Individual costs of line or transformer b, b' based on real power $P_{b,b'}(h), P_{b',b}(h)$ and reactive power $Q_{b,b'}(h), Q_{b',b}(h)$ at either end.
$\pi_b^P(h)$	Real Power Locational Marginal Price at distribution bus b during hour h , referred to as Distribution Locational Marginal Price of Real Power. It is the shadow price of the real power balance constraint.
$\pi_b^Q(h)$	Reactive Power Locational Marginal Price at distribution bus b during hour h , referred to as Distribution

	Locational Marginal Price of Reactive Power. It is the shadow price of the reactive power balance constraint.
$\pi_b^R(h)$	Reserves Locational Marginal Price at distribution bus b , referred to as Distribution Locational Marginal Price of Reserves.
$\underline{\mu}_b, \bar{\mu}_b$	Dual variable of lower and upper voltage magnitude bounds respectively.
$\underline{\gamma}_{n,n'}, \bar{\gamma}_{n,n'}$	Dual variable of lower and upper capacity constraints of transmission line n, n' respectively.
κ_α	Dual variable of capacitor α capacity constraints.

Fully Distributed Algorithm

i	Iteration Count
$v_{b,b'}(h)$	Voltage magnitude squared at end b of line (b, b') during hour h
ρ_\bullet^i	Penalty term multiplying the quadratic augmentation terms during iteration i . The subscript can be a bus b , a quantity P, Q, v or both.
$\hat{P}_b^i(h)$	Real Power Imbalance at bus b during hour h at iteration i
$\hat{Q}_b^i(h)$	Reactive Power Imbalance at bus b during hour h at iteration i

$\hat{v}_b^i(h)$	Imbalance of Voltage consistency at bus b during hour h at iteration i
$\hat{\pi}_b^{P,i}(h)$	Real power price estimate at distribution bus b during hour h at iteration i . Since it may not satisfy real power balance constraints, it is distinct from $\pi_b^{P,i}(h)$. However, it also holds that $\lim_{i \rightarrow \infty} \hat{\pi}_b^{P,i}(h) = \pi_b^P(h)$.
$\hat{\pi}_b^{Q,i}(h)$	Reactive power price estimate at distribution bus b during hour h at iteration i . Since it may not satisfy reactive power balance constraints, it is distinct from $\pi_b^{Q,i}(h)$. However, it also holds that $\lim_{i \rightarrow \infty} \hat{\pi}_b^{Q,i}(h) = \pi_b^Q(h)$.

Partially Distributed Algorithm

i	Iteration Count
$s(i)$	Stepsize used in price estimate $\hat{\pi}_b^{P,i}(h)$ and $\hat{\pi}_b^{Q,i}(h)$ updates during iteration i
$\pi_b^{P,i}(h)$	Ex-post marginal cost of real power at distribution bus b during hour h at iteration i . It is the shadow price of the real power balance constraint at the intermediate, but feasible, DER dispatch of iteration i . It holds that $\lim_{i \rightarrow \infty} \pi_b^{P,i}(h) = \pi_b^P(h)$.
$\pi_b^{Q,i}(h)$	Ex-post marginal cost of reactive power at distribution bus b during hour h at iteration i . It is the shadow price of the reactive power balance constraint at the

intermediate, but feasible, DER dispatch of iteration i . It holds that $\lim_{i \rightarrow \infty} \pi_b^{Q,i}(h) = \pi_b^Q(h)$.

$\hat{\pi}_b^{P,i}(h)$

Real power price estimate at distribution bus b during hour h at iteration i . Since it is a convex combination of $\hat{\pi}_b^{P,i-1}(h)$ and $\pi_b^{P,i}(h)$, it may not satisfy real power balance constraints, therefore it is distinct from $\pi_b^{P,i}(h)$. However, it also holds that $\lim_{i \rightarrow \infty} \hat{\pi}_b^{P,i}(h) = \pi_b^P(h)$.

$\hat{\pi}_b^{Q,i}(h)$

Reactive power price estimate at distribution bus b during hour h at iteration i . Since it is a convex combination of $\hat{\pi}_b^{Q,i-1}(h)$ and $\pi_b^{Q,i}(h)$, it may not satisfy real power balance constraints, therefore it is distinct from $\pi_b^{Q,i}(h)$. However, it also holds that $\lim_{i \rightarrow \infty} \hat{\pi}_b^{Q,i}(h) = \pi_b^Q(h)$.

List of Abbreviations

AC	Alternating Current
AIMMS	Advanced Integrated Mathematical Modeling Software
C-OPT	Centralized algorithm with hard voltage bound constraints
C-SVC	Centralized algorithm with soft voltage bound constraints
DA	Day Ahead
DC	Direct Current
DER	Distributed Energy Resource
DLMP	Distribution Locational Marginal Prices
DSO	Distribution System Operator
ED	Economic Dispatch
EV	Electric Vehicle
FDA	Fully Distributed Algorithm
FDA-OPT	FDA with hard voltage bound constraints
FDA-SVC	FDA with soft voltage bound constraints
FERC	Federal Energy Regulatory Commission
FIT	Feed-In Tariff
HA	Hour Ahead
HST	Transformer Hottest Spot Temperature
HVAC	Heating, ventilation and air conditioning
ISO	Independent System Operator
LMP	Locational Marginal Prices
NERC	North American Electric Reliability Corporation
OPF	Optimal Power Flow
PDA	Partially Distributed Algorithm
PDA-OPT	PDA with hard voltage bound constraints
PDA-SVC	PDA with soft voltage bound constraints
P-DLMP	Real power DLMP
PNNL	Pacific Northwest National Laboratory
PV	Photovoltaic
Q-DLMP	Reactive power DLMP
R-DLMP	Reserves DLMP
RT	Real Time
SoD	State of Discharge of the battery of an Electric Vehicle
SST	Solid State Transformer

TLL	Transformer Loss of Life
TOU	Time Of Use
UC	Unit Commitment

Chapter 1

Introduction

Marginal-cost based wholesale power markets were introduced in England in 1990 and in the United States in 1997, making power systems' operational planning the result of competitive bidding. Operational planning consists of the solution of a sequence of constrained minimization problems, addressing cascaded adjustments to uncertainty realizations. These problems allocate the capacity of resources amongst three key electric products: real power, reactive power and various types of reserves. Reactive power as well as some types of reserves are sometimes scheduled outside the market, based on long-term (e.g., annual) contracts or rules. They are of course provided dynamically to meet the relevant requirements.

Modern power markets co-optimize real power and the remaining types of reserves by adapting resources' schedules to price-quantity bids ("uniform" bids) from generation and demand to offer or receive service respectively. Specifically, a market operator matches these bids to maximize consumers' and generators' surplus, while ensuring that demand equals generation at all times.¹ The adoption of wholesale power markets has resulted in significant benefits including lower cost operation and decreased congestion and reserve needs.

Wholesale power markets are mature and well established in the literature and in practice alike. Across all different works in the area of power markets, that are too

¹There are more constraints taken into account for transmission power market clearing. This is just a high level description with as little detail as is needed to proceed in introducing the approaches and contributions of the thesis. See Section 4 for more details on wholesale power market clearing.

vast to explore for the scope of this thesis, the main premise of power markets remains that electricity prices are driven by competition to reflect marginal costs. In other words, electricity prices are driven to reflect the value of a service as a function of both the time that it is provided/ consumed as well as the location that is provided/ consumed at, i.e. optimal electricity prices that yield optimal resource utilization will exhibit time and locational variability.

Nowadays, power systems' operational planning and power market clearing practices are on the verge of transformation due to concurrent changes in both the generation and the demand side.

On the generation side, the adoption of renewable resources is rapidly increasing. Albeit environmentally desirable, renewables present power systems with economic and reliability challenges, mostly because of their volatility and lack of inertia. Addressing these issues with business-as-usual practices, like adding more flexible centralized generation and/ or enhancing the existing transmission and distribution infrastructure, will soon fall short of economic and sustainability goals and may prohibit the rapid integration of renewable generation that state and federal regulations mandate.

On the demand side, Distributed Energy Resources' (DERs) levels are also rising. DERs include photovoltaics, microgeneration and flexible loads like HVAC loads and electric vehicles. DERs possess various degrees of freedom. First, their capabilities allow them to exhibit attractive time-shiftable behavior. Second, non-volatile DERs (like electric vehicles and microgenerators) are able to provide reserves. Third, DERs are commonly equipped with power electronics and as such are able to transact reactive power in addition to real power and (possibly) reserves. These DER transactions are capable of transforming the distribution network by making it an active part of the grid.

Drawing experience from scheduling of traditional generating resources in wholesale power markets, we argue that time and locational price incentives can be used to optimally allocate DER capacity among real power, reactive power and reserves. This optimal DER scheduling will result in distribution network efficiencies and also provide useful synergies that can mitigate many challenges related to renewables.

This thesis is motivated by the desire to eliminate the huge inefficiencies resulting from the exclusion of distribution- network connected customers, providers and DERs from competitive power markets. Distribution markets are currently regulated and distribution pricing is rate-based. We argue that this does not allow for DERs to receive the aforementioned spatiotemporal price incentives, thereby hindering their efficient integration.

However, a simple extension of power markets allowing distribution- network connected entities to participate in the wholesale market *under the current protocol* is insufficient. The existing market practice, relying on centralized market clearing and information gathering, as well as on uniform bids and on simplified assumptions only fit to transmission networks, would be unable to capture the different nature of the distribution network (line characteristics, voltage considerations) and the intertemporal DER dynamics.

Therefore, this thesis proposes the formulation of a spatiotemporal marginal-cost based distribution power market in order to achieve optimal DER scheduling and develops and implements tractable market clearing algorithms. We concentrate on the day-ahead cycle of operational planning, that aims at scheduling resources for the next day, so as to yield the most benefits of the intertemporal nature of DERs. First, we identify the relevant costs and constraints and formulate a centralized day-ahead distribution power market that minimizes operational costs over the 24 hour daily cycle, constrained by power balance constraints, power flow constraints, voltage

magnitude constraints and constraints expressing intertemporal DER dynamics and capabilities.

The primal solution of the centralized market clearing algorithm is the DER real power, reactive power and reserves schedules and the dual solution is the dynamic marginal costs of each product. The primal solution also includes dependent variables, like real and reactive power flows and voltage magnitudes. At optimality, the primal solution provides us with the optimal DER dispatch and the dual solution provides us with the optimal marginal prices.

To put the significance of this market to perspective, we mention that explicit costs that are minimized in the distribution power market account for about 35% of total electricity costs, including generation, transmission, distribution and reliability costs. These costs include transformer degradation-related costs, that nowadays are about \$1 billion per year as well as costs due to losses over distribution network lines that are in the order of \$10 billion annually in the US.

We apply first order optimality conditions to the centralized market clearing algorithm to derive valuable relationships between the nodal prices of real power, reactive power and reserves at distribution buses with *(i)* other dual variables as well as *(ii)* sensitivities of dependent variables (voltages and power flows) and *(iii)* marginal prices at the substation bus, where distribution and transmission interface. Since these relationships reveal the building blocks of the marginal-cost based prices, we call them marginal price (or cost) unbundling equations. We also relate binding voltage bound constraints to distribution network congestion.

The large number of DERs participating in a real-size distribution power market, each of them introducing complex intertemporal constraints, combined with the non-convexity of AC power flow constraints render the centralized market clearing algorithm intractable. This motivates the use of distributed algorithms.

The literature is abundant with applications of distributed algorithms to power systems' and power markets' problems. For most of these problems, while the objective function is separable, the constraints are coupling. Therefore, dual decomposition was the first method to be applied. However, dual decomposition requires strict technical conditions to be met. Most recently, the method of alternating direction method of multipliers (ADMM) has gained popularity in many areas of active research reported in the literature because of its ability to bridge decomposability with much more relaxed technical conditions for convergence than those required by classic dual decomposition approaches.

The first distributed market clearing algorithm proposed in this thesis, called Fully Distributed Algorithm (FDA), is also based on ADMM, similar to (Kraning et al., 2014) and (Peng and Low, 2015). Nodal equality constraints are relaxed to allow for the division of the market clearing problem into smaller, DER and distribution line specific sub-problems. These subproblems are solved in parallel and are coordinated through nodal price estimates which promote and eventually enforce nodal balances. Upon convergence, nodal equality constraints hold and marginal prices are discovered.

Also, we propose and implement a second distributed market clearing algorithm, called Partially Distributed Algorithm (PDA). At each iteration of PDA, DERs self-schedule in parallel conditional upon nodal price estimates at their connection bus. These price estimates along with power flow variables are calculated centrally. This is done by solving an AC load flow and calculating its associated ex-post marginal costs through the marginal cost unbundling equations. Equivalently, we can solve a mock centralized market clearing problem, with fixed DER schedules. The primal solution of the mock centralized market clearing algorithm will provide, as discussed above, the network flows and voltages, while the dual solution will provide the ex-post marginal costs. In other words, coupling constraints are not relaxed but hold during

all iterations of PDA.

The ability to massively parallelize the subproblems means that both distributed market clearing algorithms scale to real size distribution networks deploying numerous DERs.

This work contributes to the areas of power systems modeling, power markets as well as the distributed algorithms domain. Major advancements include:

- Not only is the concept of a distribution power market pioneering, but in addition, our market formulation develops for the first time comprehensive and realistic models of the salient distribution network variable costs (e.g., transformer degradation, voltage sensitive loads) together with distribution network constraints (nodal voltage bound constraints and AC load flow), and intertemporal DER dynamics and capabilities.
- The identification of distribution network congestion as a nodal problem that occurs when voltage bound constraints are binding.
- Detailed comparison of the operational and economic benefits of the proposed granular marginal-cost based distribution prices relative to today's flat prices.
- The fully distributed ADMM-based algorithm, FDA, is applied to a much higher complexity problem than existing work in the literature, with complex intertemporal DER preferences and network constraints.
- Within FDA, we introduce and implement adaptive penalties that are updated with local information only. In addition, we use local criteria to verify convergence and terminate ADMM. The use of local penalties and local stopping criteria in our fully distributed algorithm formulation results in significantly reduced communication requirements and associated communication time bot-

tlenecks and delays as well as in decreased number of iterations required for convergence.

- The partially distributed algorithm (PDA), where DERs respond to centrally calculated price estimates and coupling constraints are not relaxed, is a novel formulation that does not fall within the traditionally explored areas of either dual decomposition or augmented-Lagrangian based methods.
- Finally, we are, to the best of our knowledge, the first to study voltage-constrained distribution market instances cleared with distributed algorithm methods. Using the aforementioned marginal price unbundling equations, we are able to decrease the deviation of nodal price estimates, obtained after a limited number of iterations, from their optimal values. Further, we model hard voltage bound constraints through appropriately designed voltage barrier functions. These result in significant convergence speed up.

Through the discovery of distribution network spatiotemporal marginal prices and the subsequent efficient integration of DERs, this thesis promises a broad societal impact. First, it promises major distribution network efficiency gains, including lower losses and increased resilience of grid infrastructure to load growth. Second, it promises to realize the much needed synergies between DERs and renewables. These synergies will, in turn, allow for speedier adoption of renewables and increased renewable integration limits from the point of view of grid safety and economic efficiency. If the renewable integration safety limits increase from today's 15% to the envisioned 45%, then emissions can be lowered by 0.5 billion to 1 billion metric tons. Further, this new market will promote investments in new technologies, products and services.

Chapter 2

Power System Fundamentals

2.1 Electricity Network And Power Fundamentals

The electricity network consists of circuits that transfer electricity from generation points to consumption points. The transportation of electricity from generation to demand is achieved through the flow of current. Current that alternates directions is referred to as Alternating Current (AC). Direct current (DC) refers to unidirectional current.

In the early days of the electric power industry, generation had to be located close to the load, so that there would be minimal losses. The invention of the transformer for stepping up and down AC voltages was instrumental in the widespread adoption of AC electric networks. With the advent of transformers, power systems can operate at high voltages to efficiently transfer electricity over great distances with low losses and then step voltages down to ensure the safe operation of electrical equipment by consumers.

While much of the AC electric system has three phases, all of our analysis and explanation will be in single- phase terms. This is because in this work, as is common, we assume that the three phases are balanced, and as such we can model them with an equivalent single phase for simplicity of exposition. Multi- phase modeling is discussed in Chapter 8.

2.1.1 Voltage and Current

AC voltages and currents have a sinusoidal behavior over time as Figure 2.1 below suggests (MIT Energy Initiative, 2015). Therefore, voltages in AC power systems are characterized by their magnitude (or amplitude), frequency and phase. Voltage is expressed by:

$$V(t) = V_{max} \cdot \cos(\omega \cdot t + \theta_V) \quad (2.1)$$

while current is expressed by:

$$I(t) = I_{max} \cdot \cos(\omega \cdot t + \theta_I) \quad (2.2)$$

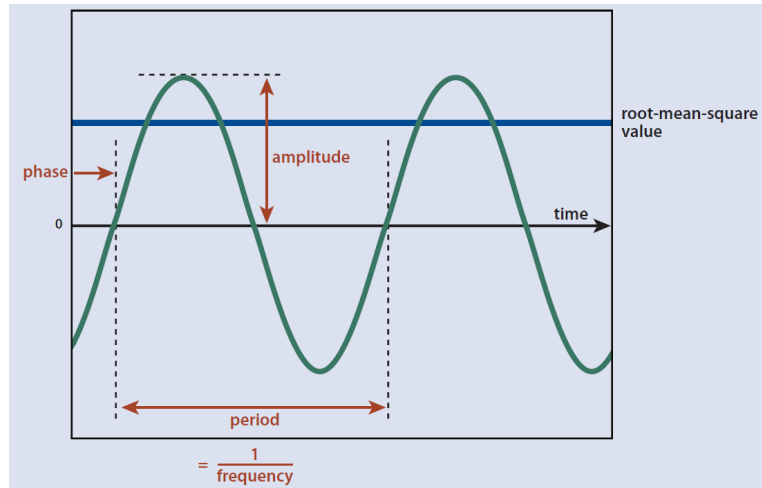


Figure 2.1: Alternating Current and Voltage over time

When voltage and current cross the vertical zero axis at the same time, i.e. their phase angle difference is zero, $\theta_V = \theta_I \Rightarrow \theta = \theta_V - \theta_I = 0$ they are called "in phase". Else, they are called "out of phase".

While the sinusoidal expression is more intuitive, in power systems analyses the frequency domain is preferred over the time domain. In the frequency domain, sinusoidal functions' amplitude and phase angle are represented by phasors (or phase

vectors), i.e. complex numbers. Therefore, we may write that:

$$\vec{V} = V \exp(j\theta_V) \quad (2.3)$$

for voltage and

$$\vec{I} = I \exp(j\theta_I) \quad (2.4)$$

for current.

V and I in equations 2.3 and 2.4 refer to the root mean square values of Figure 2.1. It holds that $V = \frac{V_{max}}{\sqrt{2}}$ and $I = \frac{I_{max}}{\sqrt{2}}$. Root mean square or effective voltage corresponds to the equivalent DC voltage that can produce the same amount of work as the AC voltage.

2.3 and 2.4 are in polar form. In rectangular form, they can be written as:

$$\vec{V} = V \cos(\theta_V) + jV \sin(\theta_V) \quad (2.5)$$

and

$$\vec{I} = I \cos(\theta_I) + jI \sin(\theta_I) \quad (2.6)$$

2.1.2 Real, Reactive, Apparent and Complex Power

Instantaneous power is defined as the product of voltage and current. Bearing in mind Figure 2.1 and equations 2.1 and 2.2 above, the phase difference of voltage and current is equal to $\theta = \theta_V - \theta_I$. For simplicity and without loss of generality, we will assume that the voltage is at zero phase angle, $\theta_V = 0$ and the current phase angle is $\theta_I = -\theta$. Therefore we have:

$$V(t) = V_{max} \cdot \cos(\omega \cdot t) \quad (2.7)$$

$$I(t) = I_{max} \cdot \cos(\omega \cdot t - \theta) \quad (2.8)$$

Instantaneous power is equal to: $V(t) \cdot I(t) = V_{max} \cdot I_{max} \cdot \cos(\omega \cdot t) \cdot \cos(\omega \cdot t - \theta) = \frac{V_{max} \cdot I_{max}}{2} \cdot \cos(\theta) \cdot (1 + \cos(2\omega t)) + \frac{V_{max} \cdot I_{max}}{2} \cdot \sin(\theta) \cdot \sin(2\omega t)$.

The first component, namely $\frac{V_{max} \cdot I_{max}}{2} \cdot \cos(\theta) \cdot (1 + \cos(2\omega t))$, has a time average of $\frac{V_{max} \cdot I_{max}}{2} \cdot \cos(\theta)$.

We call this time average real (or active) power

$$P = \frac{V_{max} \cdot I_{max}}{2} \cdot \cos(\theta) = V \cdot I \cdot \cos(\theta) \quad (2.9)$$

The second component, $\frac{V_{max} \cdot I_{max}}{2} \cdot \sin(\theta) \cdot \sin(2\omega t)$, is due to the reactive part of the load. It has a time average of zero and its amplitude is equal to $\frac{V_{max} \cdot I_{max}}{2} \cdot \sin(\theta)$. We call this magnitude reactive power:

$$Q = \frac{V_{max} \cdot I_{max}}{2} \cdot \sin(\theta) = V \cdot I \cdot \sin(\theta) \quad (2.10)$$

Because the time average of the reactive component of power is zero, we say that reactive power produces no useful work. Reactive power is responsible for a significant part of the system's losses. Reactive power is also strongly related to voltage control and can support voltages as needed for system reliability. Major blackouts in Europe and North America in recent years have been linked to insufficient reactive power supply, leading to voltage collapse. Also notable is the cost of committing inefficient generators close to urban load centers for the purpose of providing reactive power compensation.

From equations 2.9 and 2.10 it is obvious that if the phase angle difference of voltage and current is zero, $\theta = 0$, then real power is positive and reactive power is zero.

If $\theta \geq 0$, then we say that voltage leads the current, in which case reactive power is consumed $Q \geq 0$ and the load is called inductive. $\theta = 90$ makes for a purely inductive load with $P = 0$ and $Q \geq 0$.

If $\theta \leq 0$, then we say that voltage lags the current, in which case reactive power is produced $Q \leq 0$ and the load is called capacitive. $\theta = -90$ makes for a purely capacitive load with $P = 0$ and $Q \leq 0$.

As will be seen in the next Chapter, distribution lines produce or consume reactive power depending on their electrical characteristics and surroundings (underground or overhead). Generators and power electronics can also produce or consume reactive power.

We can also derive 2.9 and 2.10 starting from the phasors of voltage and current 2.3 and 2.4 and keeping the same assumptions of $\theta_V = 0$ and $\theta_I = -\theta$. We define complex power as:

$$\vec{S} = \vec{V} * \vec{I}^* = V \cdot I \cdot \exp(j\theta) = VI\cos(\theta) + jVI\sin(\theta) \quad (2.11)$$

Real (or active) power P is the real part of the complex power.

$$P = \Re(S) = VI\cos(\theta) \quad (2.12)$$

Reactive power Q is the imaginary part of complex power.

$$Q = \Im(S) = VI\sin(\theta) \quad (2.13)$$

Apparent power S is the absolute value of complex power or:

$$S = |\vec{S}| = \sqrt{P^2 + Q^2} = V \cdot I \quad (2.14)$$

The power factor ϕ is defined as the ratio of real power to apparent power, namely:

$$\phi = \frac{P}{S} = \frac{V \cdot I \cdot \cos(\theta)}{V \cdot I} = \cos(\theta) \quad (2.15)$$

2.1.3 Reserves

The most important goal of power systems operation is reliability: matching demand and generation at all times despite unexpected system events, while keeping voltages and frequency within bounds.

Ancillary services are defined as services other than energy that ensure the reliable operation of the grid (Shahidehpour et al., 2002). (Operating) reserves are a type of ancillary services, defined by NERC as "the capability above firm demand required to provide for load forecasting error, equipment forced and scheduled outages and local area protection" (North American Electric Reliability Corporation, 2008).

The North American Electric Reliability Corporation (NERC) distinguishes different types of reserves based on whether they are employed during normal system conditions or contingencies. In the category of non-event reserves, regulation (service) reserves respond within seconds to imbalances of generation and demand caused by the random nature of demand. Load following reserves also belong in the non-event reserves category and serve the same purpose as regulation reserves, but are slower to respond and can do so in the time scale of minutes. On the other hand, contingency reserves are responsible for system frequency control in the case of sudden and rare system events. Several sub-categories of reserves are defined within the contingency reserves category.

The Union for the Coordination of the Transmission of Electricity (UCTE) separates reserves into different categories:

1. Primary reserves: Local automatic control that stabilizes system frequency within seconds.
2. Secondary reserves: Central automatic control that brings frequency back to its nominal value within minutes.

3. Tertiary reserves: Manual changes to ensure system reliability in the case that more reserves are required after primary and secondary reserves have been used. It allows resources able to provide fast primary reserves to go back to being available for reserve provision.

Primary, secondary and tertiary reserves alike are responsible for frequency control during normal system operation as well as during system contingencies. (Ela et al., 2011) analyzed how the different reserve classifications defined by UCTE and FERC correspond to each other.

The mismatch of demand and generation (plus net imports) could be in either direction. As a result, reserves are bi-directional:

- Up, meaning that generation should be increased to serve additional load (caused either by unaccounted for, but normal, demand fluctuations or by contingencies), or
- Down, meaning that generation should be decreased because demand needs are less (again, caused either by unaccounted for, but normal, demand fluctuations or by contingencies)

Reserves can be symmetric, i.e. the amount of up reserves promised is equal to the amount of down reserves promised or up and down reserves can be separate services, meaning that the quantities of up and down reserves need not be equal.

Power systems are required to secure certain amounts of reserves. Regulation service reserves minimum requirements are at about 1% of the peak load. The composite amount of all reserves is calculated based on network metrics (e.g., the amount of reserves required for the system to survive the worst outage) or based on cost measures. Sometimes, reserves as well as other ancillary services are provided by generators through contracts.

On the reserves front there have been the following recent changes: first, regulation reserves are recently being provided competitively, through the wholesale power market clearing process and second, reserves can also be provided by entities on the demand side of the grid. Chapter 4 describes the former while Chapter 7 describes the latter.

2.1.4 Transmission and Distribution Networks

AC electric power systems are categorized based on their voltage magnitude levels: ¹

- High Voltage networks, also referred to as Transmission Networks, and
- Medium and Low Voltage networks, also referred to as Distribution Networks.

Voltage levels above 60kV are categorized as transmission voltages. Transmission voltages are steadily rising with the highest voltage in commercial use being 765kV in the US. A transmission line of 1000kV is used in China.²

Lower voltages belong to distribution networks. Primary distribution lines range from 4 to 34.5kV. Secondary distribution lines, i.e. lines that connect loads directly to the secondary (low voltage) side of distribution transformers are 120V or 240V in the US.

Transmission and distribution networks differ also in terms of their topology. Distribution networks, while constructed with some meshed capabilities through line switching options that enable alternative spanning tree configurations, are operated radially by switching line connections so as to obtain a radial spanning tree that serves all loads. This is done for ease of protection as well as cost efficiency. However, in large cities, distribution networks are designed and operated as meshed networks

¹In this work, we do not mention the sub-transmission network and assume it is part of the transmission network, for clarity of exposition in what follows.

²Similar Ultra High Voltage lines have been constructed in Russia and Japan but currently operate at lower voltages.

(eg. New York City). Transmission networks are also designed and operated in a meshed configuration.

Both transmission and distribution networks operate on the same frequency. The AC system of the United States and Canada operates at a standard frequency of 60Hz, while the standard frequency in Europe is 50Hz.

2.2 Calculation of Power Flow

In power systems studies, we are oftentimes interested in calculating real and reactive power flows on the electricity network resources, like lines and transformers, as well as line currents and voltages. This section presents exact and approximate models commonly used to calculate these quantities. The models are systems of equations, commonly referred to as power flow equations.

We will be presenting the basic and exact model, called Alternating Current Power Flow equations, and proceed with approximations of that model, based on the voltage level and topology of the electricity network that we are interested in: the transmission network (meshed) or the distribution network (tree).

2.2.1 Slack (swing) Bus

A slack or swing bus is not a physical bus, i.e., it is not present in actual power networks, however every power system model has a slack bus. In a power flow problem, flows and losses on each line are unknown. Therefore, nodal power balance equations contain unknowns. As a result, the power injection in some bus needs to be left unspecified otherwise, the power balance equations would be overspecified and the power flow would not be solvable. In practice, this means that the slack bus makes up for system losses.

When a small system is connected to a large system with a single line, the large system can hold the voltage constant and generate/absorb as much power as is needed,

i.e., act like a slack bus. For example, when a distribution network branches out of a transmission bus, the latter acts like a slack bus with respect to the distribution network (Dimitrovski and Tomsovic, 2004).

2.2.2 Power Flow Equations

Alternating Current (AC) Power Flow We base the derivation of the power flow equations on the vector representation of voltages and currents shown in 2.8 and 2.7 above. We represent lines as a series resistance $r_{n,n'}$ and a series reactance $x_{n,n'}$ through the following model:

$$\vec{Z}_{n,n'} = r_{n,n'} + jx_{n,n'} \quad (2.16)$$

More details on line modeling can be found in Chapter 3 below. Similarly, we define for each line the conductance and susceptance, respectively, as:

$$G_{n,n'} = \Re\left(\frac{1}{\vec{Z}_{n,n'}}\right) = \frac{r_{n,n'}}{r_{n,n'}^2 + x_{n,n'}^2} \quad (2.17)$$

$$B_{n,n'} = \Im\left(\frac{1}{\vec{Z}_{n,n'}}\right) = -\frac{x_{n,n'}}{r_{n,n'}^2 + x_{n,n'}^2} \quad (2.18)$$

As defined above, complex power $\vec{S}_{n,n'}$ on a line connecting buses n and n' is defined as the product of \vec{V}_n and $\vec{I}_{n,n'}^*$, where $\vec{I}_{n,n'}^*$ is the conjugate of $\vec{I}_{n,n'}$.

$$\vec{S}_{n,n'} = \vec{V}_n \vec{I}_{n,n'}^* \quad (2.19)$$

It also holds that the complex voltage difference is equal to the product of the impedance with the complex current, namely:

$$\vec{V}_n - \vec{V}_{n'} = \vec{I}_{n,n'} \vec{Z}_{n,n'} \Rightarrow \vec{I}_{n,n'} = \frac{\vec{V}_n - \vec{V}_{n'}}{\vec{Z}_{n,n'}} \quad (2.20)$$

Therefore substituting 2.20 into 2.19 results in:

$$\begin{aligned}\vec{S}_{n,n'} &= \vec{V}_n \vec{I}_{n,n'}^* = \vec{V}_n \frac{\vec{V}_n^* - \vec{V}_{n'}^*}{\vec{Z}_{n,n'}^*} = \vec{V}_n (\vec{V}_n^* - \vec{V}_{n'}^*) (G_{n,n'} - jB_{n,n'}) = \\ &V_n \exp(j\theta_n) (V_n \exp(-j\theta_n) - V_{n'} \exp(-j\theta_{n'})) (G_{n,n'} - jB_{n,n'})\end{aligned}\quad (2.21)$$

Complex power $\vec{S}_{n,n'}$ is also defined as:

$$\vec{S}_{n,n'} = P_{n,n'} + jQ_{n,n'} \quad (2.22)$$

where $P_{n,n'}$ is the real power flow and $Q_{n,n'}$ is the reactive power flow. Separating the real and imaginary parts of 2.21 above yields:

$$P_{n,n'} = G_{n,n'} V_n^2 - G_{n,n'} V_n V_{n'} \cos(\theta_n - \theta_{n'}) - B_{n,n'} V_n V_{n'} \sin(\theta_n - \theta_{n'}) \quad (2.23)$$

and

$$Q_{n,n'} = -B_{n,n'} V_n^2 + B_{n,n'} V_n V_{n'} \cos(\theta_n - \theta_{n'}) - G_{n,n'} V_n V_{n'} \sin(\theta_n - \theta_{n'}) \quad (2.24)$$

Equations 2.23, 2.24 are the well-known AC power flow equations. Then, we need to relate the power flow on each line, to injections (e.g., generation) and withdrawals of power (e.g., loads) at each bus. These equations are called (nodal) power balance equations and together with the AC power flow equations, are collectively used to solve power flow problems, where all injections and withdrawals are known and we are interested in calculating the real and reactive flows on the lines, the currents and the voltages.

$$\sum_{\alpha \in A_n} P_\alpha + \sum_{n'} P_{n,n'} = 0 \quad (2.25)$$

$$\sum_{\alpha \in A_n} Q_\alpha + \sum_{n'} Q_{n,n'} = 0 \quad (2.26)$$

Approximation for Transmission Networks: Direct Current (DC) Power Flow

In transmission networks, nodal voltages remain almost constant. Therefore, voltage magnitudes are considered to be approximately equal to the nominal voltage, i.e. $V_n \approx 1$ per unit. Also, the angle differences over a transmission line are considered very small. Using that $\sin(\theta) \approx \theta$ and $\cos(\theta) \approx 1$ for very small θ in equation 2.23 yields the following approximation for real power flow:

$$P_{n,n'} = -B_{n,n'}(\theta_n - \theta_{n'}) \quad (2.27)$$

Also, the resistance of transmission lines is much smaller than their reactance, therefore the conductance $G_{n,n'}$ is also small and can be ignored from equations 2.23 and 2.24 above. Combined with the above assumptions on constant voltage magnitude and small angle differences, equation 2.24 becomes:

$$Q_{n,n'} = 0 \quad (2.28)$$

In other words, reactive power flows on transmission lines are ignored.

Transmission network power flow problems can be alternatively written using the shift factor formulation (Goldis, 2015), (Caramanis et al., 2016). The shift factor formulation contains fewer although denser constraints based on line flow sensitivities or shift factors.

Approximations for distribution networks: Relaxed Branch Flow Model

The equations that follow were first proposed by (Baran and Wu, 1989). They are based on simplifications of the AC power flow equations for a tree network. As such, these equations are appropriate for a distribution network.

While the AC power flow equations 2.23 and 2.24 are a result of substituting 2.20

into 2.19, the equations of this approximation are obtained by taking the magnitude squared of 2.20 and substituting 2.19. As a result, voltage and current are represented by their square magnitude only. In other words, voltage and current now lie on a circle of radius equal to the corresponding vector magnitude, rather than on a point on the complex plane. This results in a decreased number of variables, since it does away with voltage angles. The process is as follows:

$$\begin{aligned}
|\vec{V}_{b'}|^2 &= |\vec{V}_b - \vec{I}_{b,b'} \vec{Z}_{b,b'}|^2 \\
|\vec{V}_{b'}|^2 &= (\vec{V}_b - \vec{I}_{b,b'} \vec{Z}_{b,b'}) \cdot (\vec{V}_b^* - \vec{I}_{b,b'}^* \vec{Z}_{b,b'}^*) \\
v_{b'} &= v_b + l_{b,b'}(r_{b,b'}^2 + x_{b,b'}^2) - \vec{V}_b \cdot \vec{I}_{b,b'}^* \cdot \vec{Z}_{b,b'}^* - \vec{V}_b^* \cdot \vec{I}_{b,b'} \cdot \vec{Z}_{b,b'}
\end{aligned}$$

We continue by substituting 2.19:

$$\begin{aligned}
v_{b'} &= v_b + l_{b,b'}(r_{b,b'}^2 + x_{b,b'}^2) - \vec{S}_{b,b'} \cdot \vec{Z}_{b,b'}^* - \vec{S}_{b,b'}^* \cdot \vec{Z}_{b,b'} \\
v_{b'} &= v_b + l_{b,b'}(r_{b,b'}^2 + x_{b,b'}^2) - 2 \cdot (r_{b,b'} \cdot P_{b,b'} + x_{b,b'} \cdot Q_{b,b'})
\end{aligned}$$

where $v_b = V_b^2$ and $l_{b,b'} = I_{b,b'}^2$. Notice the change of subscripts from n, n' , denoting transmission network buses, to b, b' , that denote distribution network buses, since this approximation is used for distribution networks.

The equality of two complex numbers means that their real parts and imaginary parts are both equal, or if they are written in polar form, that their magnitude and angle are equal. Taking the square of the magnitude of the voltage drop constraint, means that we are equating the magnitudes only, a looser constraint than the equality of the complex voltages. The angle equation can be thought of as superfluous because of the following reasoning: Each solution of the equality of the squared magnitudes will provide us with a unique value of the angle difference on a line, namely $\angle \vec{V}_b - \vec{V}_{b'} = \angle \vec{Z}_{b,b'} \vec{I}_{b,b'} \Rightarrow \angle \vec{V}_b - \vec{V}_{b'} = \arctan\left(\frac{\Im(\vec{Z}_{b,b'} \vec{I}_{b,b'})}{\Re(\vec{Z}_{b,b'} \vec{I}_{b,b'})}\right)$. For tree networks where the substation bus voltage angle is fixed to 0 and there is a unique ancestor to each bus, this phase

difference is adequate to calculate unique voltage angles for all buses.

We adopt these equations and follow (Farivar and Low, 2013) in naming them Relaxed Branch Flow model. The model consists of the aforementioned power flow equations (that replace equations 2.23 and 2.24 for distribution power flow problems) and power balance equations 2.25 and 2.26.

$$l_{b,b'} = I_{b,b'}^2 = \frac{P_{b,b'}^2 + Q_{b,b'}^2}{v_b} \quad (2.29)$$

$$v_{b'} = v_b - 2 \cdot (r_{b,b'} P_{b,b'} + x_{b,b'} Q_{b,b'}) + (r_{b,b'}^2 + x_{b,b'}^2) \cdot l_{b,b'} \quad (2.30)$$

$$P_{b,b'} + P_{b',b} = r_{b,b'} \cdot l_{b,b'} \quad (2.31)$$

$$Q_{b,b'} + Q_{b',b} = x_{b,b'} \cdot l_{b,b'} \quad (2.32)$$

$$\sum_{\alpha \in A_b} P_\alpha + \sum_{b'} P_{b,b'} = 0 \quad (2.33)$$

$$\sum_{\alpha \in A_b} Q_\alpha + \sum_{b'} Q_{b,b'} = 0 \quad (2.34)$$

The first two equations were derived above, the third and fourth represent the real and reactive power losses over a distribution line while the last two are the real and reactive power balance equations.

(Li et al., 2012a) provides a second order cone relaxation of the relaxed branch flow model, by substituting equality constraints 2.29 with inequalities and analytically derives sufficient conditions for it to be exact. For most practical cases the relaxation turns out to be exact even when sufficient conditions are not met.

We refer the reader to (Zimmerman, 1995), where a multitude of other power flow methods, relevant to distribution networks are included.

2.2.3 Optimal Power Flow

The power balance equations that together with power flow equations are used to solve power flow problems include the injections and withdrawals of network devices (e.g., generators, loads). When we are only interested in calculating line flows, currents and bus voltages and all injections and withdrawals are known, then call this problem a power flow problem.

Another common power systems' problem is the Optimal Power Flow or OPF for short. In an OPF problem, the injections or withdrawals of devices may not be fixed. Device injections and withdrawals are treated as decision variables and are selected relative to a given objective function. In other words, that objective's optimization is performed subject to the power flow equations ((2.29)-(2.32) for a distribution OPF problem, 2.27 for a transmission OPF problem) and power balance equations (2.25) and (2.26) as well as additional unknown injection/ withdrawal related constraints (eg. generator capacity constraints).

Chapter 3

Power System Components

This section is dedicated to describing power system components later used in this thesis. We mention traditional power systems elements, like generators, transformers, loads and shunt capacitors, as well as new power systems elements, like solid state transformers and elements that are referred to as Distributed Energy Resources. Distributed Energy Resources (DERs) are connected to the distribution network and include most notably amongst others photovoltaics, distributed volt/var compensating devices, and flexible loads like electric vehicles, smart thermostats and storage.

We remind the reader of our sign convention: negative output values denote generation (injection), while positive output values denote consumption (withdrawal). Also, flow on a line out of a bus is positive, while flow on a line into a bus is negative.

3.1 Electricity Network Resources

3.1.1 Lines

Lines in the transmission network are called transmission lines, while lines in the distribution network are called distribution lines. Transmission and distribution lines are characterized by their capacity.

Transmission line capacity is almost always respected when system operators decide how to allocate power amongst transmission lines. This is made possible by the aforementioned meshed topology of transmission networks. On the other hand, distribution lines are commonly overloaded above their capacity. This is allowed

because due to the tree topology, there might be no other option to serve distribution-network connected loads.

Transmission lines are mostly overhead, with only about 0.5% being underground. Distribution lines are more evenly divided between underground and overhead. Typically, large urban centers are served with underground distribution lines.

Lastly, with regard to modeling, transmission and distribution lines are represented by the π -model that consists of:

- A series resistance $r_{b,b'}$
- A series reactance $x_{b,b'}$
- Two shunt reactances, one at the line start point and one at the line end point.

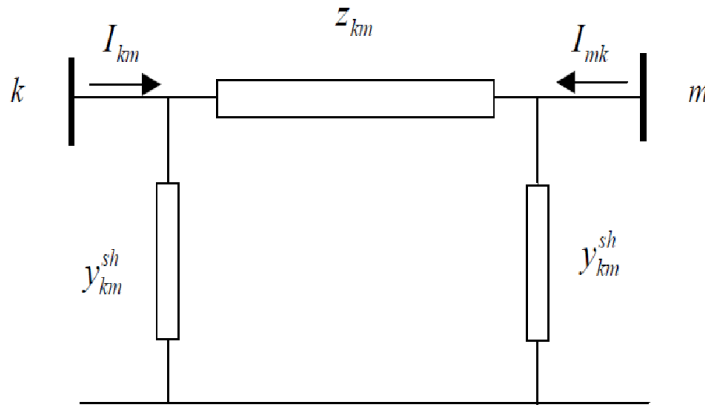


Figure 3-1: Complete transmission/distribution line model.

For simplicity, in this thesis we will disregard shunt elements and represent lines by a series resistance and reactance. As mentioned above, transmission lines have higher reactance than resistance. Overhead lines have a positive reactance, meaning that they behave like inductors and consume reactive power, while underground lines have negative reactance, i.e. they behave like capacitors and provide reactive power.

Distribution lines do not have costs for the flow through them, therefore we use $f_{b,b'}(P_{b,b'}(h), Q_{b,b'}(h), P_{b',b}(h), Q_{b',b}(h)) = 0$.

3.1.2 Transformers

Transformers are, as mentioned above, crucial elements of AC power systems. Using induction, they transform the magnitude of AC voltages, keeping the same frequency. A transformer is characterized by the primary and secondary voltages, as well as by its rated capacity. The primary voltage can be thought of as the input voltage that will be transformed and the secondary voltage can be thought of as the output, or the transformed voltage.

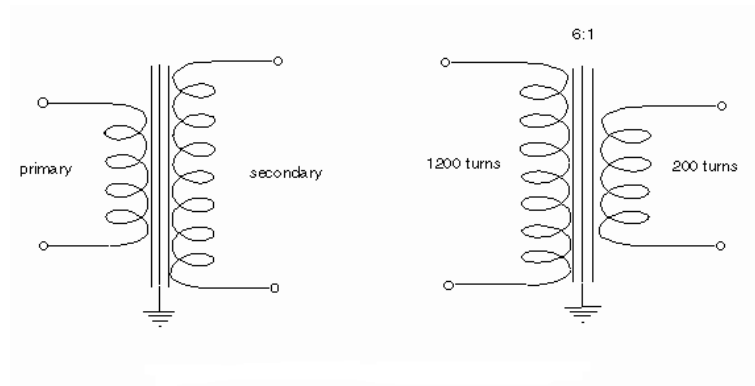


Figure 3-2: Transformer's primary and secondary coils and their ratio.

Figure 3-2 shows the transformer turns. The ratio of the primary turns N_1 to the secondary turns N_2 equals the ratio of the primary voltage V_1 to the secondary voltage V_2 , namely:

$$\frac{N_1}{N_2} = \frac{V_1}{V_2} \quad (3.1)$$

For a step-up transformer, where $V_1 \leq V_2$, the primary turns are less than the secondary turns, $N_1 \leq N_2$, as is the case for the leftmost pair of primary- secondary coils shown in Figure 3-2 above.

For a step-down transformer, where $V_1 \geq V_2$, the primary turns are more than

the secondary turns, $N_1 \geq N_2$, as is the case for the rightmost pair of primary-secondary coils shown in Figure 3-2 above.

The transformer rated capacity, similarly to a line capacity, shows how much power can flow through the transformer.

In this work, we use a simplified transformer model, where the transformer is modeled similar to a line, i.e. represented by a series resistance and reactance. More complex models can include shunt elements to the transformer model.

Types of Transformers

As mentioned above, transformers are able to transform voltage magnitude. They do this with induction between their primary and secondary coils. In *traditional transformers*, the ratio of number of turns in the primary coil to the number of turns in the secondary coil is fixed, therefore the ratio of primary to secondary transformer voltage is also fixed.

This is not the case for *tap-changing transformers*. They are equipped with a tap changer, that acts like a connection point selection across the secondary windings. This way, the primary to secondary turns ratio may be varied, thus changing the primary to secondary voltage ratio. The tap changing mechanism can be manual or automated and the tap changes can be made during no load conditions or on-load conditions.

An *autotransformer* is a type of tap-changing transformer. The two windings of a tap-changing transformer are connected in series and become one winding. Therefore, portions of this single winding make up both the primary and the secondary coils. In other words, the two sides of an autotransformer are connected physically, in addition to being connected through induction. The tap-changer allows the secondary voltage to be varied, but this time the relationship of the primary voltage to the secondary voltage given the primary and secondary coils is $\frac{V_1}{V_2} = \frac{N_1+N_2}{N_1}$, as can be seen in Figure

3.3 below.

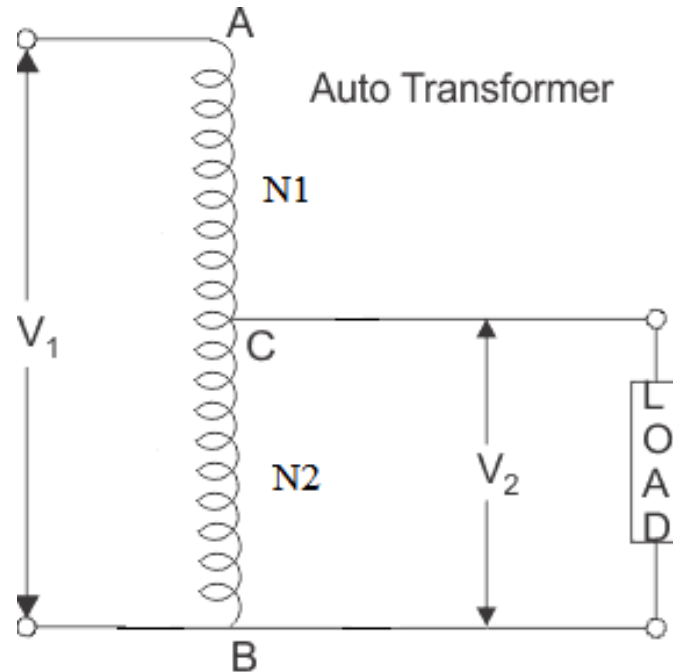


Figure 3.3: Autotransformer's coils.

Voltage regulators that are autotransformers with automatic tap-changers are especially applicable to distribution networks. They can be installed in medium or low voltage circuits, close to the substation or further into the distribution network and aim at keeping voltages flat. This task is performed through changing the turns ratio, as in any tap-transformer.

An even more recent transformer type is called *solid state transformer (SST)*. Unlike traditional and tap-changing transformers, that change the voltage magnitude operating on the 50 or 60Hz frequency, a SST employs power electronics, to change the voltage magnitude operating on a much higher frequency, commonly in the order of kHz. In specific, the steps that a SST follows to transform 50/60 Hz AC voltages are as follows:

1. Power electronics convert the primary voltage to a voltage of the same magni-

tude and higher frequency.

2. A high-frequency transformer, that is much smaller and lighter than low-frequency transformers, steps the voltage magnitude up or down, while maintaining the high frequency.
3. Finally, power electronics re-shape the AC voltage back to the 50/60Hz frequency.

This results in SSTs having much less weight and volume than traditional transformers. Other benefits include real power control, as well as reactive power compensation abilities (She et al., 2012).

Transformer Hottest Spot Temperature

Similar to lines, transformers are also characterized by a rated capacity. However, it is common for transformers to be temporarily loaded beyond that capacity, in which case the transformer is called overloaded. This is even more common a phenomenon for distribution network transformers, first because the network is radial and such overloading might be necessary to ensure service to distribution customers and second because of the bi-directional flows caused by the recent increased presence of distributed energy resources (see Section 3.4 and Chapter 4).

The flow through a transformer affects the temperatures inside the transformer and therefore affects its performance. Much work in the literature has been devoted to studying the evolution of temperatures inside a transformer. The crucial factor affecting a transformer's performance turns out to be the hottest spot temperature (HST), namely the highest temperature that develops in the transformer's insulation. Other factors like moisture and oxygen content, that can contribute to the performance of the transformer, have a lesser effect now due to new oil preservation technologies.

We refer the reader to (IEEE, 1996) for transformer hottest spot temperature formulas. In this work, we assume that the hottest spot temperature of a transformer is calculated as:

$$\theta_{b,b'}^{HS}(h) = \theta_{b,b'}^{HS}(h-1) - k_1 \cdot \left(\frac{\theta_{b,b'}^{HS}(h) + \theta_{b,b'}^{HS}(h-1)}{2} - T^{out}(h) \right) + k_2 \cdot \left(\frac{S_{b,b'}(h)}{S_{b,b'}^N} \right)^2 \quad (3.2)$$

where $\theta_{b,b'}^{HS}(h), \theta_{b,b'}^{HS}(h-1)$ is the average hottest spot temperature during hours h and $h-1$ respectively, $S_{b,b'}$ is the apparent flow through the transformer, $S_{b,b'}^N$ is the rated capacity of the transformer and $k_1, k_2 \geq 0$ are parameters.

If we assume short transition periods from one hour's equilibrium hottest spot temperature to the next hour's hottest spot temperature, i.e., that there is no impact of the previous hour's hottest spot temperature $\theta_{b,b'}^{HS}(h-1)$, then we can use the relation:

$$\theta_{b,b'}^{HS}(h) = k_1 \cdot T^{out}(h) + k_2 \cdot \left(\frac{S_{b,b'}(h)}{S_{b,b'}^N} \right)^2 \quad (3.3)$$

Parameters $k_1, k_2 \geq 0$ should be calibrated such that:

- Under nominal loading conditions, i.e. $S_{b,b'}(h) = S_{b,b'}^N$, the insulation temperature should be $\theta_{b,b'}^{HS}(h) = 110C$.
- When the transformer is overloaded, $S_{b,b'}(h) \geq S_{b,b'}^N$, and $\theta_{b,b'}^{HS}(h) \geq 110C$.
- When the transformer is underloaded, $S_{b,b'}(h) \leq S_{b,b'}^N$, and $\theta_{b,b'}^{HS}(h) \leq 110C$.

If the hottest spot temperature in a transformer exceeds 180C, the transformer's insulation might be inadvertently damaged. Therefore, in calibrating k_1 and k_2 , a high loading (of the order of $1.5 \leq \frac{S_{b,b'}}{S_{b,b'}^N} \leq 2$) is assumed to correspond to a hottest spot temperature of 180C.

Transformer Economic Life Degradation

The hottest spot temperature is linked to the insulation's deterioration over time through the Arrhenius reaction rate. The aging acceleration factor is therefore calculated as (IEEE, 1996):

$$\Gamma_{b,b'}(h) = \exp\left(\frac{15000}{383} - \frac{15000}{273 + \theta_{b,b'}^{HS}(h)}\right) \quad (3.4)$$

This equation relates the transformer's lost economic life to each clock hour of loading that causes hottest spot temperatures of $\theta_{b,b'}^{HS}(h)$.

- Under nominal loading conditions, i.e. $S_{b,b'}(h) = S_{b,b'}^N$, the insulation temperature should be $\theta_{b,b'}^{HS}(h) = 110C$, and then from equation 3.4, the transformer loses one hour of economic life per clock hour of nominal loading.
- When the transformer is overloaded, $S_{b,b'}(h) \geq S_{b,b'}^N$, and $\theta_{b,b'}^{HS}(h) \geq 110C$ the transformer loses more than one hour of economic life per clock hour of overloading.
- When the transformer is underloaded, $S_{b,b'}(h) \leq S_{b,b'}^N$, and $\theta_{b,b'}^{HS}(h) \leq 110C$ the transformer loses less than one hour of economic life per clock hour of underloading.

The last two points together with the more detailed hottest spot temperature evolution equation (3.2) relate to the practical conclusion that a transformer's life might not be greatly affected if overloading periods are followed by underloading periods.

The individual costs of a transformer are therefore equal to:

$$f_{b,b'}(P_{b,b'}(h), Q_{b,b'}(h), P_{b',b}(h), Q_{b',b}(h)) = c_{b,b'}^{tr} \cdot \Gamma_{b,b'}(h)$$

, where $c_{b,b'}^{tr}$ is the cost of transformer b, b' per hour of economic life.

Equation 3.4 is convex with respect to $\theta_{b,b'}^{HS}(h)$ for all practical values of $\theta_{b,b'}^{HS}(h)$. (The inflection point occurs at $\theta_{b,b'}^{HS}(h) = 7227C$.) Equations 3.3 and 3.2 can both easily be seen to be convex with respect to $S_{b,b'}(h)$, therefore the aging acceleration factor $\Gamma_{b,b'}(h)$ is convex with respect to $S_{b,b'}(h)$.

3.1.3 Shunt Capacitors

Shunt capacitors or capacitor banks are capacitors placed as shunt elements to the electricity network, i.e. they are connected in line-to-neutral. A capacitor stores electrical energy and can provide it back to the system in the form of reactive power. Therefore, shunt capacitors or capacitor banks are employed to provide reactive power for the basic goal of voltage control. Capacitors are normally connected after a switch that connects or disconnects them from the rest of the system. Nowadays about 19,000 capacitors are used to control system voltages at all voltage levels. Most of them, about 12,000, are used by distribution utilities to control distribution voltages (US Department of Energy, 2011). Utilities place capacitors at the end of long distribution lines and switch them on to prevent undervoltages during periods of high load.

Through the provision of reactive power, shunt capacitors can also work as "power factor correcting devices". Injecting reactive power next to an inductive load reduces net reactive power demand, i.e. reduces apparent flow on the line leaving real power unaffected, thereby increasing the power factor (see equation 2.15). Capacitors are called on to correct the power factor when the latter drops below 0.8.

Shunt capacitors have the disadvantage that their reactive power output is proportional to the square of the voltage (Eremia and Bulac, 2013). Capacitors can be modeled as on-or-off devices relative to their capacity C_α and the square of the bus' voltage magnitude:

$$Q_\alpha = \{-\min(C_\alpha \cdot v_b, C_\alpha), 0\} \quad (3.5)$$

We may also model them as continuously controllable devices through:

$$-\min(C_\alpha \cdot v_b, C_\alpha) \leq Q_\alpha \leq 0 \quad (3.6)$$

This is in line with the recent use of semiconductor switches (e.g., thyristors) to provide continuous control of the output of many reactive power compensating devices (e.g., SVC, STATCOM).

We assume zero individual costs for shunt capacitors $f_\alpha(P_\alpha(h), Q_\alpha(h)) = 0$.

3.2 Generators

Generators are able to provide real and reactive power. The most important generator characteristic is its capacity, C_α . Simplistic generator models often use rectangle constraints for real and reactive output limits. This means that real and reactive power outputs are treated as if they were independent. For a more realistic model of generators, the well-known D-curves shown in Figure 3.4 are used. We approximate the D-curve with a half-circle.

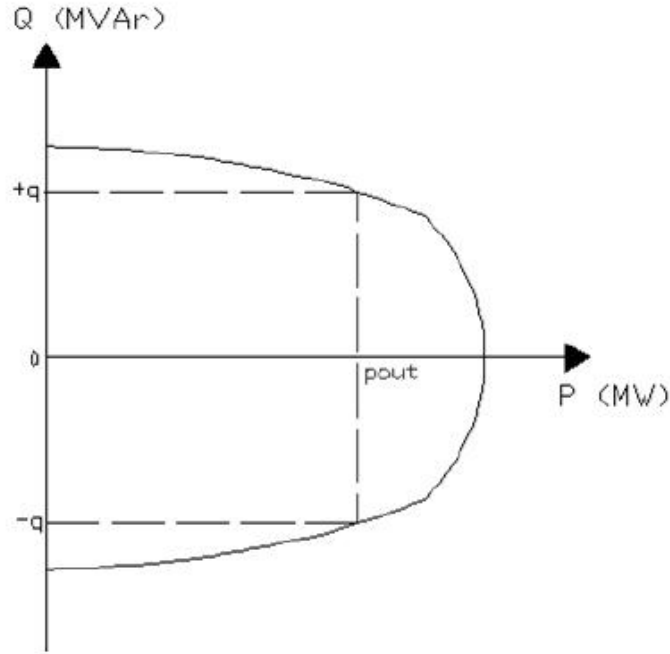


Figure 3-4: Generator's D curve, relating real and reactive power output to capacity.

Therefore, the relevant equations describing generators' outputs in real and reactive power are as follows:

$$P_{\alpha} \leq 0$$

$$P_{\alpha}^2 + Q_{\alpha}^2 \leq C_{\alpha}^2.$$

With regard to costs, generators' variable costs for real power production depend on the generator type (e.g., different fuel type) and are generally modeled as a linear function of them $f_{\alpha}(P_{\alpha}(h), Q_{\alpha}(h)) = c_{\alpha} \cdot P_{\alpha}(h)$. Fuel costs for the production of reactive power are considered to be negligible. However, depending on where the operating point is located on the half circle of Figure 3-4 the generator might incur other costs for providing reactive power. Indeed, if the generator's operating point is on the circumference, meaning that $P_{\alpha}^2 + Q_{\alpha}^2 = C_{\alpha}^2$, then there is a trade-off relationship between real and reactive power. In other words, in order to produce more

reactive power, the generator has to cut back on real power production. Such costs are referred to as "opportunity costs". Opportunity costs will be discussed in greater detail in Chapter 5.

3.3 Traditional Loads

The simpler load model found in power systems analyses is the constant power load. However, most loads are optimized to work at some voltage level \check{v} . As a result, the power consumption of loads has been shown to differ based on their voltage v when $v \neq \check{v}$ (Fairley, 2010). This is more significant for inductive loads (i.e. loads consuming reactive power). Conservation Voltage Reduction (CVR) is the reduction of energy consumption resulting from bringing feeder voltage closer to \check{v} .

In order to reflect the effect of voltage magnitude on the consumption, loads can be modeled using the ZIP model (Pacific Northwest National Laboratory, 2010). In the latter, a load is assumed to be made up of a constant impedance part (Z), a constant current part (I) and a constant power part (P). Voltage magnitude affects the consumption of the constant impedance and constant current components (Pacific Northwest National Laboratory, 2010).

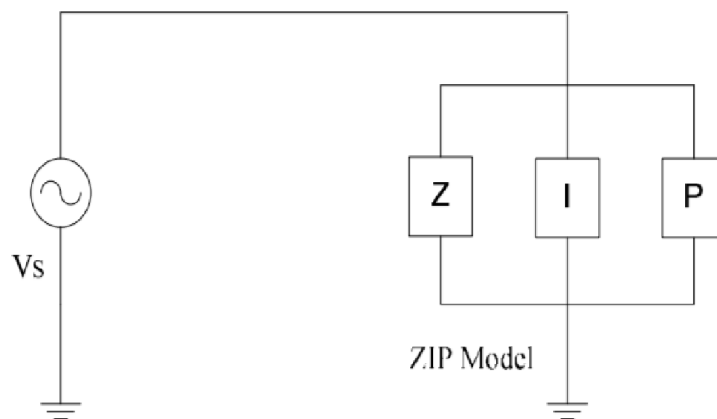


Figure 3-5: ZIP model for traditional loads.

In this work, we incorporate the effect of voltage magnitudes on the real power consumption of loads through the use of the following model: A load is optimized to work with voltage of \check{v} and then consumes P_α . We call P_α the energy service requirement of this load. For deviations of the voltage v from \check{v} , the power consumed by the load becomes:

$$\check{P}_\alpha = P_\alpha \cdot (1 + w \cdot (v - \check{v})^2) \quad (3.7)$$

If we assume that these loads have a constant power factor $\cos(\theta_\alpha)$ and that they are inductive, then their reactive power consumption is written as:

$$\check{Q}_\alpha(h) = \check{P}_\alpha(h) \cdot \frac{\sqrt{1 - \cos^2(\theta_\alpha)}}{\cos(\theta_\alpha)} \quad (3.8)$$

We assume zero individual costs for traditional loads $f_\alpha(P_\alpha(h), Q_\alpha(h)) = 0$.

The abovementioned loads are inflexible or fixed, because their energy service requirement $P_\alpha(h)$ does not change depending on system conditions. However, system conditions, namely the voltage magnitude at their connection bus, affect the real consumption of the load. We call these loads traditional loads in contrast to other loads, we will later detail, that are flexible. See section 3.4.2 below.

3.4 Distributed Energy Resources

The distribution network is currently increasingly populated with Distributed Energy Resources (DERs). DERs include photovoltaics, microgenerators as well as flexible loads, like electric vehicles, HVAC loads and storage. DERs are capable of attractive time-shiftable behavior. Also, DERs are commonly interfaced with power electronics, meaning that they are also able to provide reactive power. For example, photovoltaic panels produce DC real power and are connected to the grid through a DC-to-AC converter (inverter). Also, electric vehicles can charge their batteries with DC current through the grid by means of a charger equipped with AC-to-DC converter.

Power electronics accompanying DERs work in the following way: take the case of the inverters of photovoltaics that are equipped with power electronics. When the amount of real power transferred from the panel to the grid is below the limit of the inverter, then the inverters power electronics have excess capacity. That excess capacity can be put to dual use, or in simpler terms, that excess capacity can be used to produce reactive power. In fact, power electronics interfaced DERs are able to behave like a capacitor and inject reactive power to the grid when voltages are low or behave like an inductor and consume/ absorb reactive power when voltages are high. The same thing can happen for the converter in the charger of an electric vehicle.

On the other hand, power electronics are not always accompanying a device that provides/ consumes real power. Distributed Volt/Var devices that only inject/ consume reactive power fall within the power electronics spectrum and can be referred to as stand-alone power electronics. In this case, all of their capacity can be used to provide/consume reactive power.

The section continues with specific analysis of the DERs most relevant to this work.

3.4.1 Distributed Generation Types

Photovoltaics

The amount of real power generated from a PV panel during a certain hour is a percentage of its nameplate capacity C_α . That percentage k_3 expresses the fixed solar irradiation levels of this hour. The real power injection is described by:

$$-k_3 \cdot C_\alpha \leq P_\alpha(h) \leq 0 \quad (3.9)$$

The amount of power able to reach the grid is also limited by the inverter capacity. For the remainder of this work, as is common in the literature, we assume that

the inverter is oversized and therefore the limiting factor is the nameplate capacity. As a result, if the solar irradiation is not 100%, then the remainder of the nameplate capacity can be used to provide reactive power.

The equations that describe the relationship of the real and reactive power capabilities of a photovoltaic installation depend on the inverter type. The inverter must operate off a DC bus to be able to provide or consume reactive power. When the sun is shining, $k_3 > 0$, the DC bus is provided by the panels, in which case the real and reactive power outputs are connected through the quadratic relationship which holds also for conventional fossil generators:

$$P_\alpha^2(h) + Q_\alpha^2(h) \leq C_\alpha^2 \quad (3.10)$$

The losses of real power because of the inverter are of the order of $3\% \cdot Q_\alpha$.

If $k_3 = 0$, as is the case at night, reactive power provision is only possible if the inverter is equipped with a capacitor that can act as a DC bus. The capacitor will be charged through a battery or an AC source. In this case however, losses in addition to the 3% in the inverter would be incurred because of the charging/ discharging efficiency of the capacitor.

If the inverter is not equipped with a capacitor, then the quadratic relationship only holds when $k_3 > 0$. If $k_3 = 0$, the photovoltaic cannot provide reactive power, despite having excess capacity.

Some PV arrays utilize a DC-to-DC converter connected between the panels and the inverter. The converter steps the panel voltage up or down so as to maximize the efficiency in converting solar power to electrical power.

In this work, we assume that the PV is equipped with a capacitor, therefore reactive power provision when $k_3 = 0$ is possible. We also disregard losses because of the inverter and the capacitor charging.

A photovoltaic installation is assumed in our models to incur no operating cost to produce real or reactive power, $f_\alpha(P_\alpha(h), Q_\alpha(h)) = 0$.

Wind and microgeneration

Other types of real power generating DERs are also available: renewable like wind generators, and non-renewable like microgenerators, with or without CHP (Combined Heat and Power). Wind generators can provide real power as allowed by the hourly wind conditions, but cannot provide reactive power. Microgenerators' real and reactive power output is described by constraints similar to centralized generators.

3.4.2 Flexible Loads

Electric Vehicles

The electric vehicle (EV) charging station, depending on its voltage, can provide a certain amount of power per hour, r_α . The charger also has a capacity, C_α , that dictates the maximum battery charging rate it can handle. In addition to these two factors, the amount of energy that can be stored into the battery of the EV is also limited by the uncharged state of the battery. If the charger is not using all of its capacity, then the unused portion can be used to provide reactive power.

We translate the above description into the following equations describing the behavior of electric vehicles, assuming that they cannot discharge, i.e. while they are plugged in, they do not provide real power to the grid:

$$0 \leq P_\alpha(h) \leq r_\alpha, \alpha \in E, h_{arr} \leq h \leq h_{dep} \quad (3.11)$$

$$x_\alpha(h_{dep}) = x_\alpha(h_{arr}) - \sum_{h=h_{arr}}^{h_{dep}} P_\alpha(h), \alpha \in E \quad (3.12)$$

$$x_\alpha(h_{dep}) \geq 0, \alpha \in E \quad (3.13)$$

$$P_\alpha(h)^2 + Q_\alpha(h)^2 \leq C_\alpha(h)^2, \alpha \in E, h_{arr} \leq h \leq h_{dep} \quad (3.14)$$

Electric vehicles incur uncharged battery costs, that they need to replace with fuel, $f_\alpha(P_\alpha(h), Q_\alpha(h)) = u(x_\alpha(h_{dep}))$. They are zero when $x_\alpha(h_{dep}) = 0$ and positive otherwise.

Space Conditioning

Building space conditioning currently accounts for a significant proportion of the overall energy consumption. Given a comfort zone of temperatures, a smart thermostat is able to shift consumption between hours, also known as pre-heating and pre-cooling. This is done through embedded decision support software, that detects signals from the network. These signals are most times related to prices.

For the case of heating, the smart thermostat model is described by the following equations, if we assume a constant power factor $\cos(\theta_\alpha)$:

$$\underline{T}_\alpha^{in} \leq T_\alpha^{in}(h) \leq \bar{T}_\alpha^{in} \quad (3.15)$$

$$0 \leq P_\alpha(h) \leq C_\alpha \quad (3.16)$$

$$T_\alpha^{in}(h) = T_\alpha^{in}(h-1) + k_4 \cdot P_\alpha(h) - k_5 \cdot \left(\frac{T_\alpha^{in}(h) + T_\alpha^{in}(h-1)}{2} - T^{out}(h) \right) \quad (3.17)$$

$$Q_\alpha(h) = P_\alpha(h) \cdot \frac{\sqrt{1 - \cos^2(\theta_\alpha)}}{\cos(\theta_\alpha)} \quad (3.18)$$

Equation 3.17 shows that the inside temperature of the building is equal to the temperature of the previous hour, increased by a component based on the consumption of the pump but also decreased because of heat dissipation to the outside environment. Specifically, the decrease of the inside temperature because of the outside temperatures is relative to the temperature difference inside and outside the building.

For the case of cooling, the temperature evolution equation becomes:

$$T_\alpha^{in}(h) = T_\alpha^{in}(h-1) - k_4 \cdot P_\alpha(h) + k_5 \cdot (T^{out}(h) - \frac{T_\alpha^{in}(h) + T_\alpha^{in}(h-1)}{2}) \quad (3.19)$$

Equation 3.19 can be similarly interpreted: the inside temperature of the building is equal to the temperature of the previous hour, decreased by a component based on the consumption of the pump but also increased because of the outside temperatures.

We assume no individual costs for smart thermostats, $f_\alpha(P_\alpha(h), Q_\alpha(h)) = 0$.

Storage

Battery, flywheel and similar storage options have been relatively expensive, which is why power systems cannot rely on storage for system reliability. Storage is mostly used for islanding conditions (eg. microgrids). Recent technological breakthroughs have made storage much more affordable, leading to more interest in distribution-network connected storage not only from the literature but also from utilities. Storage capabilities are modeled similarly to those of an electric vehicle battery, minus the assumption of no discharge and of connection during certain hours only (storage is assumed to be connected at all times).

$$x_\alpha(h) = x_\alpha(h-1) - P_\alpha(h), \alpha \in E \quad (3.20)$$

$$x_\alpha(h) \geq 0, \alpha \in E \quad (3.21)$$

$$P_\alpha(h)^2 + Q_\alpha(h)^2 \leq C_\alpha(h)^2, \alpha \in E \quad (3.22)$$

With regard to cost, storage operational costs to provide power or charge should relate to and express the degradation of the battery. In this work, these costs will be ignored, $f_\alpha(P_\alpha(h), Q_\alpha(h)) = 0$, as is common in the literature.

Chapter 4

Electricity Markets

Power systems' operational planning ensures the reliable operation of power systems (adequate supply, reserves etc) by scheduling resources for the provision of three core electric products:

- Real power
- Reactive power
- Reserves, of various types, as discussed in Chapter 2.

Uncertainties in generator and line outages, demand as well as physical constraints (generator up/ down times, generator capacities, line capacities) need to be taken into account for the scheduling. Since these physical limitations require planning ahead, but uncertainty is revealed with accuracy closer to "real time", operational planning is performed in multiple, cascaded time scales. Longer-term planning is done months or weeks ahead. Shorter-term planning is performed the day before the operating day as well as throughout the day (hour ahead and minutes ahead).

Until quite recently, the electric power industry was regulated. The owners of the generating resources also owned the transmission and distribution network lines that delivered the generated power to the customers. These utilities are called vertically integrated. They performed the longer-term planning, while the shorter-term planning was performed by a control center, using a cost-of-service approach based on generator's marginal costs and capabilities.

The liberalization of the electric power industry with the introduction of deregulated electricity markets in 1990 in England, in 1997 in the United States and in 1999 in continental Europe made short-term operational planning the result of competitive bidding. Liberalized power markets have brought by a host of benefits and efficiencies including lower cost operation, decreased congestion and reserves needs.

Distribution networks are assumed to have no generation and (almost completely) price inelastic demand. Since the only generating and price-responsive entities are connected to the transmission network, all focus on competition towards cost minimization was on transmission network markets. As such, today, when we refer to a "power market" we refer to a market for electricity service in the transmission network.

This chapter proceeds with a description of transmission and distribution network pricing today. Section 4.1 describes the discovery of marginal-cost-based prices through transmission power markets. Distribution network pricing is currently rate based, as Section 4.2 discusses. Section 4.3 showcases the inefficiencies of regulated distribution power markets. The chapter concludes with Section 4.4 that proposes an alternate pricing mechanism for distribution markets, namely spatiotemporal marginal-cost-based distribution power markets.

4.1 Transmission Power Markets

Transmission power markets interact with four classes of entities:

- The generating entities
- The consuming entities: resellers and large end-users
- The transmission system owners
- The Independent System Operator (ISO).

Electricity resellers, that include electric utility companies, competitive power suppliers and electricity marketers, group demand of individual distribution-network connected customers and purchase the requisite amount of energy in the transmission markets. Because of this grouping of customers by the resellers, transmission markets are often also referred to as wholesale markets. Recently, large end-users were given the option to purchase electricity directly from the transmission markets, rather than be served through an intermediary.

The first two classes of entities, which make up the competitive sector of power systems, submit price-quantity bids and are scheduled through the market to receive/offer service. On the other hand, the last two entities are regulated. The transmission system owners are responsible for building and maintaining the transmission system following the ISO instructions. The ISO's role is to facilitate the market operation, in many ways, including transmission network control. In other words, in deregulated markets transmission ownership and transmission control are independent and unbundled from generation, demand and retailing. Since the transmission network is a natural monopoly, regulation of the ISO and the transmission ownership ensures non-discriminatory access to the network for all competing entities.¹

The ISO performs longer-term and shorter-term operational planning. For the shorter-term, the ISO performs a task called Unit Commitment (UC) to decide which units should be operating (online or committed units) the next day. UC is a hard computational task since it includes binary decision variables.

Power markets schedule the resources deemed online through UC for the provision of real power, reactive power and reserves. Of these three core products, modern power markets co-optimize real power and some types of reserves. The remaining electrical products, reactive power and the remaining types of reserves, are scheduled

¹We note that there is also the possibility for suppliers and resellers (or end users) to form a "bilateral contract" in which they agree to sell/ buy service to/ from each other at freely negotiated prices.

outside the market, i.e. they are provided dynamically but not competitively. For example, for reactive power, as discussed in Chapter 3, transmission line reactance is much higher than their resistance, therefore reactive power losses are very high over transmission lines. As such, reactive power provision in transmission markets would be a monopoly or oligopoly at best. In other words, transmission markets do not have the makings for competitive reactive power provision. Rather, reactive demand and generation are matched outside of the power market, by contracting interconnected generators to provide reactive power as needed.

Following the multisettlement structure of operational planning, power markets clear in multiple time scales: Day Ahead, Hour Ahead and Real Time.

The Day-Ahead market runs the day before the operating day and typically closes at noon. For the Day-Ahead (DA) market, the ISO accepts price-quantity bids from generation and demand.² These bids can be thought of as reservation prices: Generating entities' bids for real power show the amount of power they are willing to offer when prices equal or exceed their bid. The bids for reserves show the amount of capacity they are willing to hold on stand-by state so that they can be able to provide it as reserves if called upon closer to real time. Consuming entities' bids show the amount of power they are willing to buy when the price does not exceed their bid.

The ISO uses these bids to solve an Economic Dispatch (ED) problem: maximize generators' and consumers' surplus, based on the bids, over the entire 24 hours of the operating day, with the decision variables being, among others, the generators' MW output over the 24 hours. This surplus maximization is of course performed subject to various constraints, like power flow constraints, generators' capacity constraints, transmission line capacity constraints, contingency constraints and reserve requirements. The absence of binary decision variables makes DA ED a much simpler

²We abuse the word demand to refer to resellers. This is done for simplicity and for clarity in differentiating it from generation.

problem to solve than UC.

A simplified version of the Day Ahead transmission power market clearing problem is shown below. Here, we use the B theta model presented in Section 2.2.2. Alternatively, the Day Ahead transmission power market clearing problem can also be modeled as a shift factor version written with fewer but denser constraints based on line flow sensitivities or shift factors (Goldis, 2015), (Caramanis et al., 2016).

$$\underset{P_\alpha(h), R_\alpha(h)}{\text{minimize}} \sum_{\alpha \in G, h} -c_\alpha \cdot P_\alpha(h) - c_\alpha^R \cdot R_\alpha(h) \quad (4.1)$$

$$\text{subject to } \sum_{\alpha, \alpha \in G, D} P_\alpha(h) + \text{losses} = 0 \forall h \rightarrow \pi^P(h) \quad (4.2)$$

$$\sum_{\alpha, \alpha \in G_n, D_n} P_\alpha(h) + \sum_{n, n'} P_{n, n'}(h) = 0, \forall h \rightarrow \pi_n^P(h) \quad (4.3)$$

$$- \sum_{\alpha, \alpha \in G} R_\alpha(h) \geq \underline{R} \rightarrow \pi^R(h) \quad (4.4)$$

$$-C_\alpha \leq R_\alpha(h) + P_\alpha(h) \quad (4.5)$$

$$P_\alpha(h) \leq R_\alpha(h), \forall h \quad (4.6)$$

$$P_{n, n'}(h) = -B_{n, n'} \cdot (\theta_n(h) - \theta_{n'}(h)), \forall h \quad (4.7)$$

$$\underline{P}_{n, n'} \leq P_{n, n'}(h) \leq \bar{P}_{n, n'}, \forall h \rightarrow \gamma_{n, n'}(h) \quad (4.8)$$

In this process, the wholesale market discovers spot prices for electricity, widely known as the Locational Marginal Price (LMP), specifically Day Ahead LMP (DA LMP). This is the cost of supplying the next MW of load at a specific location after considering generator marginal costs, congestion costs and losses. It is the shadow price $\pi_n^P(h)$. The price for reserves is $\pi^R(h)$ and is zonal rather than locational. In other words, it is a single price for all transmission buses n (and their connected devices) in the transmission area with reserve requirement \underline{R} .

Considering an additional infinitesimal and costless injection at transmission bus

n , namely $P_{\dot{g}_n}(h)$, we can rewrite the problem above as (Liu et al., 2009), (Schweppe et al., 1988):

$$\underset{P_\alpha(h), R_\alpha(h), P_{\dot{g}_n}(h)}{\text{minimize}} \sum_{\alpha \in G, h} -c_\alpha \cdot P_\alpha(h) - c_\alpha^R \cdot R_\alpha(h) \quad (4.9)$$

$$\text{subject to } \sum_{\alpha, \alpha \in G, D} P_\alpha(h) + P_{\dot{g}_n}(h) + \text{losses} = 0 \forall h \rightarrow \pi^P(h) \quad (4.10)$$

$$\sum_{\alpha, \alpha \in G_n, D_n} P_\alpha(h) + P_{\dot{g}_n}(h) + \sum_{n, n'} P_{n, n'}(h) = 0, \forall h \rightarrow \pi_n^P(h) \quad (4.11)$$

$$- \sum_{\alpha, \alpha \in G} R_\alpha(h) \geq \underline{R} \rightarrow \pi^R(h) \quad (4.12)$$

$$-C_\alpha \leq R_\alpha(h) + P_\alpha(h) \quad (4.13)$$

$$P_\alpha(h) \leq R_\alpha(h), \forall h \quad (4.14)$$

$$P_{n, n'}(h) = -B_{n, n'} \cdot (\theta_n(h) - \theta_{n'}(h)), \forall h \quad (4.15)$$

$$\underline{P}_{n, n'} \leq P_{n, n'}(h) \leq \bar{P}_{n, n'}, \forall h \rightarrow \gamma_{n, n'}(h) \quad (4.16)$$

$$-\epsilon \leq P_{\dot{g}_n}(h) \leq 0 \quad (4.17)$$

By virtue of the zero generating cost, the shadow price of constraint $-\epsilon \leq P_{\dot{g}_n}(h) \leq 0$ is $\pi_n^P(h)$. We use $\gamma_{n, n'}(h) = \bar{\gamma}_{n, n'}(h) - \underline{\gamma}_{n, n'}(h)$. The Lagrangian of the problem at hour h is written as:

$$\begin{aligned} \mathcal{L}(h) = & \sum_{\alpha \in G} -c_\alpha \cdot P_\alpha(h) - c_\alpha^R \cdot R_\alpha(h) + \sum_{n, n'} \gamma_{n, n'}(h) \cdot P_{n, n'}(h) \\ & + \pi^P(h) \cdot \left(\sum_{\alpha, \alpha \in G, D} P_\alpha(h) + P_{\dot{g}_n}(h) + \text{losses} \right) + \pi_n^P(h) \cdot (-\epsilon - P_{\dot{g}_n}(h)) \end{aligned} \quad (4.18)$$

In the above, we have excluded the nodal power balance constraint and the power flow constraint, since they always hold. We take the derivative of the Lagrangian with respect to $P_{\dot{g}_n}(h)$, bearing in mind that:

- The derivative of terms containing other decision variables is zero

- $\frac{\partial \mathcal{L}(h)}{\partial P_{g_n}(h)} = 0$

We conclude that the LMPs of real power are equal to:

$$\pi_n^P(h) = \pi^P(h) \cdot \left(1 + \frac{\partial \text{losses}}{\partial P_{g_n}(h)}\right) + \sum_{n,n'} \gamma_{n,n'}(h) \cdot \frac{\partial P_{n,n'}(h)}{\partial P_{g_n}(h)} \quad (4.19)$$

We provide a short explanation of the above components of the LMP:

- $\pi^P(h)$ is called the energy component, because it is the same for all buses
- $\pi^P(h) \cdot \frac{\partial \text{losses}}{\partial P_{g_n}(h)}$ is called the loss component.
- $\sum_{n,n'} \gamma_{n,n'}(h) \cdot \frac{\partial P_{n,n'}(h)}{\partial P_{g_n}(h)}$ is called the congestion component. Congestion occurs when a transmission line capacity constraint is binding. Then it holds that $\gamma_{n,n'}(h) \neq 0$, so this component of the LMP is non-zero only when congestion occurs.

The second time scale in the multisettlement transmission power market clearing process is Hour Ahead. In Hour Ahead (HA) markets, the ISO accepts new price-quantity bids from demand and generation, that reflect updated demand patterns as well as updated generation information, to solve an Economic Dispatch (ED) problem. Similarly to the DA ED, HA ED also matches bids to maximize generators' and consumers' surplus. The difference is that for the HA ED problem, the decision variable is the single period output of the committed generators. The decreased number of decision variables in the time domain makes HA ED a simpler problem to solve compared to DA ED. This is expected; since it runs closer to "real time" it should clear fast enough. Since hour ahead markets update generator schedules, they also result in updated LMPs.

Further adjustments as uncertainty is revealed happen in markets that close minutes ahead. They can be 5 or 10 minute ahead markets that we refer to as Real

Time markets. Reserves are only promised in Day Ahead and Hour Ahead markets, but are actually deployed in time scales closer to real time, in the Real Time markets or even seconds ahead of real time, depending on the type of reserves.

LMP discovery through wholesale power markets that was described above is instructive to the formulation of spatiotemporal distribution power markets, whose description follows in Section 4.4. Distribution power markets will discover Distribution Locational Marginal Prices (DLMPs). Despite numerous differences between the two markets, that are also discussed in Section 4.4 (including additional market products like reactive power and voltage magnitude considerations), the LMP discovery process is instructive since DLMPs and LMPs have the same economic interpretation: they show the marginal value of an electric product at a specific hour and bus. As will be shown later in the thesis, while DLMP discovery is "distinct from and more complex than" (Tabors et al., 2017) LMP discovery, LMPs at the interface of transmission and distribution networks, that we call the substation bus, are key drivers of DLMPs (Tabors et al., 2017).

4.2 Distribution Network Operation Today

As mentioned above, nowadays customers at the distribution network are served through intermediaries. The distribution network market is regulated, with rules on prices aiming at achieving the following goals (Brown and Faruqui, 2014):

1. Economic efficiency
2. Equity between different customer groups (eg. industrial, commercial, residential)
3. Revenue stability for the utility
4. Bill stability for the customers

In keeping with revenue and bill stability goals, retail prices are agreed beforehand, when the customer and the utility engage in a contract. Retail prices consist of the following components:

- A base charge (or connection charge), that is independent of consumption
- The largest, most important component of the electric bill is the energy costs, which are based on consumption. The energy costs may be calculated on:
 - a fixed \$/kWh price
 - a variable rate per kWh. Variable \$/kWh pricing structures include:
 1. Pricing where each level of consumption in kW may come at different rates per kWh. These charges are based on peak demand and are called *demand charges*.
 2. Time of Use pricing (TOU). Under this concept, rates per kWh are set higher during projected on- peak hours and lower during projected off- peak hours. However, TOU is not currently used as a means to incentivize customer behavior but rather as a fair treatment to customers actually costing less to the utility company by consuming during off- peak hours for any reason.

The above components of the agreed rates are designed by utilities such that they recover the costs they incur to buy the requisite amount of power (demand plus losses) from wholesale markets plus other operational costs, like distribution network resource upgrades, repairs and replacements as well as some rate of profit. In addition, different classes of customers (industrial, commercial, residential) are subject to different rates (eg. different fixed \$/ kWh for each class of customers) and maybe even different energy cost calculations (eg. demand charges and/or TOU for larger industrial customers but fixed \$/kWh prices for residential customers).

Last but not least, the utility company has to provide quality service to customers. Additional to the actual adequacy of energy, this also relates to maintaining voltage levels and avoiding over-voltages and under-voltages that can cause malfunctioning of the retail customers' electrical equipment or even pose security risks for customers. Today, utilities employ capacitors to adjust reactive power injections and keep voltages within desired bounds. Capacitor bank switching is in most cases based on previous experience with voltages sagging in certain areas and certain hours.

4.3 Problems with today's practice

Power systems and power markets are on the verge of massive transformation because of changes on both the generation and the demand side.

On the generation side, the integration of renewable generation is increasing. Federal and state regulations, trying to keep up with aggressive emission and sustainability goals, push for rapid and increasing renewable integration. To this end, renewables are treated as must-take resources in power markets: they bid zero costs in the DA and RT power markets and are thus always cleared to provide real power. However, this increased renewable deployment presents power systems with a plethora of challenges. The most significant challenges are related to renewables' volatility. Power system operators that had to deal with demand uncertainty only now have to incorporate the volatility of generation too. Reported negative impacts of the intermittency of renewables include undergeneration instances, resulting in loss of load, as well as overgeneration instances. The latter are becoming increasingly frequent. Germany faced such issues in 2010 and 2013 on low-load sunny days, when generation exceeded demand. So did California in 2012. In fact, during these over-generation instances energy prices are suppressed, even becoming negative. Low energy prices cause reliable, baseline units to lose money, urging them to disconnect from the grid

and challenging power system reliability. Several other issues, like frequency problems, are related to renewables' lack of rotating inertia.

At the same time, the demand side is also undergoing major changes because of the introduction of Distributed Energy Resources (DERs). With respect to remuneration for the provision of electricity, the most commonly used method is to reward DERs at the retail energy rates. Generation credits for customer owned DERs can be used to offset customer charges for consumption. Generation and demand do not have to be coincident and can be subtracted over a longer time period. This technique is called *net metering*. A good example can be shown in Figure 4-1 below, that presents the power output of a residential rooftop solar together with the household load consumption over a 24 hour period.

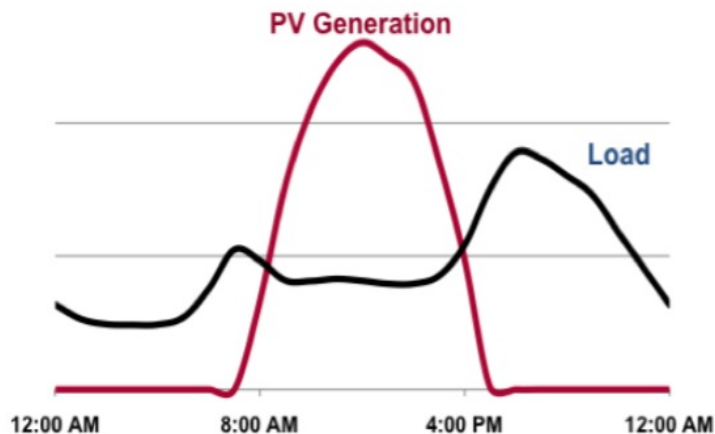


Figure 4-1: Residential demand and rooftop solar generation over a 24 hour period.

It can be easily seen that over the 24 hours depicted, the net demand (load minus PV generation) is almost zero. Therefore, with net metering, this household will pay zero dollars to the utility. However, the utility incurs transmission and distribution network costs for the injection and withdrawal of power. Since the utility is not getting paid back for these costs, it might end up not turning a profit.

Focusing on solar, as the most populous DER type, (Faruqui, 2012) mentions that decreasing costs of solar panels together with net metering at retail rates lead to customers increasingly opting for solar. Though the decreased load, this propagates to decreased utility revenues. Utilities then proceed to raise retail prices, further incentivizing customers to turn to solar and creating an infinite loop of revenue and network problems.

Specifically, utilities are implementing the following methods to deal with revenue loss (Flores-Espino, 2015):

1. Adjustments to customer's bills: Several ways to reinforce utilities within the net metering practice have been proposed. The most important ones are:
 - Increased fixed charges and decreased energy rates: While increased fixed charges almost guarantee a rise in utility earnings, this measure affects customers regardless of whether they own load-accompanying DERs. It also does not promote energy conservation, since it is paired with decreased energy rates.
 - Minimum bills: In the retail bills described above, if the amount billed to the customer is less than a minimum threshold, then the customer will pay the threshold value. This measure has a lesser effect on the utility's profits than increased fixed rates, because (given a low threshold) it is only effective when the net consumption is around zero.
2. DER Compensation plans: DER compensation plans are used to separate generation from consumption and remunerate it accordingly, in the form of the so called Feed-In Tariffs (FIT) or Value Of Solar programs, specifically targeted to PV. In essence what these programs do is charge customers for their consumption based on the agreed retail rates and then reward DER generation

with rates calculated on (estimates of) the utility cost savings because of this generation. Then, the cost savings are divided by the amount of the total DER generation, to determine a \$/kWh remuneration rate. It is common for utilities to offer such a fixed rate of remuneration for the duration of the contract, based on their estimated cost savings.

In what follows in this chapter, we propose an alternate pricing mechanism for distribution network markets.

4.4 Thesis Proposition: Spatiotemporal Distribution Electricity Markets

The previous section showcased that the static pricing methods used in today's regulated distribution network markets are unable to accommodate the rising levels of DERs. The increased network activity makes techniques like net metering and average pricing more and more unsuitable.

Static prices are unable to provide DERs with the incentives needed to optimally use their degrees of freedom: the capability for time-shiftable real power consumption, the provision of reserves and the provision of reactive power. Drawing experience from the scheduling of traditional generating resources in marginal-cost based wholesale markets and inspired by the efficiency gains resulting from the adoption of these markets, we propose the introduction of a spatiotemporal marginal-cost based, distribution power market. In this market, DERs will compete with each other and will strive to optimally allocate their capacity by submitting bids to provide/ receive service. Like the transmission network, the distribution network is also a natural monopoly, therefore fair access to all competing participants must be ensured. This is what the distribution system operator (DSO) will do, amongst other tasks. The distribution market operator will also match DERs' bids to equate demand and sup-

ply while minimizing a bid-based cost function and taking several other constraints into account.

We focus on Day Ahead distribution power markets to harness the intertemporal nature of DERs. To proceed in determining distribution power market products, relevant costs and constraints, we elaborate on the key differences between distribution and transmission networks.

- Voltage related differences: Not only are the operating voltages of transmission networks much higher than the distribution network operating voltages, but also the centralized generators are able to keep voltage magnitudes constant across transmission buses. The absence of entities with such capabilities in distribution networks means that voltage magnitudes at distribution buses are upper and lower bounded.
- Differences in the electrical characteristics of transmission and distribution lines. Resistance is much smaller than reactance in transmission lines. As mentioned above, this results in high reactive power losses over transmission lines. The difference of reactance and resistance of distribution lines is much more modest.
- The electrical characteristics of transmission lines, as well as the almost constant voltage magnitudes, allow for the use linear DC approximations for the power flow equations in transmission networks. In contrast, full AC load flow equations are deemed necessary in distribution networks.

These network differences translate to differences in the market structure of dynamic distribution network markets, compared to wholesale markets:

1. Power flow equations constrain the power market clearing problem. Instead of the linear power flow equations used in wholesale markets, AC non-convex power flow equations will be used for distribution markets.

2. The high reactive power losses over transmission lines mean that local (to each reactive power demand point) providers have an advantage for reactive power provision. The creation of such oligopolistic, if not monopolistic, conditions led to reactive power being scheduled outside the wholesale markets through long-term contracts. The different electrical characteristics of distribution lines mean that reactive power can be provided competitively over distribution networks. Therefore, the proposed distribution power markets clear an additional product of reactive power, which ties in nicely with the ability of DERs to put the excess power electronics' capacity to dual use to provide reactive power. This also means that reactive power providing resources will be remunerated dynamically in distribution markets, rather than with pre-fixed, contract-based prices as in wholesale markets.
3. Differences in the market participant capabilities:
 - Market participants in distribution power markets are DERs, which have intertemporal dynamics. While this capability adds flexibility, it makes the distribution power market problem hard to solve. The expression of such dynamics and preferences constitutes a "complex" bid, versus the price-quantity "uniform" bids of wholesale power markets participants.
 - Distribution market participants are an order of magnitude more than the transmission power market participants.
4. When clearing a wholesale market, distribution (net) demand is treated as tentatively fixed. In clearing distribution power markets, while we cannot assume that transmission network generators' outputs are fixed, we assume that the LMPs at the substation bus (i.e. the interface of transmission and distribution) are fixed. This is equivalent to assuming that the marginal generators do not

change.

5. Moreover, in wholesale markets, the demand of all distribution buses in feeders connected to the same substation is considered to be located at the substation, i.e. distribution feeders are bundled to a single bus. Similar to this demand aggregation to the substation, in distribution power markets the transmission network is approximated by substation connected generators only.

The detailed exposition of the differences in the market formulations goes to show that a simple extension of power markets allowing distribution-network connected entities to participate in the wholesale market *under the current protocol* is insufficient. Indeed, while the minimum size requirement to participate in wholesale power markets keeps decreasing, even if it were to reach the adequate levels for distribution-network connected providers and consumers to be allowed to participate, the existing market practice, relying on centralized market clearing and information gathering, as well as on uniform bids and on simplified assumptions only fit to transmission networks, would be inconsistent with and unable to capture the different nature of the distribution network (line characteristics, voltage considerations) and the intertemporal DER dynamics.

In conclusion, the envisioned Distribution Power Markets clear three products:

1. Real power
2. Reactive power
3. Reserves

DERs will compete to provide real power, reactive power and reserves and optimally allocate their capacity among these three products. Similarly to existing power markets, DERs will be scheduled by a system operator (in this case the distribution

system operator or DSO), who solves the Day Ahead market clearing problem. It is the minimization of bid-based and operational costs subject to:

- AC power flow constraints
- Power balance constraints
- DER dynamics and capabilities constraints
- Voltage bound constraints.

The DSO minimizes:

1. Real power costs, that implicitly include costs of real power losses
2. Reactive power costs, that implicitly include costs of reactive power losses
3. Transformer loss of life, while maximizing
4. Loads' utilities
5. Profit from reserves sales

The primal solution of the distribution power market clearing problem is the DER real power, reactive power and reserves schedules, as well as distribution bus voltages and power flows over distribution lines. At optimality, the primal solution is the optimal DER capacity allocation between these three products.

Wholesale markets discover locational Marginal Prices (LMPs) of real power as well as zonal prices of reserves. The LMPs of real power indicate the marginal value of an injection of real power at a specific bus and a specific time. Distribution power markets, that clear real power, reactive power and reserves, will, in direct accordance, discover Distribution Locational Marginal Prices (DLMPs). These prices are distinct for each product (real power, reactive power, reserves), are varying in the time and

space domains and express the marginal value of an injection of real power, reactive power or reserves at a specific distribution bus and a specific time. These prices will be the Lagrange multipliers corresponding to the optimal primal solution (optimal DER schedules) of the market clearing problem, or in other words, the optimal dual solution of the market clearing problem will provide the DLMPs.

The proposed distribution power market will achieve the following efficiencies:

1. Introducing competition and using all the degrees of freedom of distribution-network connected participants will lead to lower costs, more flexibility and grid resilience to load increases.
2. The distribution market explicitly minimizes variable costs (including losses, electrical equipment degradation etc). DLMPs will reflect these costs, will be time and location variant, and unbundled for each electrical product (real power, reactive power and reserves).³
3. The prices discovered by the market show the value of each market product at each location, thereby promoting the efficient integration of DERs throughout the distribution network.
4. The spatiotemporal prices can also work as investment signals and promote investments in new technologies, products and services.
5. Voltage bound constraints and power flow constraints will be included as hard constraints in the market clearing process. DERs will be providing voltage support by injections or withdrawals of reactive power, as indicated by the reactive power prices. This market-based voltage control will replace today's ad-hoc switching of capacitor banks.

³Fixed costs may not be recovered through DLMPs alone. Constant charges like a connection charge or a constant \$/kWh charge might be required to cover fixed costs.

6. The provision of reserves from DERs will contribute to the increased reserve requirements imposed by the rising levels of renewables. This way of securing reserves is less costly compared to securing an equal amount of reserves from traditional transmission-network reserve providing resources. It will also allow for the increase of the renewable penetration safety limits, that will itself lead to lower emissions.

For reasons that will become clear and discussed in detail later in the thesis, we first proceed for simplicity of exposition with day-ahead distribution power market algorithms without modeling reserves. Chapters 5 and 6 show centralized and distributed market clearing algorithms, respectively, excluding reserves. Chapter 7 completes the thesis contribution by showing day-ahead distribution market clearing algorithms complete with reserve considerations.

Chapter 5

Centralized Algorithm For Distribution Day-Ahead Power Market Clearing

5.1 Formulation

This chapter presents the formulation of the centralized day-ahead distribution power market and relevant numerical results. For simplicity of exposition, we present here the centralized market clearing formulation for real and reactive power only, and extend it to include reserve considerations in Chapter 7.

Distribution networks are connected to transmission networks at a bus called the substation bus. At this interface of transmission and distribution, we represent the transmission network by a source of real power at a constant price, as well as an auxiliary generator that provides reactive power flowing into the distribution network as needed. That constant price of real power can be thought of as the hourly LMP at the substation bus. In other words, the constant price is assumed to be the result of a wholesale power market clearing consistent with the behavior of DERs located at all distribution feeders connected to the wholesale market. In reality, this would require several iterations between each distribution feeder connected to the wholesale market and the wholesale market itself. See Chapter 8 for more details on this issue. As for the auxiliary reactive power providing generator, contrary to today's practice of contractual reactive power provision from centralized generators, it will be dynamically remunerated for the allocation of its capacity to reactive power provision.

The remuneration expresses the opportunity costs for the lost sales of real power and will depend on the amount of reactive power it provides and the substation real power LMP.

The day-ahead distribution power market clearing problem is formulated as a constrained optimization problem. The objective function is the minimization of all operational costs including:

- (i) Real power costs for real power purchases from the transmission and distribution interface
- (ii) Real power generation costs from Distributed Energy Resources (DERs) (For example, PVs have zero such costs while microgenerators have fuel costs.)
- (iii) Reactive power production fuel costs at the substation auxiliary generator
- (iv) Reactive power opportunity cost for the substation auxiliary generator
- (v) The cost of voltage modulation at the substation, as needed to maintain voltages at all distribution buses within acceptable bounds
- (vi) The cost of transformer loss of life
- (vii) The cost of not meeting loads
- (viii) Cost of uncharged EV batteries.

The minimization is performed subject to the following constraints:

- AC load flow relationships (5.2)-(5.7)
- Voltage magnitude bound constraints (5.8)
- Real and reactive power consumption of voltage sensitive loads (5.9), (5.10), (5.11), showing the efficiency of transforming the real power consumed to useful energy service work, based on the voltage magnitude.

- Real and reactive power injections/ withdrawals by DERs (5.12)
- Reactive power output of controllable shunt capacitors, which depends on their location voltage (5.13).
- Electric vehicle charging related constraints. (5.14) expresses the real power consumption limits based on the maximum charging rate capacity, while (5.15) describes the inter-temporal dynamics of the uncharged EV battery. Constraints on the EVs' capability to offer reactive power, based on the charger's capacity, are also expressed through (5.12).
- Smart thermostat related constraints. (5.16) describes the evolution of the inside temperature, given the real power consumption and the hourly outside temperatures, while (5.17) are the comfort zone constraints.

The market clearing problem in mathematical terms follows:

C-OPT: Centralized formulation with Hard Voltage Bound Constraints

$$\begin{aligned}
& \text{minimize}_{P_\alpha(h), Q_\alpha(h), v_\infty(h)} \sum_{\alpha, \alpha \in E} u_\alpha(x_\alpha(h_{dep})) + \sum_{h=1}^{24} \sum_{(b,b'), (b,b') \in tr} c_{b,b'}^{tr} \cdot \Gamma_{b,b'}(\theta_{b,b'}(h)) + \\
& \pi_\infty^P(h) \cdot P_\infty(h) - \sum_{\alpha, \alpha \in G, E} c_\alpha \cdot P_\alpha(h) + \\
& \mathcal{H}(Q_\infty(h)) + \sum_{\alpha, \alpha \in D} u_\alpha(P_\alpha(h)) + \\
& \pi_\infty^{OC}(h) \cdot (C_\infty - \sqrt{C_\infty^2 - Q_\infty^2(h)}) + \\
& c_\infty^v \cdot (v_\infty(h) - 1)^2
\end{aligned} \tag{5.1}$$

$$\text{subject to } l_{b,b'}(h) = \frac{P_{b,b'}^2 + Q_{b,b'}^2}{v_b(h)} \tag{5.2}$$

$$v_{b'}(h) - v_b(h) = -2(r_{b,b'} \cdot P_{b,b'} + x_{b,b'} \cdot Q_{b,b'}) + (r_{b,b'}^2 + x_{b,b'}^2) \cdot l_{b,b'}(h) \tag{5.3}$$

$$\sum_{\alpha, \alpha \in G_b \cup E_b} P_\alpha(h) + \sum_{\alpha, \alpha \in D_b} \check{P}_\alpha(h) + \sum_{b'} P_{b,b'}(h) = 0 \quad (5.4)$$

$$\sum_{\alpha, \alpha \in G_b \cup E_b \cup F_b} Q_\alpha(h) + \sum_{\alpha, \alpha \in D_b} \check{Q}_\alpha(h) + \sum_{b'} Q_{b,b'}(h) = 0 \quad (5.5)$$

$$P_{b,b'}(h) + P_{b',b}(h) = r_{b,b'} l_{b,b'}(h) \quad (5.6)$$

$$Q_{b,b'}(h) + Q_{b',b}(h) = x_{b,b'} l_{b,b'}(h) \quad (5.7)$$

$$\underline{v}_b \leq v_b(h) \leq \bar{v}_b \rightarrow \underline{\mu}_b(h), \bar{\mu}_b(h) \quad (5.8)$$

$$\underline{P}_\alpha \leq P_\alpha \leq \bar{P}_\alpha, \alpha \in D \quad (5.9)$$

$$\check{P}_\alpha(h) = P_\alpha(h) \cdot (1 + w \cdot (v_b(h) - \check{v})^2), \alpha \in D \quad (5.10)$$

$$\check{Q}_\alpha(h) = \check{P}_\alpha(h) \cdot \frac{\sqrt{1 - \cos^2(\theta_\alpha)}}{\cos(\theta_\alpha)}, \alpha \in D \quad (5.11)$$

$$P_\alpha^2(h) + Q_\alpha^2(h) \leq C_\alpha^2(h), \alpha \in G, E \quad (5.12)$$

$$-\min(C_\alpha, C_\alpha \cdot v_b(h)) \leq Q_\alpha(h) \leq 0, \alpha \in F \rightarrow \kappa_\alpha(h) \quad (5.13)$$

$$0 \leq P_\alpha(h) \leq r_\alpha, \alpha \in E, h_{arr} \leq h \leq h_{dep}, \alpha \in \text{DER set for EVs} \quad (5.14)$$

$$0 \leq x_\alpha(h_{dep}) = x_\alpha(h_{arr}) - \sum_{h=h_{arr}}^{h_{dep}} P_\alpha(h), \alpha \in \text{DER set for EVs} \quad (5.15)$$

$$T_\alpha^{in}(h) = T_\alpha^{in}(h-1) - k_4 \cdot P_\alpha(h) + k_5 \cdot \left(T^{out}(h) - \frac{T_\alpha^{in}(h) + T_\alpha^{in}(h-1)}{2} \right), \alpha \in \text{DER set for smart thermostats} \quad (5.16)$$

$$\underline{T}_\alpha \leq T_\alpha^{in}(h) \leq \bar{T}_\alpha, \alpha \in \text{DER set for smart thermostats} \quad (5.17)$$

For the remainder of this work, we will assume that the fuel cost of producing reactive power at the auxiliary substation generator, $\mathcal{H}(Q_\infty(h))$, is very small and therefore negligible. We note that the smart thermostat constraints, describe the evolution of the inside temperature for the case of cooling. The relevant equations for the case of heating can be found in Section 3.4.2. The transformer loss of life equation

$\Gamma_{b,b'}$ and the hottest spot temperature $\theta_{b,b'}$ that appear in the objective function (5.1) were described in Section 3.1.2.

5.2 Decision and Dependent Variables

The variables included in the above day-ahead distribution power market clearing problem are separated into dependent variables and independent variables (decision variables) in the table below (Wang et al., 2009), (Sivanagaraju, 2009):

Decision Variables	Dependent Variables
Real Power Output $P_\alpha(h)$	Real Power Flow $P_{b,b'}(h), P_\infty(h)$
Reactive Power Output $Q_\alpha(h)$	Reactive Power Flow $Q_{b,b'}(h), Q_\infty(h)$
Substation Voltage $v_\infty(h)$	Voltage Magnitudes of $b \neq \infty$
	Line Current $I_{b,b'}(h)$
	Apparent flow $S_{b,b'}(h)$

Table 5.1: Dependent and independent variables of Distribution Day Ahead Power Market clearing problem.

5.3 Components of the Distribution Locational Marginal Prices

At optimality, the primal solution is the optimal DER capacity allocation between real and reactive power. It corresponds to the optimal dual solution. The shadow prices of real and reactive power balance constraints (5.4) and (5.5), namely $\pi_b^P(h)$ and $\pi_b^Q(h)$, respectively are the locational marginal prices of each product at each distribution bus b and hour h . Heretofore, we will refer to the real power balance shadow price as the Real Power Distribution Locational Marginal Price or P-DLMP for short. Similarly, we will refer to the reactive power balance shadow price as the Reactive Power Distribution Locational Marginal Price or Q-DLMP for short. The shorthand DLMP will refer to either or both P-DLMP and Q-DLMP.

As for the inequality constraints, we direct the reader's attention to the shadow prices of the voltage bound constraints (5.8), namely $\underline{\mu}_b$ and $\bar{\mu}_b$. These are non-zero

when the voltage magnitudes bind. Specifically, only one of $\underline{\mu}_b$ and $\bar{\mu}_b$ can be non-zero for each bus b and hour h .

In what follows, we use first order optimality conditions to derive interesting relationships between P-DLMPs, Q-DLMPs, other shadow prices, sensitivities of dependent variables and substation LMPs. We call the resulting relationships *DLMP unbundling equations*.

In order to do so, we consider at each bus b a costless infinitesimal injection of real power $P_{\dot{g}_b}(h)$ and a costless infinitesimal injection of reactive power $Q_{\dot{g}_b}(h)$. As such, the market clearing problem is rewritten as:

$$\begin{aligned} & \text{minimize (5.1)} & (5.18) \\ & P_\alpha(h), Q_\alpha(h), v_\infty(h), P_{\dot{g}_b}(h), Q_{\dot{g}_b}(h) \end{aligned}$$

$$\text{subject to (5.2), (5.3), (5.6)-(5.17)} \quad (5.19)$$

$$P_{\dot{g}_b}(h) + \sum_{\alpha, \alpha \in G_b \cup E_b} P_\alpha(h) + \sum_{\alpha, \alpha \in D_b} \check{P}_\alpha(h) + \sum_{b'} P_{b,b'}(h) = 0 \quad (5.20)$$

$$Q_{\dot{g}_b}(h) + \sum_{\alpha, \alpha \in G_b \cup E_b \cup F_b} Q_\alpha(h) + \sum_{\alpha, \alpha \in D_b} \check{Q}_\alpha(h) + \sum_{b'} Q_{b,b'}(h) = 0 \quad (5.21)$$

$$-\epsilon \leq P_{\dot{g}_b}(h) \leq 0 \quad (5.22)$$

$$-\epsilon \leq Q_{\dot{g}_b}(h) \leq 0 \quad (5.23)$$

The zero generating cost of $P_{\dot{g}_b}(h)$ and $Q_{\dot{g}_b}(h)$ implies that the shadow price of constraint (5.22) is equal to $\pi_b^P(h)$ and the shadow price of constraint (5.23) is equal to $\pi_b^Q(h)$. We now write the Lagrangian in its reduced form by disregarding terms from:

- power flow constraints (5.2), (5.3), (5.6) and (5.7) and power balance constraints (5.20), (5.21). Based on Kirchoff's laws, these constraints will always hold, i.e. a change in the right hand side will equal the change in the left hand side.
- constraints (5.10) and (5.11)

- All other objective function components and constraints that only contain decision variables, since the derivative of any decision variable with respect to decision variables $P_{\dot{g}_b}(h)$ or $Q_{\dot{g}_b}(h)$ is 0, by first order optimality conditions.

Therefore, the reduced Lagrangian is equal to:

$$\mathcal{L} = \sum_h \left\{ \begin{array}{l} \pi_\infty^P(h) \cdot P_\infty(h) - \sum_{\alpha, \alpha \in E} c_\alpha \cdot P_\alpha(h) \\ + \pi_\infty^{OC}(h) \cdot (C_\infty - \sqrt{C_\infty^2 - Q_\infty^2(h)}) + \sum_{(b,b'), (b,b') \in tr} c_{b,b'}^{tr} \cdot \Gamma_{b,b'}(h) \\ + \sum_b \bar{\mu}_b \cdot (v_b(h) - \bar{v}_b) + \sum_b \mu_b \cdot (\underline{v}_b - v_b(h)) \\ + \sum_{(b,\alpha), \alpha \in F_b} \kappa_\alpha(h) \cdot (-\min(C_\alpha, C_\alpha \cdot v_b(h)) - Q_\alpha(h)) \\ + \sum_b \pi_b^P(h) \cdot (-\epsilon - P_{\dot{g}(b)}(h)) + \sum_b \pi_b^Q(h) \cdot (-\epsilon - Q_{\dot{g}(b)}(h)) \end{array} \right. \quad (5.24)$$

We proceed by noting that:

- The first order optimality conditions with respect to decision variables $P_{\dot{g}_b}(h)$ and $Q_{\dot{g}_b}(h)$ imply that $\frac{\partial \mathcal{L}}{\partial P_{\dot{g}_b}(h)} = \frac{\partial \mathcal{L}}{\partial Q_{\dot{g}_b}(h)} = 0$.
- The term in the Lagrangian arising from capacitor related constraints (5.13) can be rewritten as:

$$\min(C_\alpha, C_\alpha \cdot v_b(h)) = \begin{cases} C_\alpha, v_b(h) \geq 1. \\ C_\alpha \cdot v_b(h), v_b(h) < 1. \end{cases} \quad (5.25)$$

- We use $\mu_b(h) = \bar{\mu}_b(h) - \underline{\mu}_b(h)$.

Hence, the aforementioned optimality conditions imply that:

$$\pi_{\beta}^P(h) = \left\{ \begin{array}{l} \underbrace{\pi_{\infty}^P(h) \cdot \frac{\partial P_{\infty}(h)}{\partial P_{\dot{g}_{\beta}}(h)}}_A + \underbrace{\frac{\pi_{\infty}^{OC}(h) \cdot Q_{\infty}(h)}{\sqrt{C_{\infty}^2 - Q_{\infty}^2(h)}} \cdot \frac{\partial Q_{\infty}(h)}{\partial P_{\dot{g}_{\beta}}(h)}}_B + \\ \underbrace{\sum_{h_1 \geq h, (b,b') \in tr} c_{b,b'}^{tr} \cdot \frac{\partial \Gamma_{b,b'}(S_{b,b'}(h_1))}{\partial P_{\dot{g}_{\beta}}(h)}}_C + \underbrace{\sum_b \mu_b(h) \cdot \frac{\partial v_b(h)}{\partial P_{\dot{g}_{\beta}}(h)}}_{D_1} - \\ \underbrace{\sum_{(b,\alpha), \alpha \in F_b} \kappa_{\alpha}(h) \cdot 1_{v_b(h) < 1} \cdot C_{\alpha} \cdot \frac{\partial v_b(h)}{\partial P_{\dot{g}_{\beta}}(h)}}_{D_2} \end{array} \right. \quad (5.26)$$

and similarly for the reactive DLMP:

$$\pi_{\beta}^Q(h) = \left\{ \begin{array}{l} \underbrace{\pi_{\infty}^Q(h) \cdot \frac{\partial P_{\infty}(h)}{\partial Q_{\dot{g}_{\beta}}(h)}}_{A'} + \underbrace{\frac{\pi_{\infty}^{OC}(h) \cdot Q_{\infty}(h)}{\sqrt{C_{\infty}^2 - Q_{\infty}^2(h)}} \cdot \frac{\partial Q_{\infty}(h)}{\partial Q_{\dot{g}_{\beta}}(h)}}_{B'} + \\ \underbrace{\sum_{h_1 \geq h, (b,b') \in tr} c_{b,b'}^{tr} \cdot \frac{\partial \Gamma_{b,b'}(S_{b,b'}(h_1))}{\partial Q_{\dot{g}_{\beta}}(h)}}_{C'} + \underbrace{\sum_b \mu_b(h) \cdot \frac{\partial v_b(h)}{\partial Q_{\dot{g}_{\beta}}(h)}}_{D'_1} - \\ \underbrace{\sum_{(b,\alpha), \alpha \in F_b} \kappa_{\alpha}(h) \cdot 1_{v_b(h) < 1} \cdot C_{\alpha} \cdot \frac{\partial v_b(h)}{\partial Q_{\dot{g}_{\beta}}(h)}}_{D'_2} \end{array} \right. \quad (5.27)$$

Relations (5.26) and (5.27) are called *DLMP unbundling equations* because they show the components that make up the DLMPs. DLMPs consist of components including substation LMPs, other constraints' shadow prices and dependent variables' sensitivities. In specific, these components are:

- A, A' are the cost of sensitivity of real power flowing into the distribution network at the substation bus with respect to a costless infinitesimal injection of real and reactive power respectively. In particular, A is equal to $\pi_{\infty}^P(h) \cdot \frac{\partial P_{\infty}(h)}{\partial P_{\dot{g}_{\beta}}(h)} = \pi_{\infty}^P(h) \cdot (1 + \frac{P_{losses}(h)}{\partial P_{\dot{g}_{\beta}}(h)})$, which is equivalent to the energy and loss components of LMPs (4.19).

- B, B' are the marginal cost of sensitivity of reactive power of the auxiliary generator at the substation with respect to a costless infinitesimal injection of real and reactive power respectively.
- C, C' are the cost of sensitivity of transformer loss of life with respect to a costless infinitesimal injection of real and reactive power respectively.
- D, D' are:
 1. The sensitivity of the voltage level at each *binding* bus times the relevant Lagrange multiplier
 2. The cost of affecting the maximum reactive power output of capacitors, if their voltage is below 1 per unit.

D_1 and D'_1 are non-zero only when voltage bound constraints are binding. This is similar to the congestion component of the LMPs (4.19) that is non-zero only when the line capacity constraints are binding. We say that binding voltage bound constraints express distribution network congestion, i.e. distribution network congestion is a nodal problem and complement this statement with numerical results in Section 5.5.1.

The intuitive explanation behind the spatial variability of the DLMPs is that an equal injection at a different distribution bus will have different effect on losses, voltage magnitudes and line/ transformer flows. Also, DLMPs of both real and reactive power may be lower or higher than the substation values, since $A, A', B, B' \geq 0$ (with a subtle assumption on $\pi_\infty^P(h) \geq 0$ and $\pi_\infty^{OC}(h) \geq 0$) but $C, C', D_1, D'_1, D_2, D'_2$ can be either positive or negative (Ntakou and Caramanis, 2015).

In order to numerically evaluate the right-hand side of (5.26) and (5.27) one needs to determine the sensitivities of dependent variables, namely $\frac{\partial P_{b,b'}}{\partial P_{\dot{g}_\beta(h)}}$, $\frac{\partial Q_{b,b'}}{\partial P_{\dot{g}_\beta(h)}}$, $\frac{\partial v_b}{\partial P_{\dot{g}_\beta(h)}}$ and $\frac{\partial P_{b,b'}}{\partial Q_{\dot{g}_\beta(h)}}$, $\frac{\partial Q_{b,b'}}{\partial Q_{\dot{g}_\beta(h)}}$, $\frac{\partial v_b}{\partial Q_{\dot{g}_\beta(h)}}$. Taking the derivative of constraints (5.2), (5.3),

(5.4), (5.6), (5.5) and (5.7) we get:

$$\frac{\partial l_{b,b'}}{\partial P_{\dot{g}_\beta(h)}} = \frac{2 \cdot P_{b,b'}}{v_b} \cdot \frac{\partial P_{b,b'}}{\partial P_{\dot{g}_\beta(h)}} + \frac{2 \cdot Q_{b,b'}}{v_b} \cdot \frac{\partial Q_{b,b'}}{\partial P_{\dot{g}_\beta(h)}} - \frac{P_{b,b'}^2 + Q_{b,b'}^2}{v_b^2} \cdot \frac{\partial v_b}{\partial P_{\dot{g}_\beta(h)}} \quad (5.28)$$

$$\frac{\partial v_{b'}}{\partial P_{\dot{g}_\beta(h)}} = \frac{\partial v_b}{\partial P_{\dot{g}_\beta(h)}} - 2 \cdot R_{b,b'} \cdot \frac{\partial P_{b,b'}}{\partial P_{\dot{g}_\beta(h)}} - 2 \cdot X_{b,b'} \cdot \frac{\partial Q_{b,b'}}{\partial P_{\dot{g}_\beta(h)}} + (R_{b,b'}^2 + X_{b,b'}^2) \cdot \frac{\partial l_{b,b'}}{\partial P_{\dot{g}_\beta(h)}} \quad (5.29)$$

$$\sum_{b'} \frac{\partial P_{b,b'}}{\partial P_{\dot{g}_\beta(h)}} = \begin{cases} -1, b = \beta \\ 0, \text{else} \end{cases} \quad (5.30)$$

$$\frac{\partial P_{b,b'}}{\partial P_{\dot{g}_\beta(h)}} + \frac{\partial P_{b',b}}{\partial P_{\dot{g}_\beta(h)}} = R_{b,b'} \cdot \frac{\partial l_{b,b'}}{\partial P_{\dot{g}_\beta(h)}} \quad (5.31)$$

$$\sum_{b'} \frac{\partial Q_{b,b'}}{\partial P_{\dot{g}_\beta(h)}} = 0 \quad (5.32)$$

$$\frac{\partial Q_{b,b'}}{\partial P_{\dot{g}_\beta(h)}} + \frac{\partial Q_{b',b}}{\partial P_{\dot{g}_\beta(h)}} = X_{b,b'} \cdot \frac{\partial l_{b,b'}}{\partial P_{\dot{g}_\beta(h)}} \quad (5.33)$$

We note that while equations (5.29) are technically $2|L| = (2N - 2)$ many, only $|L| = N - 1$ are linearly independent. For the calculation of the sensitivities with respect to an infinitesimal reactive power injection, we can similarly derive the following system of equations:

$$\frac{\partial l_{b,b'}}{\partial Q_{\dot{g}_\beta(h)}} = \frac{2 \cdot P_{b,b'}}{v_b} \cdot \frac{\partial P_{b,b'}}{\partial Q_{\dot{g}_\beta(h)}} + \frac{2 \cdot Q_{b,b'}}{v_b} \cdot \frac{\partial Q_{b,b'}}{\partial Q_{\dot{g}_\beta(h)}} - \frac{P_{b,b'}^2 + Q_{b,b'}^2}{v_b^2} \cdot \frac{\partial v_b}{\partial Q_{\dot{g}_\beta(h)}} \quad (5.34)$$

$$\frac{\partial v_{b'}}{\partial Q_{\dot{g}_\beta(h)}} = \frac{\partial v_b}{\partial Q_{\dot{g}_\beta(h)}} - 2 \cdot R_{b,b'} \cdot \frac{\partial P_{b,b'}}{\partial Q_{\dot{g}_\beta(h)}} - 2 \cdot X_{b,b'} \cdot \frac{\partial Q_{b,b'}}{\partial Q_{\dot{g}_\beta(h)}} + (R_{b,b'}^2 + X_{b,b'}^2) \cdot \frac{\partial l_{b,b'}}{\partial Q_{\dot{g}_\beta(h)}} \quad (5.35)$$

$$\sum_{b'} \frac{\partial P_{b,b'}}{\partial Q_{\dot{g}_\beta(h)}} = 0 \quad (5.36)$$

$$\frac{\partial P_{b,b'}}{\partial Q_{\dot{g}_\beta(h)}} + \frac{\partial P_{b',b}}{\partial Q_{\dot{g}_\beta(h)}} = R_{b,b'} \cdot \frac{\partial l_{b,b'}}{\partial Q_{\dot{g}_\beta(h)}} \quad (5.37)$$

$$\sum_{b'} \frac{\partial Q_{b,b'}}{\partial Q_{\dot{g}_\beta(h)}} = \begin{cases} -1, b = \beta \\ 0, \text{else} \end{cases} \quad (5.38)$$

$$\frac{\partial Q_{b,b'}}{\partial Q_{\dot{g}_\beta(h)}} + \frac{\partial Q_{b',b}}{\partial Q_{\dot{g}_\beta(h)}} = X_{b,b'} \cdot \frac{\partial l_{b,b'}}{\partial Q_{\dot{g}_\beta(h)}} \quad (5.39)$$

5.4 Centralized Solution Feasibility

5.4.1 Uniqueness of Solution

As discussed in 2.2.2, relaxed branch load flow constraints are an exact reformulation of the full AC load flow constraints. The constraint set remains not convex, because of the quadratic equality constraints $l_{b,b'} = \frac{P_{b,b'}^2 + Q_{b,b'}^2}{v_b}$.

(Chiang and Baran, 1990) proves that the solution to a power flow problem with full AC load flow equations is unique, given (i) reasonable voltage bounds and (ii) radial network topology.

Although our problem is an optimal power flow problem with additional complexity, our computational experience appears to be consistent with a unique solution.

5.4.2 Existence of Solution

(Chiang and Baran, 1990) makes the assumption of reasonable voltage bounds, of the order of +/- 10%, constraining the power flow problem. While these constraints are characterized as necessary to obtain a unique solution for a power flow problem, they are not sufficient. In other words, these constraints guarantee at most one solution.

Although we model a slack bus that can provide real and reactive power as needed, it is possible that this is not enough to sustain system voltages within their bounds. In such an instance, the optimal power flow problem will be infeasible.

5.4.3 Centralized Algorithm modeling Voltage Bound Constraints with a Barrier Function

Since we identified the voltage bounds constraints as the only last source of infeasibility, in order to ensure feasibility we replace hard voltage bound constraints of the

type of (5.8) with soft constraints, namely voltage-related barrier functions in the objective function.

The hard voltage bound constraints are equivalent to penalty terms like $f(v_b(h)) = H(\underline{v} - v_b(h)) + H(v_b(h) - \bar{v})$, where H is the Heaviside function. Since these constraints are non-differentiable, we use constraints of the type $f(v_b(h)) = k_{6,b} \cdot (\exp(k_{7,b} \cdot (v_b(h) - \bar{v})) + \exp(k_{8,b} \cdot (\underline{v} - v_b(h))))$. We tune k_6 to control the contribution of this term to the objective function. In fine tuning parameters k_7, k_8 , we choose $k_7 \gg$ and $k_8 \gg$ for the resulting curve to be as close to a square wave as is practical. Such a choice of large enough k_7, k_8 will also ensure that the voltages of the new optimal solution will be close to the original optimal solution.¹ With this alteration, the centralized market clearing problem becomes:

C-SVC: Centralized formulation with soft voltage bound constraints

minimize (5.1) + $\sum_{b,h} k_{6,b} \cdot (\exp(k_{7,b} \cdot (v_b(h) - \bar{v})) + \exp(k_{8,b} \cdot (\underline{v} - v_b(h))))$

subject to (5.2)-(5.7) and (5.9)-(5.17)

We note that when adjusting the parameters in the voltage barrier functions, there is a trade-off relationship between reaching the original voltages and deviating from the original DLMPs. This is because large parameters ensure a box-like shape of the barrier function and therefore a closer distance from the original voltages, but they also magnify the voltage component of the DLMPs leading to higher DLMPs in the presence of soft voltage bound constraints than the original DLMPs with hard voltage bound constraints. Specifically, we derive below the unbundling of the DLMPs

¹Another way to model soft voltage bound constraints is with quadratic functions of the form of $k_9 \cdot 1_{v_b \geq \bar{v}} \cdot (v - \bar{v})^2 + k_{10} \cdot 1_{v_b \leq \underline{v}} \cdot (v - \underline{v})^2$. We proceed with the use of exponential functions since they are convex.

obtained as shadow prices of the power balance constraints of C-SVC.

$$\pi_{\beta}^{P,SVC}(h) = \begin{cases} \pi_{\infty}^P(h) \cdot \frac{\partial P_{\infty}(h)}{\partial P_{\dot{g}_{\beta}(h)}} + \frac{\pi_{\infty}^{QC}(h) \cdot Q_{\infty}(h)}{\sqrt{C_{\infty}^2 - Q_{\infty}^2(h)}} \cdot \frac{\partial Q_{\infty}(h)}{\partial P_{\dot{g}_{\beta}(h)}} + \\ \sum_{h_1 \geq h, (b,b') \in tr} c_{b,b'}^{tr} \cdot \frac{\partial \Gamma_{b,b'}(S_{b,b'}(h_1))}{\partial P_{\dot{g}_{\beta}(h)}} + \\ \sum_b k_{6,b} \cdot k_{7,b} \cdot \exp(k_{7,b} \cdot (v_b(h) - \bar{v})) \cdot \frac{\partial v_b(h)}{\partial P_{\dot{g}_{\beta}(h)}} - \\ \sum_b k_{6,b} \cdot k_{8,b} \cdot \exp(k_{8,b} \cdot (\underline{v} - v_b(h))) \cdot \frac{\partial v_b(h)}{\partial P_{\dot{g}_{\beta}(h)}} - \\ \sum_{(b,\alpha), \alpha \in F_b} \kappa_{\alpha}(h) \cdot 1_{v_b(h) < 1} \cdot C_{\alpha} \cdot \frac{\partial v_b(h)}{\partial P_{\dot{g}_{\beta}(h)}} \end{cases} \quad (5.40)$$

$$\pi_{\beta}^{Q,SVC}(h) = \begin{cases} \pi_{\infty}^P(h) \cdot \frac{\partial P_{\infty}(h)}{\partial Q_{\dot{g}_{\beta}(h)}} + \frac{\pi_{\infty}^{QC}(h) \cdot Q_{\infty}(h)}{\sqrt{C_{\infty}^2 - Q_{\infty}^2(h)}} \cdot \frac{\partial Q_{\infty}(h)}{\partial Q_{\dot{g}_{\beta}(h)}} + \\ \sum_{h_1 \geq h, (b,b') \in tr} c_{b,b'}^{tr} \cdot \frac{\partial \Gamma_{b,b'}(S_{b,b'}(h_1))}{\partial Q_{\dot{g}_{\beta}(h)}} + \\ \sum_b k_{6,b} \cdot k_{7,b} \cdot \exp(k_{7,b} \cdot (v_b(h) - \bar{v})) \cdot \frac{\partial v_b(h)}{\partial Q_{\dot{g}_{\beta}(h)}} - \\ \sum_b k_{6,b} \cdot k_{8,b} \cdot \exp(k_{8,b} \cdot (\underline{v} - v_b(h))) \cdot \frac{\partial v_b(h)}{\partial Q_{\dot{g}_{\beta}(h)}} - \\ \sum_{(b,\alpha), \alpha \in F_b} \kappa_{\alpha}(h) \cdot 1_{v_b(h) < 1} \cdot C_{\alpha} \cdot \frac{\partial v_b(h)}{\partial Q_{\dot{g}_{\beta}(h)}} \end{cases} \quad (5.41)$$

The sensitivities $\frac{\partial P_{b,b'}}{\partial P_{\dot{g}_{\beta}(h)}}$, $\frac{\partial Q_{b,b'}}{\partial P_{\dot{g}_{\beta}(h)}}$, $\frac{\partial v_b}{\partial P_{\dot{g}_{\beta}(h)}}$, $\frac{\partial P_{b,b'}}{\partial Q_{\dot{g}_{\beta}(h)}}$, $\frac{\partial Q_{b,b'}}{\partial Q_{\dot{g}_{\beta}(h)}}$, and $\frac{\partial v_b}{\partial Q_{\dot{g}_{\beta}(h)}}$ can be calculated as in the original problem with hard voltage bound constraints.

5.5 Numerical Results

For all the numerical results shown below, we use the AIMMS Optimization software. AIMMS provides us with the (locally) optimal primal and corresponding optimal dual solution.

5.5.1 Un-congested Distribution Network

In this section, we provide numerical results we obtained on a realistic 800 bus distribution feeder, whose specifications can be found in Appendix A. The results that follow use $w = 0$ as the relevant parameter in constraint (5.10).

Figure 5.1 shows the spread of the real power Distribution Locational Marginal Prices (DLMPs) by means of hourly minimum and maximum real power DLMP and the substation real power LMP, while Figure 5.2 shows the minimum, maximum and substation reactive power DLMP. The minimum DLMP can be seen to drop below the substation value for both real and reactive power. The maximum DLMP spikes during certain hours when transformer overloading occurs.

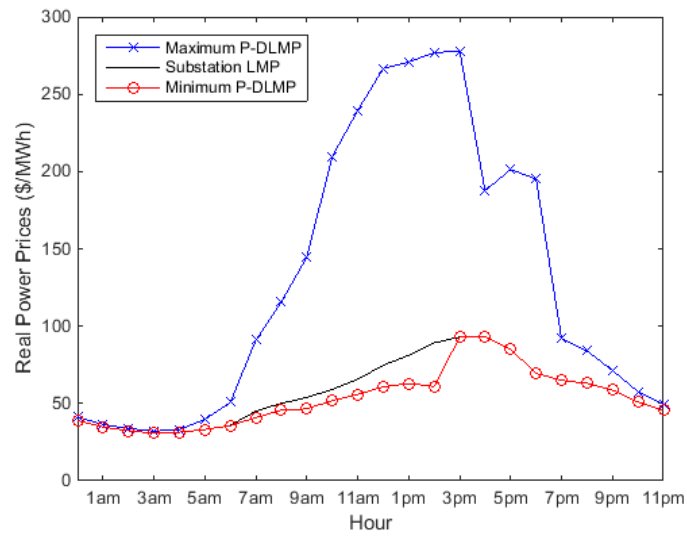


Figure 5.1: Hourly minimum, maximum and substation value of real power DLMP

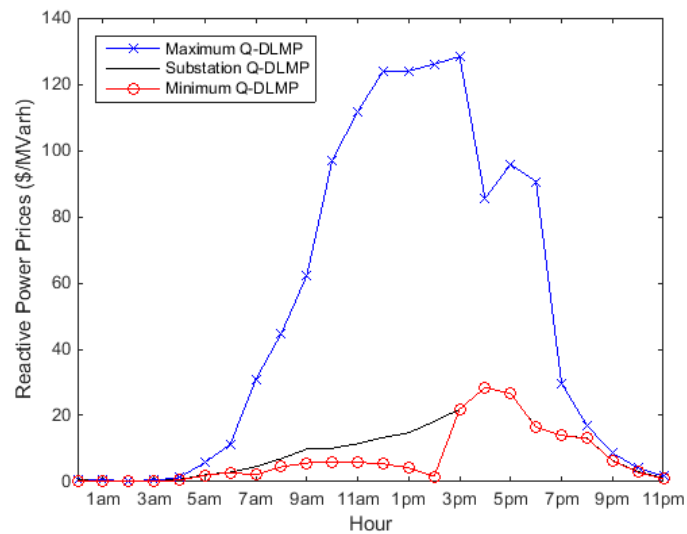


Figure 5.2: Hourly minimum, maximum and substation value of reactive power DLMP

Figures 5.3 and 5.4 show the components of real and reactive DLMPs at two interesting buses in the network. The results indicate that the transformer component as well as the voltage component can turn out to be significant contributors to marginal costs.

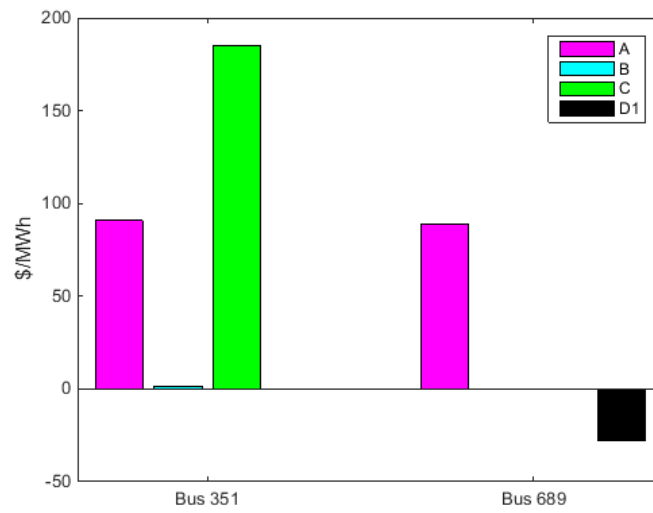


Figure 5-3: Real power DLMP components at selected buses 351 and 689 (see equation 5.26 for explanation of each component)

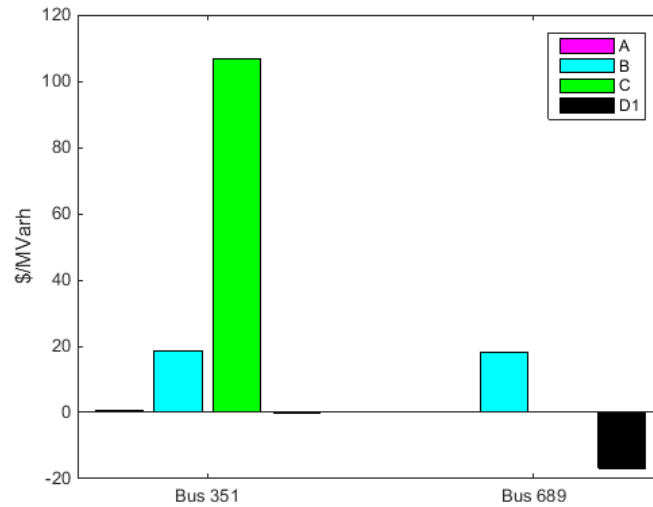


Figure 5-4: Reactive power DLMP components at selected buses 351 and 689 (see equations 5.27 for explanation of each component)

Our simulations have also revealed how congestion expresses itself in distribution networks. While in transmission networks, congestion refers to lines loaded to their capacity, in distribution networks congestion is a nodal problem because it refers to

voltage bound constraints binding (either above or below).

From a market perspective, transmission network congestion is a problem because it can increase operational costs when cheap resources generate below their capacity because all lines out of them are congested. The same can happen in a distribution power market. As our simulations reveal, PVs, whose variable costs are zero, provide below their capacity if the voltage magnitude at their connection bus binds from above.

Figure 5-5 below contributes to the argument that binding voltage bound constraints express distribution network congestion. In particular, we report the substation voltage versus the solar irradiation per hour. Since higher voltages mean lower losses, we would expect the only voltage that is a decision variable, i.e. the substation voltage, to be at the upper limit at all times. Contrary to that, we see that when irradiation is high, the substation voltage drops below the upper limit. Combined with Figure 5-6 that shows the maximum voltage among buses with photovoltaics, we conclude that during high irradiation hours, the substation voltage drops so that the voltage at buses with PVs can reach the upper bound, allowing PVs to produce as close to their capacity as they can. We note that Figures 5-5 and 5-6 only show the hours with non-zero irradiation.

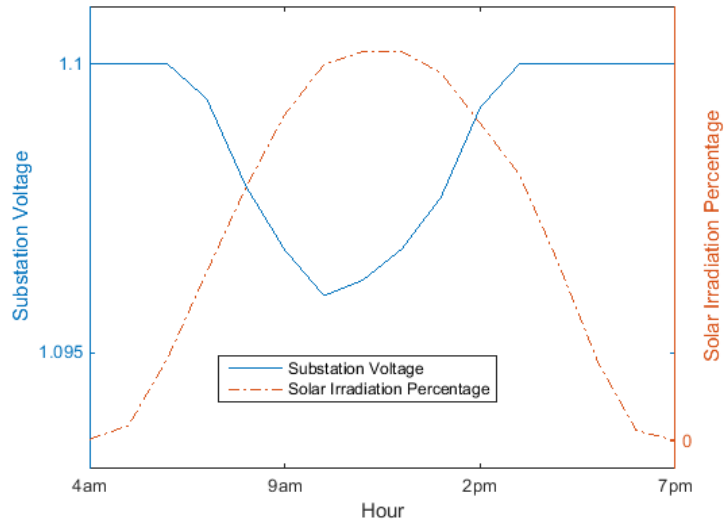


Figure 5-5: Hourly substation voltage versus solar irradiation percentage

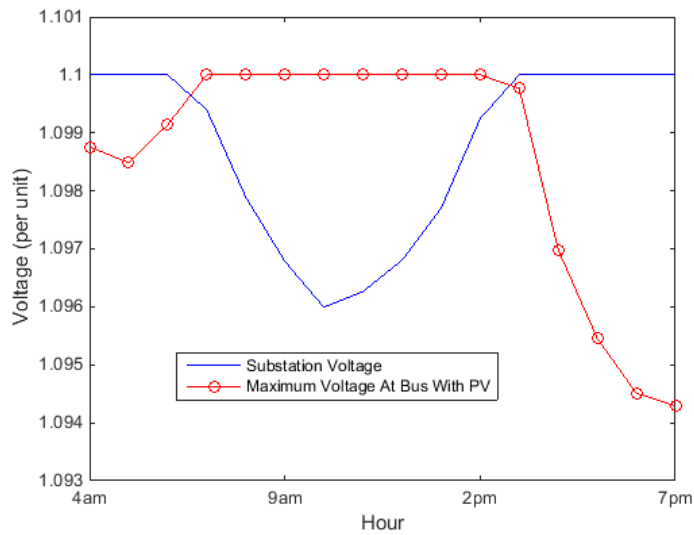


Figure 5-6: Hourly substation voltage and maximum PV voltage

5.5.2 Benefits of Distribution Network Price Granularity

Below, we discuss the network and economic benefits of the proposed granular spatiotemporal prices relative to today's flat prices. The goal of this section is to show

the benefits of time and locational incentives. To this end, we compare the following pricing schemes:

1. Flat prices: constant price for all buses and all hours
2. Spatiotemporally varying prices (DLMPs) obtained through the proposed distribution power market.

For the results that follow, we incorporate the voltage sensitivity part of the fixed loads (see constraint (5.10)) by using $\check{v} = 0.96, w = 1$.

Under flat prices, electric vehicles start charging upon connection. An important conclusion is that in the absence of locational incentives DERs are not appropriately guided/ incentivized on how to provide reactive power. This is because a spatially constant price does away with the effects of the network topology on the prices, i.e. line losses and voltage magnitudes. Therefore, the DERs do not see voltage drops or rises and as such, see no use in reactive power provision. This means that in our simulations of the 800 bus network under flat prices, PVs will be providing the maximum real power allowed by the solar irradiation at all hours and no reactive power and EVs will be charging upon connection and will also not provide reactive power.

Figure 5-7 shows the average voltage over all buses with voltage sensitive loads, with DLMPs and flat prices. For the on peak hours, the DLMP market can attain an average voltage across all load buses that is closer to \check{v} than flat prices can. The latter, lacks DER scheduling flexibility and has the substation voltage as the single decision variable to decrease costs. Therefore, it cannot maintain voltages within limits without raising voltages at load buses to be much higher than \check{v} .

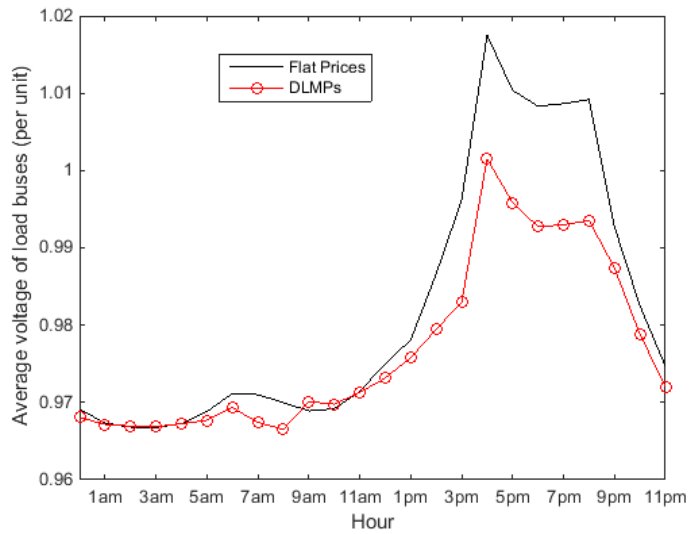


Figure 5-7: Comparison of the average voltage at load buses under flat prices and DLMPs.

Figure 5-8 reports on the ex-post net cost of all distribution participants. This is the payments minus receipts for consuming and providing, respectively, both real and reactive power. The benefit is about 17%.

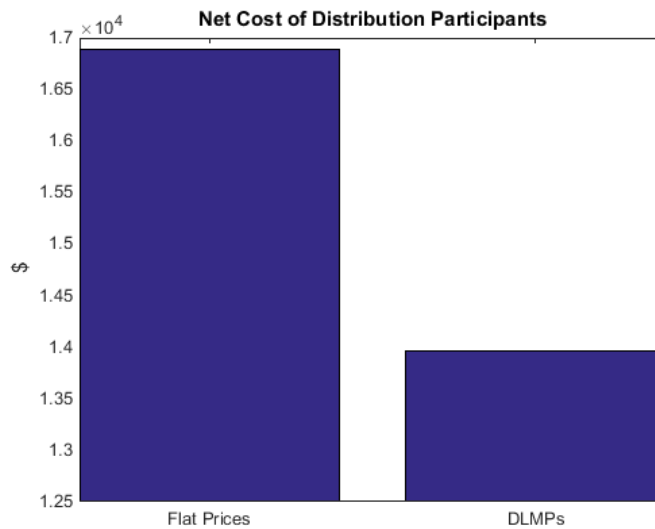


Figure 5-8: Comparison of Net Cost of Distribution Participants under flat prices and DLMPs.

The following two figures show the costs that price responsive loads incur with spatiotemporal prices versus flat prices. Figure 5-9 shows the costs of electric vehicles that appear to be decreasing by approximately 58%. Under flat prices, electric vehicles charge upon connection, not taking advantage of the lowest cost hours, and do not provide reactive power, which explains the large cost decrease electric vehicles realize under DLMPs.

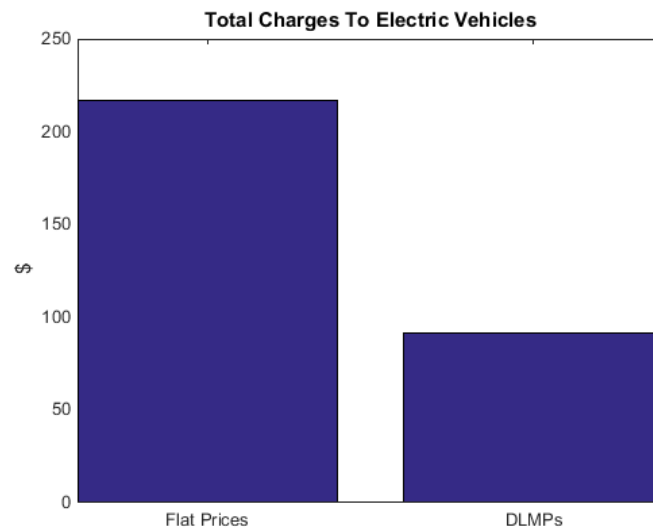


Figure 5-9: Comparison of electric vehicle (net) costs under flat prices and DLMPs.

Figure 5-10 shows the cost savings of space conditioning that are about 38%.

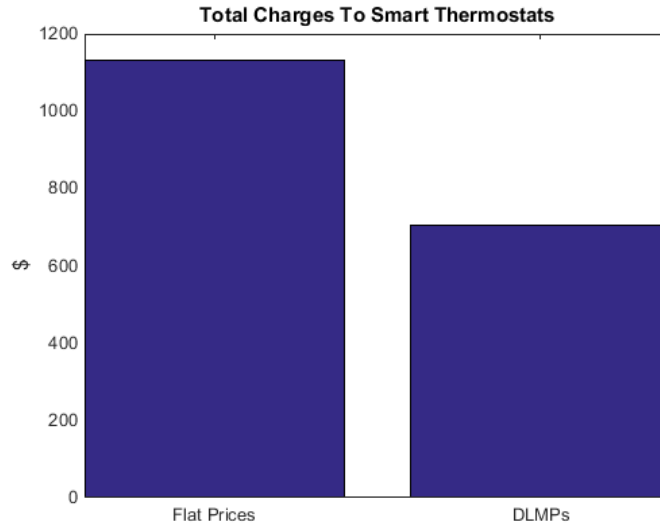


Figure 5·10: Comparison of space conditioning costs under flat prices and DLMPs.

Figures 5·11 and 5·12 elaborate on the sub-optimality of flat prices, by concentrating at bus 383, where the smart thermostat of the largest capacity is located. Figure 5·11 shows the ex-post marginal cost of real power at that bus and the consumption of the smart thermostat located at this bus, under flat pricing, while Figure 5·12 shows the same measures as they are decided in a spatiotemporal distribution power market setting. While the evolution of costs and consumption are almost inverse for the market case, with zero consumption during cost peaks, the evolution is actually about analogous when using flat prices. Consuming more as prices rise and less as prices drop is an undesirable behavior and a clear indicator of the suboptimality of fixed rate pricing.

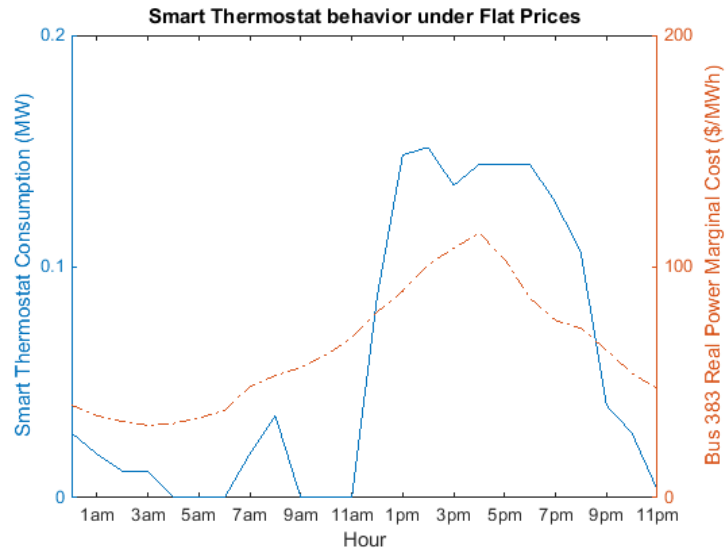


Figure 5-11: 24-hour trajectory of real power DLMP and smart thermostat consumption at bus 383 under flat prices.

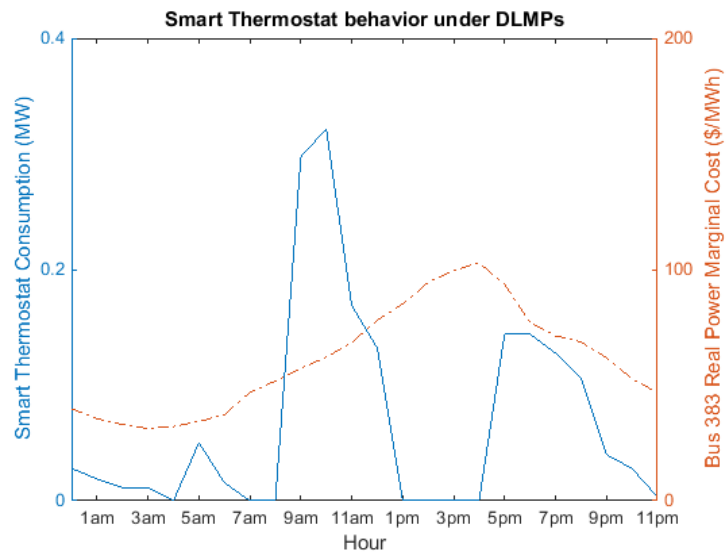


Figure 5-12: 24-hour trajectory of real power DLMP and smart thermostat consumption at bus 383 under DLMPs.

Figure 5-13 focuses on the net payments of fixed loads and depicts a very interesting conclusion: price inelastic loads will also benefit from the implementation of a spatiotemporal distribution market. Specifically, the costs of fixed loads will

drop by about 14%. The DLMP market has the flexibility to adjust all price responsive distribution participants' schedules to achieve the optimal primal solution, which corresponds to the optimal dual solution. Therefore, although the real and reactive output of the fixed loads remains unchanged, the charges they incur decrease because of the discovery of optimal marginal costs.

Figures 5-14 and 5-15 show exactly that effect on the ex-post marginal costs. Figure 5-14 contrasts the maximum real power DLMP across the distribution feeder with the maximum ex- post marginal costs of real power under flat prices, while Figure 5-15 does the same for reactive power. The absence of time and location specific information to the DERs and the resulting sub-optimal outputs of DERs, lead to shadow prices that vary greatly from the optimal result of the DLMP market. In other words, under spatiotemporal prices, the spikes of marginal costs in both real and reactive power are avoided. Notice how these spikes coincide time-wise with the spikes of the market-based DLMPs but are much larger in magnitude. The reason for these spikes is again the transformer overloading, which is more excessive under flat prices.

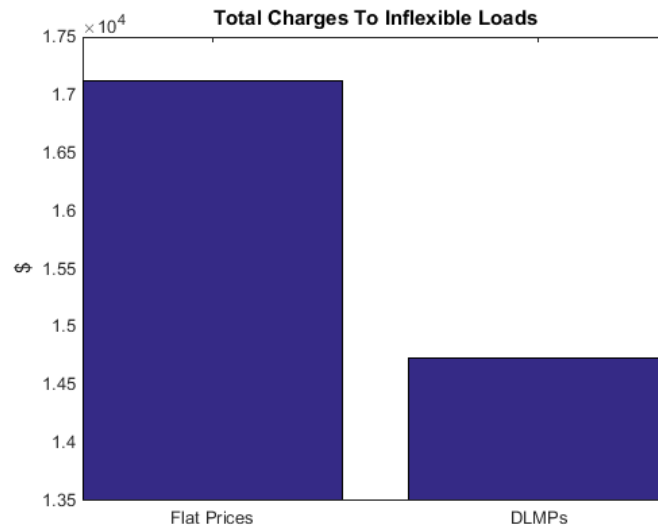


Figure 5-13: Comparison of inflexible loads costs under flat prices and DLMPs.

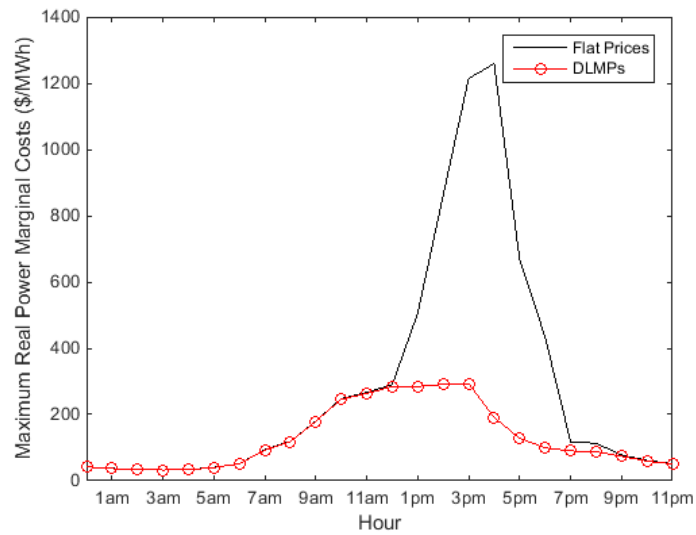


Figure 5-14: Comparison of the hourly maximum real power DLMP and the real power ex-post marginal costs under flat prices.

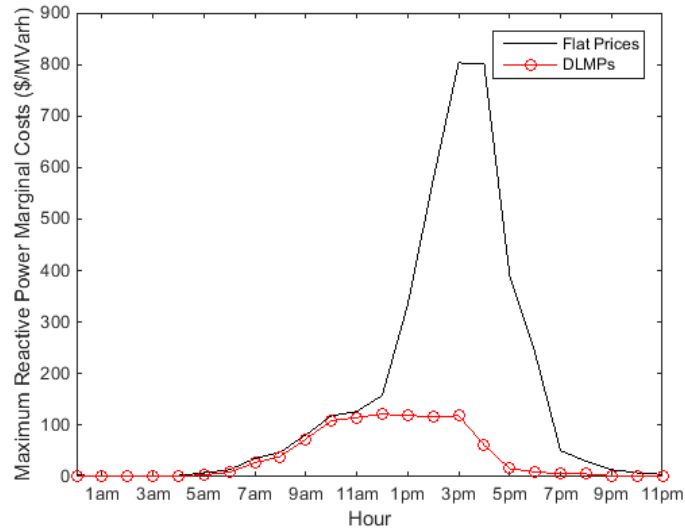


Figure 5.15: Comparison of the hourly maximum reactive power DLMP and the reactive power ex-post marginal costs under flat prices.

5.5.3 Congested Distribution Networks

For this section, we switch to the 47-bus congested distribution network. The results that follow aim at showing the closeness of the solution obtained by the centralized problem with soft voltage bound constraints, C-SVC, as compared to the centralized problem with hard voltage bound constraints, C-OPT. Figure 5.16 does so by means of illustrating the total cost for real power service paid by the curtailable loads, while Figure 5.17 shows the voltage magnitudes at all load buses.

In C-SVC voltages are at most 0.04% away from their true optimal values in C-OPT. Real power DLMPs of C-SVC differ about 1-2% from the real power DLMPs of C-OPT. This difference is much smaller than the effect of binding voltages on DLMPs. Specifically, we quantify the effect of binding voltages by decreasing the voltage lower bound \underline{v} enough for it to no longer bind. We notice that by doing so real power DLMPs are decreased by as much as 15%.

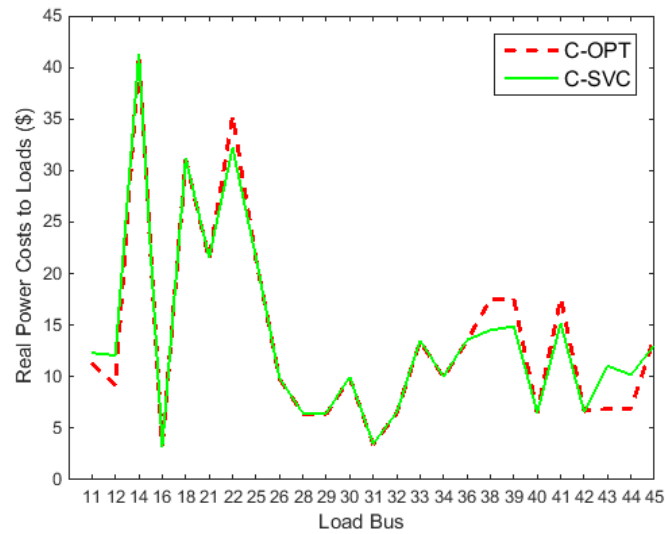


Figure 5-16: Comparison of Real Power Costs to Curtailable Loads in the presence of hard voltage bound constraints (C-OPT) and soft voltage bound constraints (C-SVC).

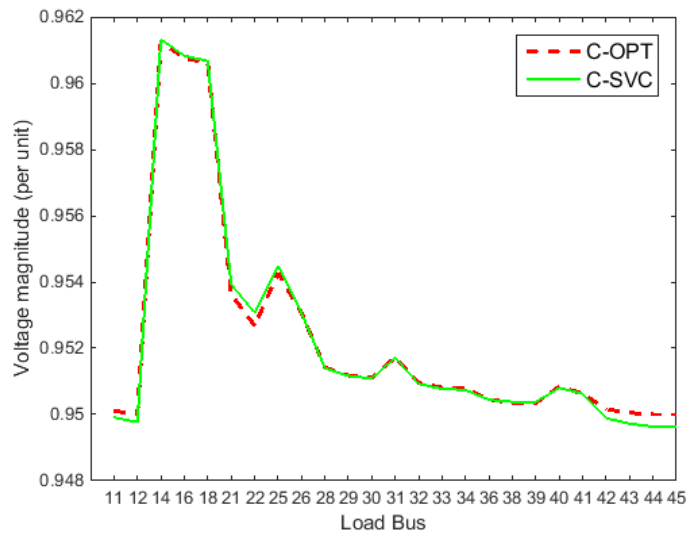


Figure 5-17: Comparison of voltage magnitudes of load buses in the presence of hard voltage bound constraints (C-OPT) and soft voltage bound constraints (C-SVC).

5.6 Computational Effort

The basic contributors to computational complexity of the centralized distribution market clearing algorithm are:

1. Market participants order in the hundreds of thousands
2. Distribution market participants' capabilities are complex and time-coupled (eg. electric vehicles, smart thermostats)
3. The optimal power flow problem is not constrained over a convex set, because of the non-convex power flow equations. Specifically, the non-convex constraint is the line current constraint (5.2) that is a quadratic equality constraint.

The number of variables grows proportionally to the network size as well as with the number of market participants, therefore the centralized market clearing algorithm can easily be seen to become intractable for real-size distribution networks. AC OPF problems are generally known to be NP hard to solve. The literature has dealt with this issue with two main approaches:

- Approximations of the AC load flow constraints that convexify the problem. Several approximations have been proposed over the years, the most popular being the B-theta model shown in Chapter 2. More recently, (Li et al., 2012a) proposed replacing the quadratic equality constraint with inequalities, yielding $l_{b,b'} \geq \frac{P_{b,b'}^2 + Q_{b,b'}^2}{v_b}$ and investigated when the relaxation is exact.
- Decomposition approaches (see Chapter 6 for more details)

Since in the distribution power market clearing problem it is not only the AC load flow constraints, but also the numerous and complex DER dynamics constraints, that contribute to the high computational burden, decomposition approaches are more

relevant to the problem that this thesis addresses. Therefore, the thesis continues with the presentation and implementation of distributed algorithms.

Chapter 6

Distributed Algorithms for Distribution Day-Ahead Power Market Clearing

The AC OPF problem aims at minimizing a certain objective (generator scheduling to minimize generation costs, or minimize losses etc) subject to AC power flow constraints, power balance constraints and voltage bound constraints. For scheduling type of AC OPF problems, as is the case for example in power market problems, additional constraints are needed (generator capacity constraints, DER dynamics etc).

The AC OPF problem is generally known to be NP hard to solve. This is due to the quadratic equality constraints that describe the line current 5.2. The computational burden is further exacerbated in the case of a problem like the centralized distribution power market clearing problem seen in Chapter 5, that, in addition to the AC load flow relationships, includes other complex constraints as well, like the intertemporal DER dynamics and the intertemporal transformer hottest spot temperature relationships.

The literature has proposed several approximations of the AC load flow constraints that convexify the problem, the most popular being the B-theta model shown in Chapter 2. More recently, (Li et al., 2012a) and (Farivar and Low, 2013) proposed replacing the quadratic equality constraint with inequalities, yielding $l_{b,b'} \geq \frac{P_{b,b'}^2 + Q_{b,b'}^2}{v_b}$ and investigated when the relaxation is exact.

The dual of the AC OPF problem has also received lots of attention in the literature. Active research reported in the literature is looking into solving the dual

of the AC OPF problem instead of the AC OPF problem itself. The dual problem is preferable because it is convex. (Lavaei and Low, 2012) and (Molzahn, 2013) examine the resulting duality gap based, amongst others, on the network topology (radial or meshed) so as to decide how close is the optimal objective function value of the dual problem to the optimal objective function value of the AC OPF (primal) problem. (Lavaei and Low, 2012) proves certain conditions as sufficient to guarantee zero duality gap (like oversatisfaction of load), but shows through simulation results that many more instances, not satisfying the sufficient conditions, have zero duality gap. (Molzahn, 2013), on the other hand, simulates instances where the duality gap is non-zero (when line capacities are low, or when shadow prices of power balance constraints of original OPF problem (i.e. nodal marginal prices) are negative).

Other researchers are trying to deal with the computational burden of OPF problems through decomposition. This is more relevant to the types of problems in this thesis since as mentioned above the computational burden of a distribution power market problem is not only caused by the AC load flow constraints but by other complex constraints too.

For OPF problems, the objective function is typically separable. For example, for loss minimization problems the objective function is the sum of line specific terms. For an economic dispatch problem, the objective function is the sum of bid-based components specific to each competing entity. However, the presence of nodal equality and inequality constraints renders the OPF problem overall non-separable.

For transmission OPF problems, the coupling nodal constraints are equality constraints: real power balance 2.25 and real power flow constraints 2.27. For distribution OPF problems, as is the distribution day-ahead power market clearing problem of Chapter 5, nodal coupling constraints are equality and inequality. Coupling equality constraints consist of real power balance constraints 5.4, reactive power balance

constraints 5.5 and voltage drop constraints 5.3. Voltage magnitude bound inequality constraints 5.8 are the coupling inequality constraints.

Constraints that contain nodal as well as line-specific variables, like 2.27 and 5.3, are not only coupling but also imply another equality constraint of consistency, that is implicit in the centralized OPF formulation. Constraints of the type of 2.27 imply voltage angle consistency, i.e. that all transmission lines going in and out of the same bus have the same angle at their ends. Constraints of the type 5.3, imply voltage magnitude consistency, meaning that that all distribution lines going in and out of the same bus have the same voltage at their ends.

The literature has studied relaxations of the coupling equality constraints to enable the decomposition of the OPF problem. We proceed with an overview of the methods used so far in the literature to distribute the computation of the OPF problem. A very high level description of the OPF problem that aims at capturing the decomposable nature of the objective function versus the coupling nature of the constraints of interest follows:

$$\begin{aligned} & \underset{x=[x_k]}{\text{minimize}} \sum_k f_k(x_k) \\ & \text{subject to } Ax = b \rightarrow \lambda \\ & \quad \quad \quad x_k \in X_k \end{aligned}$$

where we use x to collectively refer to primal variables of the OPF problem and λ to refer to the dual variables of the coupling constraints of the OPF problem.

Lagrangian-based methods have been employed, with a plethora of past work employing dual decomposition. The lagrangian of the above OPF problem is written as:

$$\mathcal{L} = \sum_k f_k(x_k) + \lambda \cdot (Ax - b) = \sum_k (f_k(x_k) + \lambda \cdot A_k \cdot x_k) - \lambda \cdot b$$

The decomposition to subproblems and the dual decomposition steps are straightforward:

- Primal variable update step $x_k^{i+1} = \operatorname{argmin}_{x_k \in X_k} f_k(x_k) + \lambda^i \cdot A_k \cdot x_k$. These individual problems can be solved in parallel.
- Dual variable update step $\lambda^{i+1} = \lambda^i + s^i \cdot (A \cdot x^{i+1} - b)$

The stepsize s^i needs to be properly adjusted to avoid oscillations (see (Bertsekas and Tsitsiklis, 1989)). Still, dual decomposition requires strict technical conditions for convergence, which motivated the use of other methods. Augmented Lagrangian based methods require looser technical conditions for convergence. The augmented Lagrangian is written as:

$$\mathcal{L} = \sum_k f_k(x_k) + \lambda \cdot (Ax - b) + \frac{\rho}{2} \cdot \|Ax - b\|_2^2$$

The quadratic augmentation terms $\frac{1}{2}\|Ax - b\|_2^2$, multiplied by the penalty ρ robustify convergence, but also destroy the straightforward splitting to subproblems that the lagrangian methods, like dual decomposition offer.

In order to enable the decomposition of the augmented Lagrangian, several past methods proposed minimizing over one variable while keeping all of the variables tentatively fixed. This resulted in the following process:

- Primal variable update step:

$$x_k^{i+1} = \operatorname{argmin}_{x_k \in X_k} f_k(x_k) + \lambda^i \cdot A_k \cdot x_k + \frac{\rho}{2} \cdot \left\| + \sum_{m \leq k} A_m x_m^{k+1} + A_k x_k + \sum_{m \geq k} A_m x_m^k - b \right\|_2^2. \text{ This is obviously separable, but results in a sequential method.}$$

- Dual variable update step $\lambda^{i+1} = \lambda^i + \rho \cdot (A \cdot x^{i+1} - b)$

Recently, the Alternating Direction Method of Multipliers (ADMM) provided a way to end up with parallelizable individual subproblems. (Boyd et al., 2011) shows

how ADMM can be applied to a multitude of optimization problems, including OPF problems. ADMM starts from the augmented Lagrangian and through the use of local and global copies of variables, bridges the decomposability of dual decomposition methods with the robustness of augmented Lagrangian methods. We refer the interested reader to (Kraning et al., 2014), (Bertsekas and Tsitsiklis, 1989) and (Ntakou and Caramanis, 2014) for the math leading to the steps of the ADMM for the simplistic OPF problem that follow below:

- Primal variable update step $x_k^{i+1} = \underset{x_k \in X_k}{\operatorname{argmin}} f_k(x_k) + \lambda^i \cdot A_k \cdot x_k + \frac{\rho}{2} \cdot \|A_k x_k - A_k x_k^i + \hat{x}^i\|_2^2$, where $\hat{x}^i = \frac{Ax^i - b}{N}$. \hat{x}^i can be thought of as the imbalance in satisfying the coupling constraint. These individual problems are fully parallelizable.
- Dual variable update step $\lambda^{i+1} = \lambda^i + \rho \cdot \hat{x}_k^{i+1}$

The quadratic augmentation terms offer robustness and help in oscillation avoidance in the calculation of the primal variables. They converge to zero.

The following guarantees hold for ADMM:

1. Upon convergence, the optimal objective function value is found.
2. Upon convergence, the optimal dual variables are found $\lim_{i \rightarrow \infty} \lambda^i \rightarrow \lambda^*$.
3. Upon convergence, the relaxed constraints hold, $\lim_{i \rightarrow \infty} \hat{x}^i \rightarrow 0$.

We now focus on interpreting the subproblems. For the case of dual decomposition, the update steps shown above can be described in words as:

- Each subproblem $x_k^{i+1} = \underset{x_k \in X_k}{\operatorname{argmin}} f_k(x_k) + \lambda^i \cdot A_k \cdot x_k$ is solved in parallel to update primal variable x_k while the dual variable λ is fixed.
- The dual variable is updated based on the violation of the relaxed constraint $Ax = b$, given the tentative x_k^{i+1} .

For an OPF problem, real power balance constraints are among the coupling constraints that are relaxed to enable the decomposition. Section 5.3 discussed that, for a power market problem, the dual variables of the power balance constraints are the locational marginal prices. As in all spot markets, this is the price that a market participant connected to this bus would pay to receive or gets paid to provide real or reactive power respectively. Therefore, the individual subproblems have an interesting power market interpretation.

The dual variables λ_i are referred to as price estimates since they converge to the nodal prices. It can easily be seen that the objective of participant k who solves the problem of deciding x_k^{i+1} is the minimization of all the costs that the participant incurs: personal costs $f_k(x_k)$ (e.g., transformer loss of life or uncharged EV battery costs) and payments/ remuneration based on the nodal price estimates $\lambda^i \cdot A_k \cdot x_k$.

This instructive interpretation is extended to the subproblems resulting from the augmented Lagrangian based decompositions like ADMM. An augmented Lagrangian, as the one used in ADMM, includes the terms in the simple Lagrangian plus quadratic terms of the relaxed constraints. The role of these constraints is to provide robustness and they converge to zero. Therefore, the interpretation of the subproblems used in ADMM is the same as the interpretation of dual decomposition subproblems: subproblems minimize all the costs that a participant incurs: personal costs (e.g., transformer loss of life or uncharged EV battery costs) and payments/ remuneration based on the nodal price estimates.

(Peng and Low, 2015), (Kraning et al., 2014) and (Chakrabarti et al., 2014) solve OPF problems using ADMM to relax relevant coupling equality constraints and enable the problem splitting.

(Peng and Low, 2015) refers to distribution networks and as such the information passing assumes a tree topology by requiring a unique ancestor for each bus. The

primal variables are the net injection at each bus, the line flows and the voltage magnitudes. Equality coupling constraints 5.4, 5.5, 5.3 are relaxed through ADMM to enable the decomposition of the original problem to bus specific subproblems. Coupling inequality constraints 5.8 remain hard constraints but are now made local to each bus subproblem. In each subproblem, the bus decides its voltage, its net injection and the flow on the unique line from its parent (direct upstream bus) based on tentative values it has received for the voltage of its parent as well as for the flows on the lines that connect it to its children (directly connected downstream buses). The flows on the lines that connect it to its children are decided in the subproblems solved by the children buses with similar logic. The dual variable update step calculates the dual variable of the relaxed constraints (nodal power balance and voltage coupling constraints) and involves the calculation of \hat{x}^i , the imbalance in satisfying the coupling constraints based on the tentative individual bus decisions.

(Kraning et al., 2014) and (Chakrabarti et al., 2014) use ADMM to solve scheduling OPF problems for transmission networks in a distributed fashion. The primal variables are the injections of each device (e.g., generator), the line flows and the voltage angles. The additional constraints of each device that should be scheduled (e.g., generator capacity constraints) dictate the splitting of the original problem below the bus level to individual device subproblems. In this context, local communication is defined as communication between the a bus and its connected devices. However the equality coupling constraints for real power balance 2.25 and real power flow 2.27, couple decisions at the bus level. Relaxing 2.25 and the voltage angle consistency constraints, allows for network resources that connect buses to each other (e.g., lines and transformers) to also solve individual subproblems. This is equivalent to distributing the load flow to line specific subproblems. Coupling equality constraints 2.27 are now local to each line subproblem. Device specific subproblems

decide on their output based on messages they have received on the output decisions of other devices or lines/ transformers connected to the same bus. Lines/transformers decide the injection (or withdrawal) at the sending end and withdrawal (or injection) at the receiving end based on the tentative outputs of the devices and other lines/ transformers connected to both ends. All of these subproblems are solved in parallel. Buses calculate the imbalance \hat{x}^i and perform the dual variable update step.

The first distributed algorithm proposed in this thesis to decompose the centralized power market problem shown in Chapter 5 falls under the category of OPF problems split to device subproblems using ADMM to relax coupling equality relationships. We will heretofore refer to this algorithm as Fully Distributed Algorithm or FDA. By relaxing real and reactive power balance (equality coupling) constraints and voltage magnitude consistency constraints, the original problem splits to DER and line/ transformer subproblems. Each DER, solves an individual cost minimization subproblem, as do lines and transformers. The objective function is based on price estimates that the buses calculate. In specific, buses perform the dual update step of ADMM by first, calculating the imbalances in satisfying the relaxed constraints \hat{x}^i and then updating the price estimates λ^i . Coupling inequality constraints, namely voltage bound inequality constraints, as well as coupling equality constraints of the type of 5.3 become local to each line subproblem.

Our work draws from (Kraning et al., 2014) and provides the following major advancements:

- We apply ADMM to a much more complex centralized problem, in a multiple commodity market, with complex network constraints and complex DER dynamics.
- We improve upon current ADMM practices by proposing local, instead of the usual global, methods to verify convergence of the ADMM process as well as

adjust the penalties multiplying the quadratic augmentation terms. These local updates lessen the communication burden and improve the convergence rate.

- In Chapter 5, distribution network congestion was linked to binding voltage bound constraints. In this Chapter, we will show that the convergence speed of FDA is slower in the presence of binding voltage inequality constraints. We can attribute this to two main reasons: First, binding inequality constraints impose an additional constraint on the voltage decisions that makes consensus on voltage harder to reach. Second, binding inequality constraints explicitly affect the nodal prices, as the DLMP unbundling equations 5.26 and 5.27 reveal. We deal with this issue in two ways: *(i)* by using the DLMP unbundling relationships 5.26 and 5.27, that provide us with the building blocks of DLMPs, to correct tentative FDA results and *(ii)* by modeling hard voltage bound inequality constraints with voltage barrier functions.

The second distributed algorithm proposed by this thesis is called Partially Distributed Algorithm (PDA). The first step is identical to classic dual decomposition. It involves the solution of individual, lagrangian-based subproblems for each DER in parallel. Each DER subproblem adjusts the DER dispatch so as to minimize the DERs personal costs plus costs based on price estimates it receives from a system operator. The second step is the calculation of updated price estimates given the tentative DER dispatch. The updated price estimates are calculated centrally through either of two equivalent ways.

- The price estimates can be calculated through solving the load flow based on the tentative DER dispatch and then using the unbundling equations 5.26 and 5.27.
- The dual solution of a mock centralized market clearing problem with fixed

DER schedules will include the price estimates.

In other words, PDA differs from classic dual decomposition in that the coupling constraints are not relaxed but rather they are enforced in every iteration. This is in line with recent work by (Li et al., 2012b) and (Joo and Ilic, 2013), where market participants respond to centrally calculated price estimates. Binding voltage inequality constraints pose feasibility and convergence challenges to PDA. We model these hard voltage bound inequality constraints with voltage barrier functions to deal with these issues.

6.1 Fully Distributed Algorithm (FDA): Distributed DER Scheduling and Power Flow

6.1.1 Problem Formulation with Hard Voltage Bound Constraints

In this section, we derive the formulation of the Fully Distributed Algorithm (FDA) for distribution Day-Ahead market clearing. Our formulation draws from (Kraning et al., 2014) as well as other works in the ADMM and proximal algorithms area. We remind the reader of the centralized algorithm for distribution Day- Ahead power market clearing problem with hard voltage bound constraints, C-OPT, by giving a higher level overview of it.

$$\underset{P_\alpha(h), Q_\alpha(h), v_\infty(h)}{\text{minimize}} \sum_{\alpha, h} f_\alpha(P_\alpha(h), Q_\alpha(h)) + \sum_{(b, b'), h} f_{b, b'}(P_{b, b'}(h), Q_{b, b'}(h), P_{b', b}(h), Q_{b', b}(h)) \quad (6.1)$$

subject to:

- Equality constraints on each line/ transformer (5.2), (5.6) and (5.7)
- DER capacity constraints (5.9)-(5.17)
- Nodal equality constraints:

- Real power balance constraints (5.4)
- Reactive power balance constraints (5.5)
- Voltage drop constraints (5.3)
- Nodal inequality constraints:
 - Voltage bound constraints (5.8)

Looking at the objective function terms and the constraints, we conclude that they are all DER and line/ transformer ¹ specific, except for the nodal equality and inequality constraints. The right hand side of constraints (5.3) contains only line/ transformer specific variables, while the left hand side includes nodal variables. Therefore, if we use $v_{b,b'}$ to denote the voltage magnitude at the end b of line b, b' , we can re-write the Day-Ahead problem as:

minimize $\sum_{\alpha,h} f_{\alpha}(P_{\alpha}(h), Q_{\alpha}(h)) + \sum_{(b,b'),h} f_{b,b'}(P_{b,b'}(h), Q_{b,b'}(h), P_{b',b}(h), Q_{b',b}(h))$
subject to:

- Constraints on each line/ transformer

1. Voltage equality constraints

$$v_{b',b}(h) - v_{b,b'}(h) = -2 \cdot (r_{b,b'} \cdot P_{b,b'}(h) + x_{b,b'} \cdot Q_{b,b'}(h)) + (r_{b,b'}^2 + x_{b,b'}^2) l_{b,b'}(h) \quad (6.2)$$

2. Voltage inequality constraints

$$\underline{v} \leq v_{b,b'}(h) \leq \bar{v} \rightarrow \mu_{b,b'}(h) \quad (6.3)$$

3. Other equality constraints (5.2), (5.6) and (5.7)

- DER capacity constraints (5.9)-(5.17)

¹In this chapter, when we refer to lines, we generally refer to a distribution line or a transformer.

- Nodal equality constraints:
 - Real power balance constraints (5.4) $\rightarrow \pi_b^P(h)$
 - Reactive power balance constraints (5.5) $\rightarrow \pi_b^Q(h)$
- Voltage consistency constraints:

$$v_{b,b'}(h) = v_{b,\beta}(h), \forall b', \beta \rightarrow \zeta_{b,b'}(h) \quad (6.4)$$

The additional voltage consistency constraints impose the same voltage on the ends of all lines sharing the same bus and allows for the voltage bound inequality constraints to be line specific. The power balance constraints, as well as the voltage consistency constraints, couple individual DER and line/ transformer decisions. In order to come up with a distributed formulation, we relax them and include them as objective function terms. Looking at applications of ADMM to common problems, the nodal power balance constraints look like exchange constraints, while voltage consistency constraints are similar to consensus constraints. Applying the proximal algorithm to the above and dropping constants, the DER specific subproblem at iteration $i+1$ can be written as (Bertsekas and Tsitsiklis, 1989), (Ntakou and Caramanis, 2014):

$$\begin{aligned} (P_a^{i+1}(h), Q_a^{i+1}(h)) = & \underset{\text{DER constraints}}{\operatorname{argmin}} \sum_h f_a(P_a(h), Q_a(h)) \\ & + \sum_h \hat{\pi}_b^{P,i}(h) \cdot P_a(h) + \sum_h \frac{\rho_P}{2} \cdot \|P_a(h) - P_a^i(h) + \hat{P}_b^i(h)\|_2^2 \\ & + \sum_h \hat{\pi}_b^{Q,i}(h) \cdot Q_a(h) + \sum_h \frac{\rho_Q}{2} \cdot \|Q_a(h) - Q_a^i(h) + \hat{Q}_b^i(h)\|_2^2 \end{aligned} \quad (6.5)$$

subject to DER constraints.

where we use the following relations: ²

$$\hat{P}_b^i(h) = \frac{\sum_{\alpha \in A_b} P_\alpha^i(h) + \sum_{b'} P_{b,b'}^i(h)}{|A_b| + |H_b|} \quad (6.6)$$

$$\hat{Q}_b^i(h) = \frac{\sum_{\alpha \in A_b} Q_\alpha^i(h) + \sum_{b'} Q_{b,b'}^i(h)}{|A_b| + |H_b|} \quad (6.7)$$

For a distribution line/ transformer (b, b') we can write with similar logic:

$$\begin{aligned} & (P_{b,b'}^{i+1}(h), Q_{b,b'}^{i+1}(h), v_{b,b'}^{i+1}(h), P_{b',b}^{i+1}(h), Q_{b',b}^{i+1}(h), v_{b',b}^{i+1}(h)) = \\ & \operatorname{argmin} \sum_h f_{b,b'}(P_{b,b'}(h), Q_{b,b'}(h), P_{b',b}(h), Q_{b',b}(h)) \\ & + \sum_h \hat{\pi}_b^{P,i}(h) \cdot P_{b,b'}(h) + \sum_h \frac{\rho_P}{2} \cdot \|P_{b,b'}(h) - P_{b,b'}^i(h) + \hat{P}_b^i(h)\|_2^2 \\ & + \sum_h \hat{\pi}_{b'}^{P,i}(h) \cdot P_{b',b}(h) + \sum_h \frac{\rho_P}{2} \cdot \|P_{b',b}(h) - P_{b',b}^i(h) + \hat{P}_{b'}^i(h)\|_2^2 \\ & + \sum_h \hat{\pi}_b^{Q,i}(h) \cdot Q_{b,b'}(h) + \sum_h \frac{\rho_Q}{2} \cdot \|Q_{b,b'}(h) - Q_{b,b'}^i(h) + \hat{Q}_b^i(h)\|_2^2 \\ & + \sum_h \hat{\pi}_{b'}^{Q,i}(h) \cdot Q_{b',b}(h) + \sum_h \frac{\rho_Q}{2} \cdot \|Q_{b',b}(h) - Q_{b',b}^i(h) + \hat{Q}_{b'}^i(h)\|_2^2 \\ & + \sum_h \zeta_{b,b'}^i(h) \cdot v_{b,b'}(h) + \sum_h \frac{\rho_v}{2} \cdot \|v_{b,b'}(h) - \hat{v}_b^i(h)\|_2^2 \\ & + \sum_h \zeta_{b',b}^i(h) \cdot v_{b',b}(h) + \sum_h \frac{\rho_v}{2} \cdot \|v_{b',b}(h) - \hat{v}_{b'}^i(h)\|_2^2 \end{aligned} \quad (6.8)$$

subject to line equality constraints (6.2), (5.2), (5.6) and (5.7)

and line inequality constraints (6.3)

²Note the notation change from $\pi_b^P(h)$ to $\hat{\pi}_b^{P,i}(h)$ and similarly for reactive power. Throughout this thesis we are using $\pi_b^P(h)$, $\pi_b^Q(h)$, $\pi_b^{P,i}(h)$ and $\pi_b^{Q,i}(h)$ to refer to the ex-post marginal costs of a solution that satisfies nodal power balance and voltage consistency constraints. In other words, $\pi_b^P(h)$, $\pi_b^Q(h)$, $\pi_b^{P,i}(h)$ and $\pi_b^{Q,i}(h)$ are shadow prices of the power balance constraints. $\hat{\pi}_b^{P,i}(h)$ and $\hat{\pi}_b^{Q,i}(h)$ refer to intermediate, tentative price estimates that might not satisfy power balance and voltage consistency for all iterations i . As can be seen from the convergence guarantees that follow, we will have that $\lim_{i \rightarrow \infty} \hat{\pi}_b^{P,i}(h) = \pi_b^P(h)$ and $\lim_{i \rightarrow \infty} \hat{\pi}_b^{Q,i}(h) = \pi_b^Q(h)$.

where we have defined:

$$\hat{v}_b^i(h) = \frac{\sum_{b',(b,b') \in H_b} v_{b,b'}(h)}{|H_b|} \quad (6.9)$$

The coupling voltage bound inequality constraints are now local to each line subproblem.

The price updates are performed following the rules below:

$$\hat{\pi}_b^{P,i+1}(h) = \hat{\pi}_b^{P,i}(h) + \rho_P \cdot \hat{P}_b^{i+1}(h) \quad (6.10)$$

$$\hat{\pi}_b^{Q,i+1}(h) = \hat{\pi}_b^{Q,i}(h) + \rho_Q \cdot \hat{Q}_b^{i+1}(h) \quad (6.11)$$

$$\zeta_{b,b'}^{i+1}(h) = \zeta_{b,b'}^i(h) + \rho_v \cdot (v_{b,b'}^{i+1}(h) - \hat{v}_b^{i+1}(h)) \quad (6.12)$$

The DER and line/transformers subproblems' objective function can be rewritten in the following shorter form (called "scaled form" in (Kraning et al., 2014) and (Boyd et al., 2011)) by combining the linear and quadratic terms in each objective function (6.5) and (6.8).

$$\begin{aligned} (P_a^{i+1}(h), Q_a^{i+1}(h)) = & \underset{\text{DER constraints}}{\operatorname{argmin}} \sum_h f_a(P_a(h), Q_a(h)) \\ & + \sum_h \frac{\rho_P}{2} \cdot \|P_a(h) - P_a^i(h) + \hat{P}_b^i(h) + u_b^i(h)\|_2^2 \\ & + \sum_h \frac{\rho_Q}{2} \cdot \|Q_a(h) - Q_a^i(h) + \hat{Q}_b^i(h) + \lambda_b^i(h)\|_2^2 \end{aligned} \quad (6.13)$$

subject to DER constraints.

and

$$\begin{aligned}
& (P_{b,b'}^{i+1}(h), Q_{b,b'}^{i+1}(h), v_{b,b'}^{i+1}(h), P_{b',b}^{i+1}(h), Q_{b',b}^{i+1}(h), v_{b',b}^{i+1}(h)) = \\
& \operatorname{argmin} \sum_h f_{b,b'}(P_{b,b'}(h), Q_{b,b'}(h), P_{b',b}(h), Q_{b',b}(h)) \\
& + \sum_h \frac{\rho_P}{2} \cdot \|P_{b,b'}(h) - P_{b,b'}^i(h) + \hat{P}_b^i(h) + u_b^i(h)\|_2^2 \\
& + \sum_h \frac{\rho_P}{2} \cdot \|P_{b',b}(h) - P_{b',b}^i(h) + \hat{P}_{b'}^i(h) + u_{b'}^i(h)\|_2^2 \\
& + \sum_h \frac{\rho_Q}{2} \cdot \|Q_{b,b'}(h) - Q_{b,b'}^i(h) + \hat{Q}_b^i(h) + \lambda_b^i(h)\|_2^2 \\
& + \sum_h \frac{\rho_Q}{2} \cdot \|Q_{b',b}(h) - Q_{b',b}^i(h) + \hat{Q}_{b'}^i(h) + \lambda_{b'}^i(h)\|_2^2 \\
& + \sum_h \frac{\rho_v}{2} \cdot \|v_{b,b'}(h) - \hat{v}_b^i(h) + \sigma_{b,b'}^i(h)\|_2^2 \\
& + \sum_h \frac{\rho_v}{2} \cdot \|v_{b',b}(h) - \hat{v}_{b'}^i(h) + \sigma_{b',b}^i(h)\|_2^2
\end{aligned} \tag{6.14}$$

subject to line equality constraints (6.2), (5.2), (5.6) and (5.7)

and line inequality constraints (6.3)

where we have used: $u_b^i(h) = \frac{\hat{\pi}_b^{P,i}(h)}{\rho_P}$

$$\begin{aligned}
\lambda_b^i(h) &= \frac{\hat{\pi}_b^{Q,i}(h)}{\rho_Q} \\
\sigma_{b,b'}^i(h) &= \frac{\zeta_{b,b'}^i(h)}{\rho_v}.
\end{aligned}$$

For the remainder of the thesis, we will be using the formulation described by 6.5 and 6.8 since it is more intuitive and instructive to the process that FDA follows: DERs self-schedule by solving problems aiming at minimizing their overall costs, that are comprised of individual costs $f_\alpha(h)$ plus what DERs pay for real and reactive power $\hat{\pi}_b^P(h) \cdot P_\alpha(h) + \hat{\pi}_b^Q(h) \cdot Q_\alpha(h)$.

The line subproblems can have a similar interpretation if one thinks of lines as an entity that buys real/ reactive power from its one end and sells it to the other end. Then $\hat{\pi}_b^{P,i}(h) \cdot P_{b,b'}(h) + \hat{\pi}_{b'}^{P,i}(h) \cdot P_{b',b}(h)$ (same for reactive power) can be interpreted as

costs that the line wants to minimize. A line also minimizes costs $f_{b,b'}(h)$. Note that, as discussed in Chapter 3, $f_{b,b'}(h)$ is the transformer degradation costs for transformer lines, while $f_{b,b'}(h) = 0$ for non-transformer lines.

The remainder of the terms in the objective functions, i.e., the second norm squared terms like $\|P_a(h) - P_a^i(h) + \hat{P}_b^i(h)\|_2^2$, are augmentation terms whose role is to robustify convergence. As iterations progress and convergence is achieved, these augmentation terms converge to zero.

The Fully Distributed Algorithm with hard voltage bound constraints (FDA-OPT) is finally described as:

FDA-OPT: Fully Distributed Algorithm with Hard voltage bound constraints

1. Initialize $i \leftarrow 1$.
2. For $\alpha \in D, G, E, F$ solve:

$$\underset{P_\alpha(h), Q_\alpha(h)}{\text{minimize}} \sum_h \begin{cases} f_\alpha(P_\alpha(h), Q_\alpha(h)) \\ + \hat{\pi}_b^{P,i}(h) \cdot P_\alpha(h) + \text{augmentation terms for } P_\alpha(h) \\ + \hat{\pi}_b^{Q,i}(h) \cdot Q_\alpha(h) + \text{augmentation terms in } Q_\alpha(h) \end{cases} \quad (6.15)$$

subject to DER constraints.

3. For $(b, b') \in H$ solve:

$$\begin{array}{l}
\text{minimize} \\
P_{b,b'}(h), P_{b',b}(h) \\
Q_{b,b'}(h), Q_{b',b}(h) \\
v_{b,b'}(h), v_{b',b}(h)
\end{array}
\sum_h \left\{ \begin{array}{l}
f_{b,b'}(P_{b,b'}(h), Q_{b,b'}(h), P_{b',b}(h), Q_{b',b}(h)) \\
+\hat{\pi}_b^{P,i}(h) \cdot P_{b,b'}(h) + \hat{\pi}_{b'}^{P,i}(h) \cdot P_{b',b}(h) \\
+\text{augmentation terms for } P_{b,b'}(h), P_{b',b}(h) \\
+\hat{\pi}_b^{Q,i}(h) \cdot Q_{b,b'}(h) + \hat{\pi}_{b'}^{Q,i}(h) \cdot Q_{b',b}(h) \\
+\text{augmentation terms for } Q_{b,b'}(h), Q_{b',b}(h) \\
+\zeta_{b,b'}^i(h) \cdot v_{b,b'}(h) + \zeta_{b',b}^i(h) \cdot v_{b',b}(h) \\
+\text{augmentation terms for } v_{b,b'}(h), v_{b',b}(h)
\end{array} \right. \quad (6.16)$$

subject to line equality constraints (6.2), (5.2), (5.6) and (5.7)

and line inequality constraints (6.3)

4. For all buses update:

$$\begin{aligned}
\hat{\pi}_b^{P,i+1}(h) &= \hat{\pi}_b^{P,i}(h) + \rho_P \cdot \hat{P}_b^{i+1}(h) \\
\hat{\pi}_b^{Q,i+1}(h) &= \hat{\pi}_b^{Q,i}(h) + \rho_Q \cdot \hat{Q}_b^{i+1}(h) \\
\zeta_{b,b'}^{i+1}(h) &= \zeta_{b,b'}^i(h) + \rho_v \cdot (v_{b,b'}^{i+1}(h) - \hat{v}_b^{i+1}(h)) \\
v_b^{i+1}(h) &= \frac{\sum_{b',(b,b') \in H_b} v_{b,b'}^{i+1}(h)}{|H_b|} \\
\mu_b^{i+1}(h) &= \sum_{b',(b,b') \in H_b} \mu_{b,b'}^{i+1}(h)
\end{aligned}$$

5. If tolerance criterion satisfied, terminate. Else, $i \leftarrow i + 1$ and go to 2.

The method is based on ADMM, therefore the following convergence guarantees hold (Kraning et al., 2014), (Boyd et al., 2011):

- Real and reactive power balance and voltage consistency are achieved, i.e.

$$\lim_{i \rightarrow \infty} \hat{P}_b^i(h) = 0, \lim_{i \rightarrow \infty} \hat{Q}_b^i(h) = 0 \text{ and } \lim_{i \rightarrow \infty} v_{b,b'}^i(h) - \hat{v}_b^i(h) = 0.$$

- The optimal objective function value is reached.

- The optimal prices are found, i.e. $\lim_{i \rightarrow \infty} \hat{\pi}_b^{P,i}(h) = \pi_b^P(h)$ and $\lim_{i \rightarrow \infty} \hat{\pi}_b^{Q,i}(h) = \pi_b^Q(h)$.

6.1.2 Stopping Criteria

This section elaborates on step 5 of the above iterative algorithm. The stopping criteria are based on the imbalances in satisfying the power balance and voltage consistency constraints and their change from the previous iteration. We define the vector of constraint imbalances, across all buses b and hours h as:

$$\mathbf{s}^i = (\hat{\mathbf{P}}^i, \hat{\mathbf{Q}}^i, \mathbf{v}^i - \hat{\mathbf{v}}^i) \quad (6.17)$$

and the vector of imbalance changes as:

$$\Delta \mathbf{s}^i = (\rho_P \cdot (\mathbf{P}^i - \hat{\mathbf{P}}^i) - (\mathbf{P}^{i-1} - \hat{\mathbf{P}}^{i-1}), \rho_Q \cdot (\mathbf{Q}^i - \hat{\mathbf{Q}}^i) - (\mathbf{Q}^{i-1} - \hat{\mathbf{Q}}^{i-1}), \rho_v \cdot (\hat{\mathbf{v}}^i - \hat{\mathbf{v}}^{i-1})) \quad (6.18)$$

where:

- $\hat{\mathbf{P}}^i = [\hat{\mathbf{P}}_{\mathbf{b}}^i]$, $\hat{\mathbf{P}}_{\mathbf{b}}^i = [\hat{P}_b^i(h)]'$,
- $\hat{\mathbf{Q}}^i = [\hat{\mathbf{Q}}_{\mathbf{b}}^i]$, $\hat{\mathbf{Q}}_{\mathbf{b}}^i = [\hat{Q}_b^i(h)]'$ and
- $\mathbf{v}^i - \hat{\mathbf{v}}^i = [\mathbf{v}_{\mathbf{b},\mathbf{b}'}^i - \hat{\mathbf{v}}_{\mathbf{b}}^i]$, $\mathbf{v}_{\mathbf{b},\mathbf{b}'}^i = [v_{b,b'}^i(h)]'$, $\hat{\mathbf{v}}_{\mathbf{b}}^i = [\hat{v}_b^i(h)]'$.

Based on (Kraning et al., 2014) and (Boyd et al., 2011), the stopping criterion is defined as:

$$\|\mathbf{s}^i\| \leq \epsilon \wedge \|\Delta \mathbf{s}^i\| \leq \epsilon \quad (6.19)$$

However, stopping criteria of the form of (6.19) require that some agent, i.e. the system operator, needs to obtain the imbalances and imbalance changes of all distribution buses. To do away with this need and lessen the communication burden associated with FDA, we propose a local stopping method. At each iteration of FDA,

each bus determines the value of a flag as below:

$$\text{flag}(b, i) = \begin{cases} 1, & \text{if } \|\mathbf{s}_b^i\| \leq \epsilon \wedge \|\Delta \mathbf{s}_b^i\| \leq \epsilon \\ 0, & \text{else} \end{cases} \quad (6.20)$$

where we define $\mathbf{s}_b^i = (\hat{\mathbf{P}}_b^i, \hat{\mathbf{Q}}_b^i, \mathbf{v}_b^i - \hat{\mathbf{v}}_b^i)$ and $\Delta \mathbf{s}_b^i = (\rho_P \cdot (\mathbf{P}_b^i - \hat{\mathbf{P}}_b^i) - (\mathbf{P}_b^{i-1} - \hat{\mathbf{P}}_b^{i-1}), \rho_Q \cdot (\mathbf{Q}_b^i - \hat{\mathbf{Q}}_b^i) - (\mathbf{Q}_b^{i-1} - \hat{\mathbf{Q}}_b^{i-1}), \rho_v \cdot (\hat{\mathbf{v}}_b^i - \hat{\mathbf{v}}_b^{i-1}))$.

A value of 1 indicates local convergence. At the beginning of iteration cycle $i + 1$, each bus b communicates the value of its flag $\text{flag}(b, i)$ to its direct upstream nets. The upstream bus b' receives the message and at the end of iteration $i + 1$ adds to it the value of its own flag $\text{flag}(b', i + 1)$ and communicates the sum to its direct upstream bus. If the value of the sum at the substation is equal to the number of buses in the network and if that is true for as many iterations as the depth of the tree (i.e. number of buses in the longest distribution line), then it follows logically that all flags were 1 at the same time and the algorithm has converged (Wainwright et al., 2003).

6.1.3 Iterative Penalty Change

As described in (Kraning et al., 2014), updating the penalty at each iteration can make convergence faster. This is performed during step 4 of the algorithm shown above. However, the update rules proposed in (Kraning et al., 2014) require global communication. Moreover, in order to guarantee convergence, changes to the penalty should stop after some iterations. (Kraning et al., 2014) and (Boyd et al., 2011) limit the penalty updates to some number of initial iterations and disallow penalty updates after that limit is exceeded.

This thesis proposes an alternate penalty update that not only is local but also does away with the need to count the number of penalty updates. Like our

proposed local stopping criterion, the penalty update rule is based on the imbalances in satisfying the power balance and voltage consistency constraints and their change relative to the previous iteration. As iterations progress, imbalances and their changes decrease, therefore the penalty changes will also decrease until they do no longer change. Specifically, in the case of a centrally adapted penalty $\rho^i = \rho_P^i = \rho_Q^i = \rho_v^i$, the proposed penalty change is:

$$\rho^{i+1} = \begin{cases} \rho^i \cdot (1 + (\|\mathbf{s}^{i+1}\| + \|\Delta\mathbf{s}^{i+1}\|)), & \text{if } \frac{\|\mathbf{s}^{i+1}\|}{\|\Delta\mathbf{s}^{i+1}\|} > 5 \wedge \|\mathbf{s}^{i+1}\| + \|\Delta\mathbf{s}^{i+1}\| < 0.3 \\ 1.3 \cdot \rho^i, & \text{if } \frac{\|\mathbf{s}^{i+1}\|}{\|\Delta\mathbf{s}^{i+1}\|} > 5 \wedge \|\mathbf{s}^{i+1}\| + \|\Delta\mathbf{s}^{i+1}\| \geq 0.3 \\ \rho^i \cdot (1 - (\|\mathbf{s}^{i+1}\| + \|\Delta\mathbf{s}^{i+1}\|)), & \text{if } \frac{\|\Delta\mathbf{s}^{i+1}\|}{\|\mathbf{s}^{i+1}\|} > 5 \wedge \|\mathbf{s}^{i+1}\| + \|\Delta\mathbf{s}^{i+1}\| < 0.3 \\ 0.7 \cdot \rho^i, & \text{if } \frac{\|\Delta\mathbf{s}^{i+1}\|}{\|\mathbf{s}^{i+1}\|} > 5 \wedge \|\mathbf{s}^{i+1}\| + \|\Delta\mathbf{s}^{i+1}\| \geq 0.3 \\ \rho^i, & \text{else} \end{cases} \quad (6.21)$$

Penalties can also be specific to each bus, in which case the update rule is:

$$\rho_b^{i+1} = \begin{cases} \rho_b^i \cdot (1 + (\|\mathbf{s}_b^{i+1}\| + \|\Delta\mathbf{s}_b^{i+1}\|)), & \text{if } \frac{\|\mathbf{s}_b^{i+1}\|}{\|\Delta\mathbf{s}_b^{i+1}\|} > 5 \wedge \|\mathbf{s}_b^{i+1}\| + \|\Delta\mathbf{s}_b^{i+1}\| < 0.3 \\ 1.3 \cdot \rho_b^i, & \text{if } \frac{\|\mathbf{s}_b^{i+1}\|}{\|\Delta\mathbf{s}_b^{i+1}\|} > 5 \wedge \|\mathbf{s}_b^{i+1}\| + \|\Delta\mathbf{s}_b^{i+1}\| \geq 0.3 \\ \rho_b^i \cdot (1 - (\|\mathbf{s}_b^{i+1}\| + \|\Delta\mathbf{s}_b^{i+1}\|)), & \text{if } \frac{\|\Delta\mathbf{s}_b^{i+1}\|}{\|\mathbf{s}_b^{i+1}\|} > 5 \wedge \|\mathbf{s}_b^{i+1}\| + \|\Delta\mathbf{s}_b^{i+1}\| < 0.3 \\ 0.7 \cdot \rho_b^i, & \text{if } \frac{\|\Delta\mathbf{s}_b^{i+1}\|}{\|\mathbf{s}_b^{i+1}\|} > 5 \wedge \|\mathbf{s}_b^{i+1}\| + \|\Delta\mathbf{s}_b^{i+1}\| \geq 0.3 \\ \rho_b^i, & \text{else} \end{cases} \quad (6.22)$$

Finally, as per our original FDA problem derivation, penalties can be specific to each quantity. This is important because the quantities that each term is specific to, namely real power, reactive power and voltage, are not necessarily of the same order of magnitude. Bus-and-quantity specific penalties' update rules are not explicitly described but follow easily. In the case of iterative penalty changes, Step 4 of the

FDA algorithm becomes (shown for bus-specific penalty changes):

$$\begin{aligned}
\hat{\pi}_b^{P,i+1}(h) &= \hat{\pi}_b^{P,i}(h) + \rho_b^i \cdot \hat{P}_b^{i+1}(h) \\
\hat{\pi}_b^{Q,i+1}(h) &= \hat{\pi}_b^{Q,i}(h) + \rho_b^i \cdot \hat{Q}_b^{i+1}(h) \\
\zeta_{b,b'}^{i+1}(h) &= \zeta_{b,b'}^i(h) + \rho_b^i \cdot (v_{b,b'}^{i+1}(h) - \hat{v}_b^{i+1}(h)) \\
v_b^{i+1}(h) &= \frac{\sum_{b',(b,b') \in H_b} v_{b,b'}^{i+1}(h)}{|H_b|} \\
\mu_b^{i+1}(h) &= \sum_{b',(b,b') \in H_b} \mu_{b,b'}^{i+1}(h) \\
\rho_b^{i+1} &= \rho_b^{i+1}(\rho_b^i, \|\mathbf{s}_b^{i+1}\|, \|\Delta \mathbf{s}_b^{i+1}\|) \\
\hat{\pi}_b^{P,i+1}(h) &:= \frac{\rho_b^i}{\rho_b^{i+1}} \cdot \hat{\pi}_b^{P,i+1}(h) \\
\hat{\pi}_b^{Q,i+1}(h) &:= \frac{\rho_b^i}{\rho_b^{i+1}} \cdot \hat{\pi}_b^{Q,i+1}(h) \\
\zeta_{b,b'}^{i+1}(h) &:= \frac{\rho_b^i}{\rho_b^{i+1}} \cdot \zeta_{b,b'}^{i+1}(h)
\end{aligned}$$

6.1.4 Synchronization of Device Solutions to Nodal Price Updates

In the description of the algorithm shown above we assume that all device subproblems complete solving before buses update the price variables. In other words, updates are synchronous.

While synchronization is a necessary condition to guarantee convergence of ADMM, it causes bottlenecks related to the slowest computational time among line and DER subproblems. Recent work has investigated asynchronous algorithms. In our case, asynchronous updates would allow for buses to update their nodal prices and penalties after receiving the tentative schedules of only some of the connected devices.

Literature is promising in the general direction of asynchronous implementations. (Bertsekas and Tsitsiklis, 1989) discusses problems that can converge under asynchronous implementations as well as benefits and problems associated with asynchronous updates. Recent work on techniques for convergence of asynchronous algorithms is too vast to investigate for the scope of this work. We mention (Zhang and Kwok, 2014), (Li and Marden, 2012) and (Wei and Ozdaglar, 2013) as representa-

tive work. On the more specific literature of asynchronous distributed algorithms for power systems, (Li et al., 2014) concentrates on voltage control and proves through a Lyapunov function that updates with no communication at all result in convergence.

6.1.5 Enhancements for Voltage Congested Distribution Networks

Because of the nature of FDA, where voltage bound inequality constraints are local to each line subproblem, solving instances where these constraints bind at the optimal solution can be challenging for two main reasons. First, binding voltage inequality constraints are an additional constraint imposed on voltage decisions, making voltage consensus harder to reach. Second, as revealed by the DLMP unbundling equations 5.26 and 5.27 active voltage bound constraints explicitly affect nodal prices.

In the case of binding voltage bound constraints, where $\mu_b(h) \neq 0$, we notice that before full convergence to the primal and dual variables is achieved, it is possible to have busses with $\mu_b(h) \neq 0$ and $v_b(h) \neq \bar{v} \wedge v_b(h) \neq \underline{v}$. Also, numerical results indicate that convergence is slower in the presence of binding voltage bound constraints. This is our motivation for enhancements to the above structure of FDA. Our efforts concentrate around:

1. A correction process applied to non-fully converged prices based on the DLMP unbundling equations.
2. Modeling of hard voltage bound inequality constraints with barrier-function-based soft voltage constraints, as in the modification of the centralized algorithms shown in Section 5.4.

Price Estimate Correction Process

With the motivation that binding voltage bound constraints affect DLMPs, in this section, we use equations 5.26 and 5.27 that show the building blocks of the real and

reactive power DLMPs to correct price estimates obtained by intermediate iterations of FDA. The premises upon which relations 5.26 and 5.27 are derived do not hold for not fully converged iterations of FDA. Specifically, at each iteration of FDA-OPT, the discrepancy in satisfying 5.26 and 5.27 is equal to:

$$\epsilon_{\beta}^{P,i}(h) = \begin{cases} -\pi_{\beta}^{P,i}(h) + \pi_{\infty}^P(h) \cdot \frac{\partial P_{\infty}^i(h)}{\partial P_{\dot{g}\beta}(h)} + \frac{\pi_{\infty}^{OC}(h) \cdot Q_{\infty}^i(h)}{\sqrt{C_{\infty}^2 - (Q_{\infty}^i(h))^2}} \cdot \frac{\partial Q_{\infty}^i(h)}{\partial P_{\dot{g}\beta}(h)} + \\ \sum_{h_1 \geq h, (b,b') \in tr} c_{b,b'}^{tr} \cdot \frac{\partial \Gamma_{b,b'}(S_{b,b'}^i(h_1))}{\partial P_{\dot{g}\beta}(h)} + \sum_b \mu_b(h) \cdot \frac{\partial v_b^i(h)}{\partial P_{\dot{g}\beta}(h)} - \\ \sum_{(b,\alpha), \alpha \in F_b} \kappa_{\alpha}(h) \cdot 1_{v_b^i(h) < 1} \cdot C_{\alpha} \cdot \frac{\partial v_b^i(h)}{\partial P_{\dot{g}\beta}(h)} \end{cases} \quad (6.23)$$

$$\epsilon_{\beta}^{Q,i}(h) = \begin{cases} -\pi_{\beta}^{Q,i}(h) + \pi_{\infty}^P(h) \cdot \frac{\partial P_{\infty}^i(h)}{\partial Q_{\dot{g}\beta}(h)} + \frac{\pi_{\infty}^{OC}(h) \cdot Q_{\infty}^i(h)}{\sqrt{C_{\infty}^2 - (Q_{\infty}^i(h))^2}} \cdot \frac{\partial Q_{\infty}^i(h)}{\partial Q_{\dot{g}\beta}(h)} + \\ \sum_{h_1 \geq h, (b,b') \in tr} c_{b,b'}^{tr} \cdot \frac{\partial \Gamma_{b,b'}(S_{b,b'}^i(h_1))}{\partial Q_{\dot{g}\beta}(h)} + \sum_b \mu_b(h) \cdot \frac{\partial v_b^i(h)}{\partial Q_{\dot{g}\beta}(h)} - \\ \sum_{(b,\alpha), \alpha \in F_b} \kappa_{\alpha}(h) \cdot 1_{v_b^i(h) < 1} \cdot C_{\alpha} \cdot \frac{\partial v_b^i(h)}{\partial Q_{\dot{g}\beta}(h)} \end{cases} \quad (6.24)$$

We aim at minimizing the discrepancies $\epsilon_{\beta}^{P,i}(h), \forall \beta, h$ and $\epsilon_{\beta}^{Q,i}(h), \forall \beta, h$. We perform the minimization using $P_{b,b'}^i(h), Q_{b,b'}^i(h), v_b^i(h), \pi_b^{P,i}(h), \pi_b^{Q,i}(h)$ as parameters and $\mu_b(h)$ as the decision variables. The resulting price estimate correction process is of the form:

1. Corrected voltage bound inequality constraint shadow prices are the solution of the following problem:

$$\underset{\mu \geq 0}{\text{minimize}} \|\mathbf{A}_{\mathbf{P}}^i \cdot \mu - \mathbf{c}_{\mathbf{P}}^i\|_2^2 \quad (6.25)$$

for voltages binding above and

$$\underset{\mu \leq 0}{\text{minimize}} \|\mathbf{A}_{\mathbf{P}}^i \cdot \mu - \mathbf{c}_{\mathbf{P}}^i\|_2^2 \quad (6.26)$$

for voltages binding below, where:

- $\mu = [\mu_b(h)]$

- $A_P^i = [\frac{\partial v_b^i(h)}{\partial P_{\dot{g}_\beta}(h)}]$
- $c_P^i = [\pi_\beta^{P,i}(h) - \pi_\infty^P(h) \cdot \frac{\partial P_\infty^i(h)}{\partial P_{\dot{g}_\beta}(h)} - \frac{\pi_\infty^{OC}(h) \cdot Q_\infty^i(h)}{\sqrt{C_\infty^2 - (Q_\infty^i(h))^2}} \cdot \frac{\partial Q_\infty^i(h)}{\partial P_{\dot{g}_\beta}(h)} - \sum_{h_1 \geq h, (b,b') \in tr} c_{b,b'}^{tr} \cdot \frac{\partial \Gamma_{b,b'}(S_{b,b'}^i(h_1))}{\partial P_{\dot{g}_\beta}(h)} + \sum_{(b,\alpha), \alpha \in F_b} \kappa_\alpha(h) \cdot 1_{v_b^i(h) < 1} \cdot C_\alpha \cdot \frac{\partial v_b(h)}{\partial P_{\dot{g}_\beta}(h)}]$

It follows easily that the reactive power DLMP-based correction process is equivalent.³

$$\underset{\mu \geq 0}{\text{minimize}} \|\mathbf{A}_Q^i \cdot \mu - \mathbf{c}_Q^i\|_2^2 \quad (6.27)$$

and for voltages binding below:

$$\underset{\mu \leq 0}{\text{minimize}} \|\mathbf{A}_Q^i \cdot \mu - \mathbf{c}_Q^i\|_2^2 \quad (6.28)$$

where:

- $A_Q^i = [\frac{\partial v_b^i(h)}{\partial Q_{\dot{g}_\beta}(h)}]$
- $c_Q^i = [\pi_\beta^{Q,i}(h) - \pi_\infty^P(h) \cdot \frac{\partial P_\infty^i(h)}{\partial Q_{\dot{g}_\beta}(h)} - \frac{\pi_\infty^{OC}(h) \cdot Q_\infty^i(h)}{\sqrt{C_\infty^2 - (Q_\infty^i(h))^2}} \cdot \frac{\partial Q_\infty^i(h)}{\partial Q_{\dot{g}_\beta}(h)} - \sum_{h_1 \geq h, (b,b') \in tr} c_{b,b'}^{tr} \cdot \frac{\partial \Gamma_{b,b'}(S_{b,b'}^i(h_1))}{\partial Q_{\dot{g}_\beta}(h)} + \sum_{(b,\alpha), \alpha \in F_b} \kappa_\alpha(h) \cdot 1_{v_b^i(h) < 1} \cdot C_\alpha \cdot \frac{\partial v_b(h)}{\partial Q_{\dot{g}_\beta}(h)}]$

2. Using the corrected μ into 5.26 and 5.27 together with tentative FDA results

$P_{b,b'}^i$, $Q_{b,b'}^i$ and v_b^i allows us to get corrected price estimates.

Going back to our original statement about the nature of FDA leaving room for solutions with $\mu_b(h) \neq 0$ and $v_b(h) \neq \bar{v} \wedge v_b(h) \neq \underline{v}$, in performing the minimizations of (6.25) and (6.27) we take into account only the buses whose voltage is binding as candidates for $\mu_b(h) \neq 0$. The numerical effects of the price estimate correction process are shown in Section 6.1.6. Admittedly, the implementation of this correction process requires that global information be gathered by some agent. Therefore, the

³We remind the reader that $\mu_b(h) = \bar{\mu}_b(h) - \underline{\mu}_b(h)$, where $\bar{\mu}_b(h), \underline{\mu}_b(h) \geq 0$. When voltages bind above, $\bar{\mu}_b(h) \geq 0, \underline{\mu}_b(h) = 0 \Rightarrow \mu_b(h) = \bar{\mu}_b(h) \Rightarrow \mu_b(h) \geq 0$. When voltages bind from below, $\bar{\mu}_b(h) = 0, \underline{\mu}_b(h) \geq 0 \Rightarrow \mu_b(h) = -\underline{\mu}_b(h) \Rightarrow \mu_b(h) \leq 0$.

periodicity of implementing it should be such that the computational requirements are still low.

FDA modeling Voltage Bound Constraints with a Barrier Function

The formulation of FDA with voltage barrier functions is based off of (5.4). We show below the modified formulation of FDA that we refer to as FDA-SVC, standing for Soft Voltage Constraints. The only changes compared to FDA-OPT appear in Step 3, where the distribution line subproblem is shown, as well as Step 4:

FDA-SVC: Fully Distributed Algorithm with Soft Voltage Constraints

1. Initialize $i \leftarrow 1$.
2. For $\alpha \in D, G, E, F$ solve:

$$\underset{P_\alpha(h), Q_\alpha(h)}{\text{minimize}} \sum_h \begin{cases} f_a(P_a(h), Q_a(h)) \\ + \hat{\pi}_b^{P,i}(h) \cdot P_a(h) + \text{augmentation terms for } P_a(h) \\ + \hat{\pi}_b^{Q,i}(h) \cdot Q_a(h) + \text{augmentation terms in } Q_a(h) \end{cases} \quad (6.29)$$

subject to DER capacity constraints.

3. For $(b, b') \in H$ solve:

$$\begin{array}{l}
\text{minimize} \\
P_{b,b'}(h), P_{b',b}(h) \\
Q_{b,b'}(h), Q_{b',b}(h) \\
v_{b,b'}(h), v_{b',b}(h)
\end{array}
\sum_h \left\{ \begin{array}{l}
f_{b,b'}(P_{b,b'}(h), Q_{b,b'}(h), P_{b',b}(h), Q_{b',b}(h)) \\
+ \hat{\pi}_b^{P,i}(h) \cdot P_{b,b'}(h) + \hat{\pi}_{b'}^{P,i}(h) \cdot P_{b',b}(h) \\
+ \text{augmentation terms for } P_{b,b'}(h), P_{b',b}(h) \\
+ \hat{\pi}_b^{Q,i}(h) \cdot Q_{b,b'}(h) + \hat{\pi}_{b'}^{Q,i}(h) \cdot Q_{b',b}(h) \\
+ \text{augmentation terms for } Q_{b,b'}(h), Q_{b',b}(h) \\
+ \zeta_{b,b'}^i(h) \cdot v_{b,b'}(h) \\
+ \frac{k_{6,b}}{|H_b|} \cdot \exp(k_{7,b} \cdot (v_{b,b'}(h) - \bar{v})) \\
+ \frac{k_{6,b}}{|H_b|} \cdot \exp(k_{8,b} \cdot (\underline{v} - v_{b,b'}(h))) \\
+ \zeta_{b',b}^i(h) \cdot v_{b',b}(h) \\
+ \frac{k_{6,b'}}{|H_{b'}|} \cdot \exp(k_{7,b'} \cdot (v_{b',b}(h) - \bar{v})) \\
+ \frac{k_{6,b'}}{|H_{b'}|} \cdot \exp(k_{8,b'} \cdot (\underline{v} - v_{b',b}(h))) \\
+ \text{augmentation terms for } v_{b,b'}(h), v_{b',b}(h)
\end{array} \right. \quad (6.30)$$

subject to line equality constraints (6.2), (5.2), (5.6) and (5.7)

4. For all buses update:

$$\begin{aligned}
\hat{\pi}_b^{P,i+1}(h) &= \hat{\pi}_b^{P,i}(h) + \rho_P \cdot \hat{P}_b^{i+1}(h) \\
\hat{\pi}_b^{Q,i+1}(h) &= \hat{\pi}_b^{Q,i}(h) + \rho_Q \cdot \hat{Q}_b^{i+1}(h) \\
\zeta_{b,b'}^{i+1}(h) &= \zeta_{b,b'}^i(h) + \rho_v \cdot (v_{b,b'}^{i+1}(h) - \hat{v}_b^{i+1}(h)) \\
v_b^{i+1}(h) &= \frac{\sum_{b',(b,b') \in H_b} v_{b,b'}^{i+1}(h)}{|H_b|} \\
\mu_b^{i+1}(h) &= \sum_{b',(b,b') \in H_b} \mu_{b,b'}^{i+1}(h)
\end{aligned}$$

5. If tolerance criterion satisfied, terminate. Else, $i \leftarrow i + 1$ and go to 2.

Note the change in the multiplier of the voltage barrier function terms $k_{6,b}$. We

divide by the degree of each bus b (i.e. the number of lines entering or exiting bus b), since in FDA-SVC this term is used for each line, rather than each bus as in C-SCV.

6.1.6 Numerical Results using FDA

This section is dedicated to the numerical results using the Fully Distributed Algorithm (FDA). We use the 47-bus network described in Appendix A and adjust the DER presence and capabilities to induce or relieve congestion. We start with results on non-congested conditions and continue with congested instances.

FDA Results on Uncongested Networks

We begin by comparing the iterations needed for convergence with the use of:

1. Constant penalty
2. Centrally adapted penalty
3. Bus-specific penalty
4. Bus-and-quantity specific penalty

ρ^1	Constant	Centrally Adapted	Bus Specific	Bus& Quantity
5	1205	409	196	205
10	2298	514	261	241
20	1595	519	355	331
50	>> 5000	442	417	342

Table 6.1: Number of iterations required for convergence using Fully Distributed Algorithms with various penalty updates rules.

We conclude that a large constant penalty can indeed result in no convergence. On the other hand, local penalties result not only in lower communication burden but also in decreased number of iterations needed for convergence.

The following figures show the evolution of a centrally adapted penalty and the evolution of bus-specific penalties, respectively, starting from much different initial values.

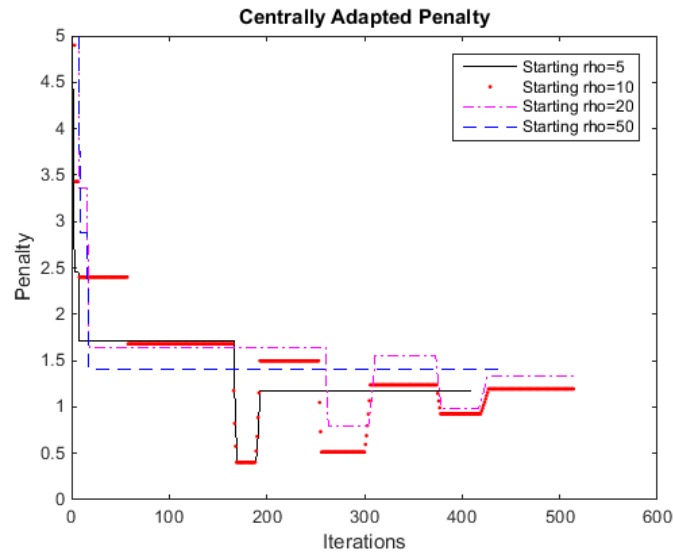


Figure 6-1: Evolution of centrally adapted penalty across iterations.

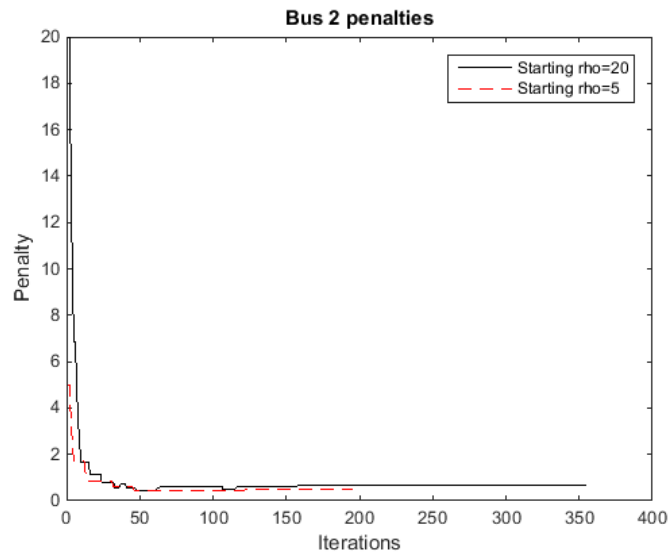


Figure 6-2: Evolution of bus-specific penalty across iterations at a specific distribution bus, starting from different penalty values.

In addition, to underline the importance of locational penalties, we show the

updates of bus-specific penalty for two different distribution buses starting from the same penalty value.

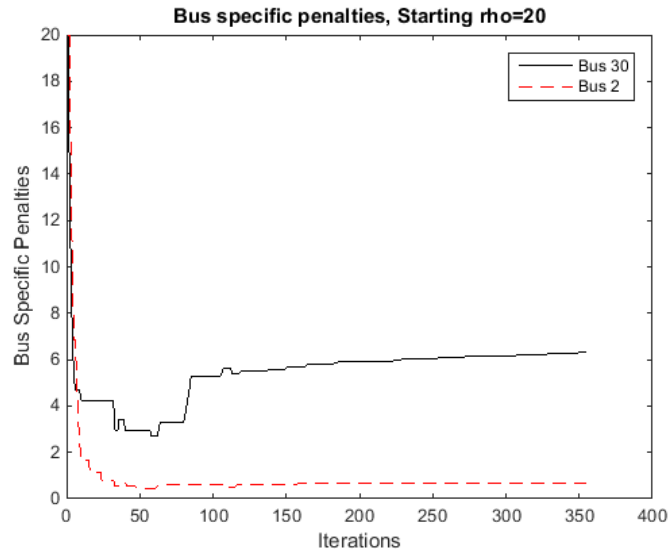


Figure 6-3: Evolution of bus-specific penalty across iterations at two distribution buses, starting from the same initial penalty value.

The two figures below show the updates of the bus-and-quantity specific penalties for two different buses.

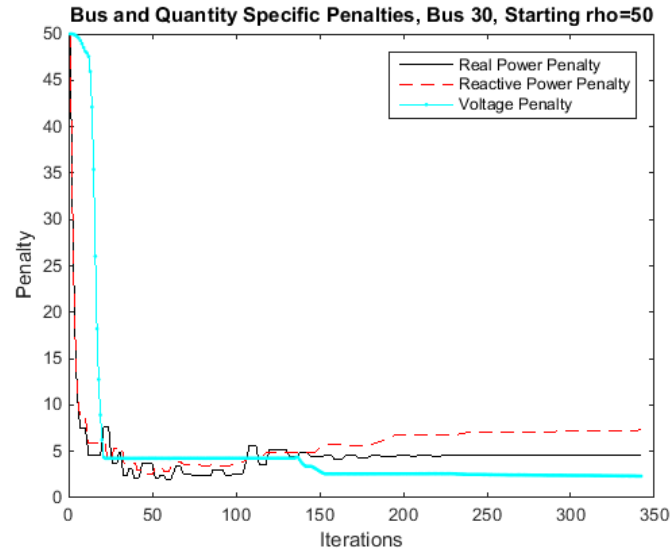


Figure 6-4: Updates of bus-specific penalty of real power, reactive power and voltage consistency across iterations at distribution bus 30.

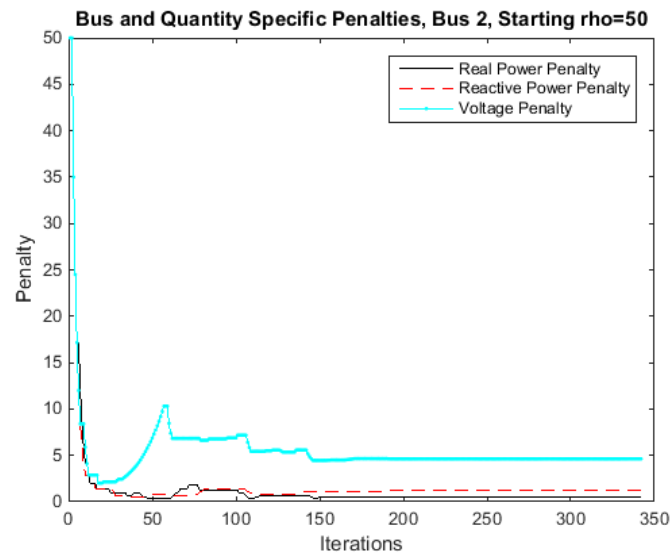


Figure 6-5: Updates of bus-specific penalty of real power, reactive power and voltage consistency across iterations at distribution bus 2.

We reach the following conclusions regarding penalties:

1. In agreement with (Kraning et al., 2014), the choice of the starting value of the penalty is not important, if the penalty is allowed to change for many iterations.

2. Our choice of penalty update rules, based on imbalances and the imbalances' changes, indeed leaves the penalties unchanged for many iterations before convergence, as is desired for ADMM's theoretical convergence guarantees.
3. Bus specific penalties can vary significantly across buses, as in Figure 6-3.
4. Starting from the same initial value and specifying quantity and bus specific penalties, can result in penalties for each quantity varying greatly in the space domain, as in Figures 6-5 and 6-4.

The following figures show the convergence of the prices of real and reactive power, by means of the maximum and average deviation across iterations, with the use of bus and quantity specific penalties that are initialized at 50.

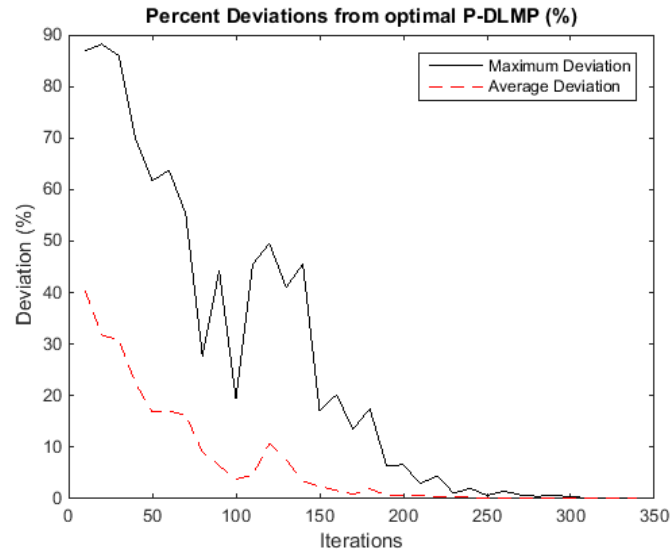


Figure 6-6: Percent deviation of real power price estimates from optimal reactive power price across iterations.

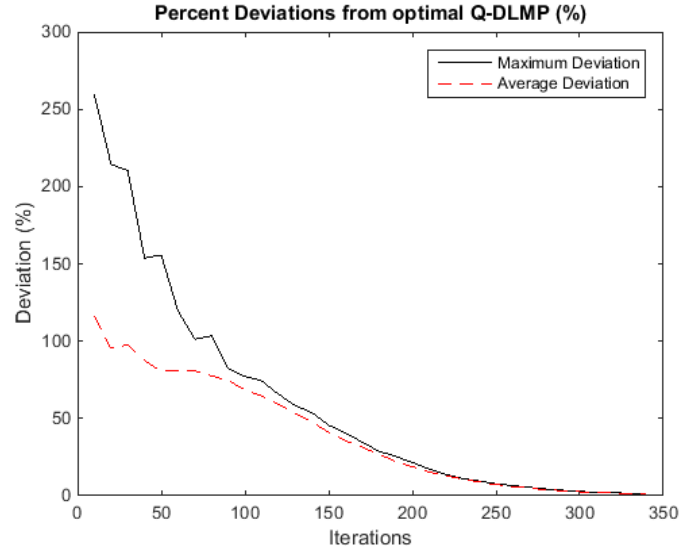


Figure 6.7: Percent deviation of reactive power price estimates from optimal reactive power price across iterations.

For completeness, the tables below show the deviation from the optimal real and reactive DLMPs, for bus specific penalties and for all tested starting values of the penalty (Ntakou and Caramanis, 2014).

ρ^I	Average Deviation	Minimum Deviation	Maximum Deviation
5	0.0513	0.0001	0.2821
10	0.0585	0.0001	0.5445
20	0.0895	0.0003	0.5553
50	0.0290	0.0000	0.1706

Table 6.2: Average, minimum and maximum deviation of real power prices from P-DLMPs (%) at convergence, with the use of bus specific penalties.

ρ^I	Average Deviation	Minimum Deviation	Maximum Deviation
5	0.6435	0.4048	0.8442
10	1.3242	0.8299	1.5025
20	1.3455	0.8738	1.5254
50	1.2026	0.9728	1.3571

Table 6.3: Average, minimum and maximum deviation of reactive power prices from Q-DLMPs (%) at convergence, with the use of bus specific penalties.

The tables below show the same metrics for bus-and-quantity specific penalties and for all tested starting values of the penalty.

ρ^I	Average Deviation	Minimum Deviation	Maximum Deviation
5	0.0476	0.0005	0.2016
10	0.0171	0.0001	0.0523
20	0.0176	0.0032	0.0808
50	0.0255	0.0003	0.1413

Table 6.4: Average, minimum and maximum deviation of real power prices from P-DLMPs (%) at convergence, with the use of bus-and-quantity specific penalties.

ρ^I	Average Deviation	Minimum Deviation	Maximum Deviation
5	0.1547	0.0497	0.2162
10	1.6385	1.2788	1.7887
20	1.3719	1.1010	1.4991
50	1.1715	0.9868	1.3566

Table 6.5: Average, minimum and maximum deviation of reactive power prices from Q-DLMPs (%) at convergence, with the use of bus-and-quantity specific penalties.

(Peng and Low, 2015) examines how the network size and the network diameter (distance, measured in number of lines, of the two furthest buses) affect the number of iterations required for convergence of ADMM to solve an OPF problem over a tree network. Through simulations, (Peng and Low, 2015) concludes that the network distance is the most important factor affecting the convergence speed. We contribute to this result by comparing the convergence speed of FDA for the 47-bus network, whose results are shown above, to the convergence speed of FDA for a 253-bus network, that on top of higher network size, also has a larger diameter. This results in slower convergence (Ntakou and Caramanis, 2014). The specifications of both networks can be found in the Appendix.

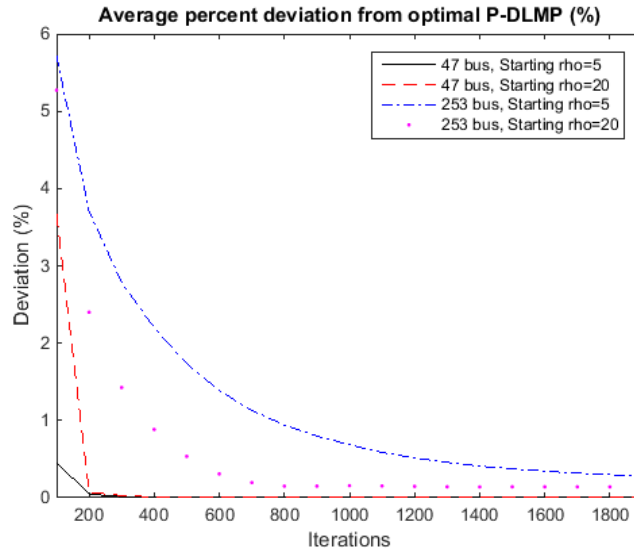


Figure 6-8: Average percent deviation of real power price estimates from optimal real power price across iterations, 47-bus network versus 253-bus network.

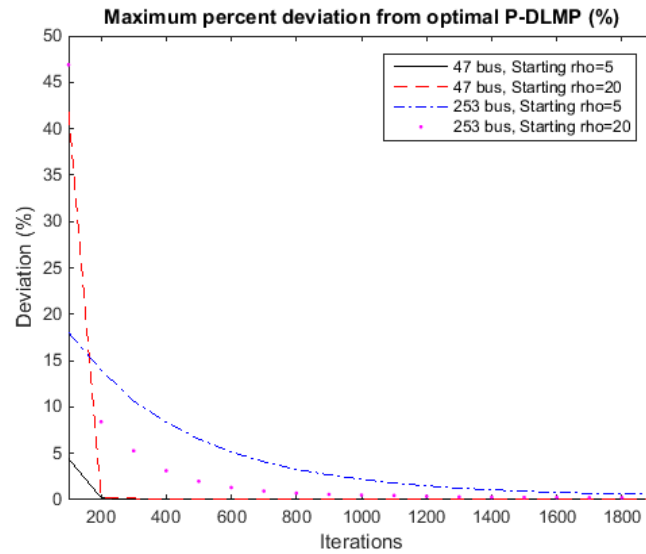


Figure 6-9: Maximum percent deviation of real power price estimates from optimal real power price across iterations, 47-bus network versus 253-bus network.

FDA Results on Congested Networks

We simulate a congested instance of the 47-bus network A, where hard voltage bound inequality constraints bind (Ntakou and Caramanis, 2016).

Motivated by the superiority of results with the use of bus-and-quantity specific penalties, we proceed in the analysis of FDA for congested conditions using bus-and-quantity specific penalties.

The figure below shows that the sum of voltage shadow prices over all distribution buses, $\sum_b \mu_b^i(h) = \sum_{b,b'} \mu_{b,b'}^i(h)$ converges to the optimal sum in a small number of iterations.

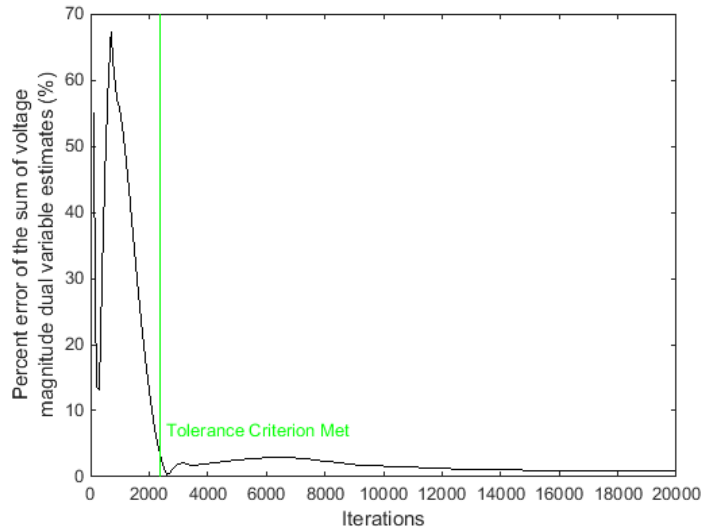


Figure 6-10: Percent deviation of the sum of the voltage magnitude shadow prices across all buses from the optimal value across iterations.

However, individual values $\mu_b^i(h)$ take much longer to converge. The following two figures show the percent deviation of real and reactive power price estimates across iterations, respectively, by means of the minimum, average and maximum deviation.

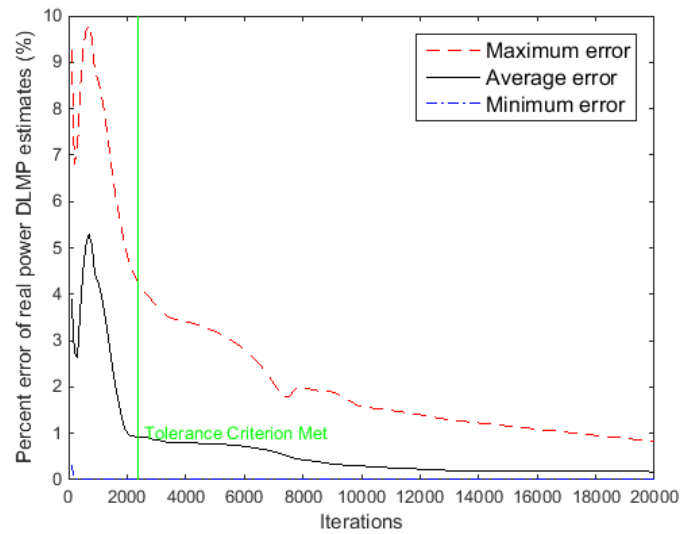


Figure 6-11: Minimum, average and maximum percent deviation of real power price estimates across all buses from the optimal value across iterations.

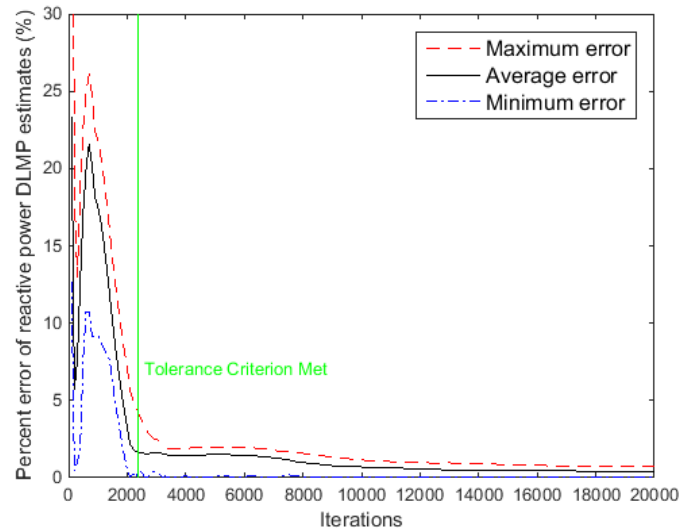


Figure 6-12: Minimum, average and maximum percent deviation of reactive power price estimates across all buses from the optimal value across iterations.

Figure 6-13 below, zooms into Figures 6-11 and 6-12 above, to show the percent deviation of real and reactive power price estimates many iterations after the tolerance

criterion is met.

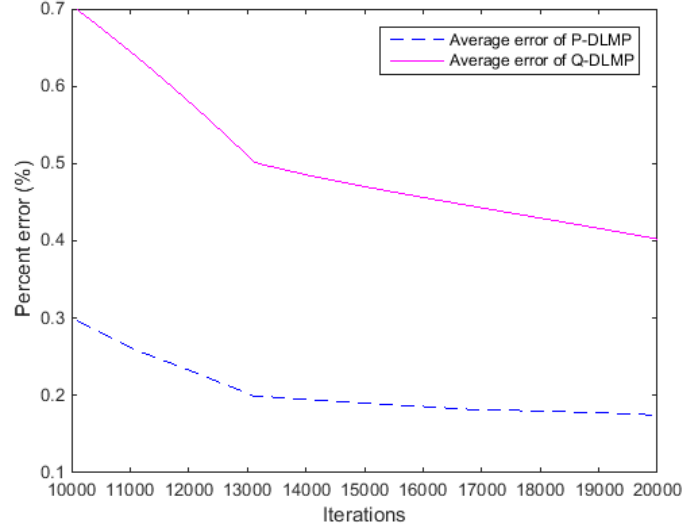


Figure 6-13: Average percent deviation of the real and reactive power price estimates across all buses from the optimal value long after convergence.

We conclude that the slow convergence of the individual $\mu_b^i(h)$ values propagates to a decreased rate of convergence of the real and reactive power marginal costs.

To proceed, we show the discrepancy in satisfying the first order optimality constraints 6.23. In specific, the figure below shows the maximum and average values of the ratio $\frac{100 \cdot \epsilon_b^P(i)(h)}{\pi_b^{P,i}(h)}$ across iterations and over all distribution buses.

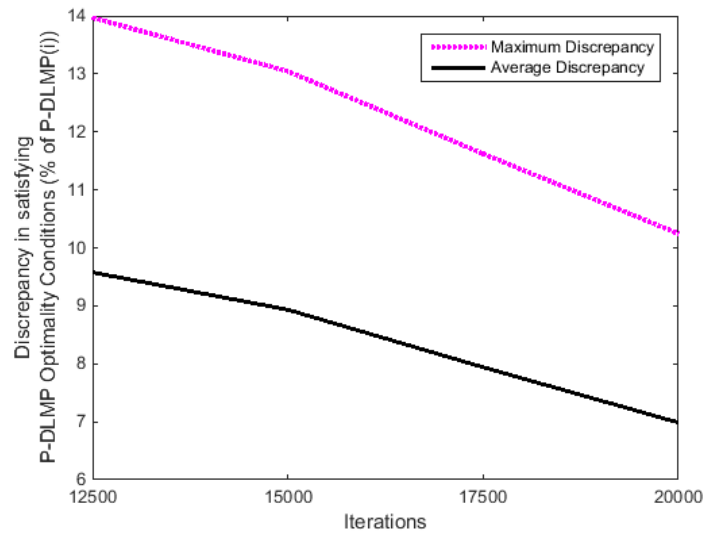


Figure 6-14: Deviation in satisfying first order optimality conditions of real power DLMPs as a percentage of the benchmark real power DLMP.

The results of the proposed price estimate correction process follow below. First, voltage bound inequality constraints' shadow prices are corrected through 6.25 and 6.27 as shown in Figure 6-15 below. Figure 6-15 only shows buses that correspond to non-zero voltage magnitude shadow prices for at least one of the methods that we compare.

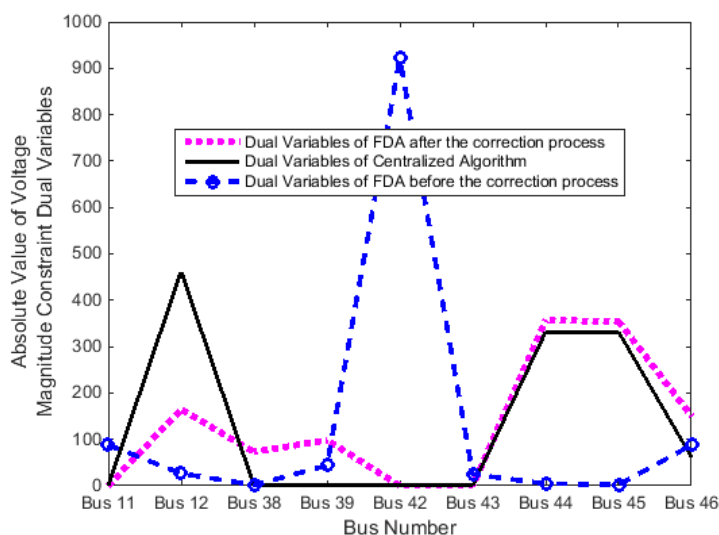


Figure 6-15: Shadow prices of voltage bound constraints, before and after the correction process.

Compared to the optimal solution, obtained by the centralized solution, that we use as a benchmark, the correction process results in 2 additional buses appearing to be binding, versus 4 additional buses in the unassisted FDA results. For the 2 additional buses, the shadow prices assigned are very small. Interestingly, the sum of the voltage magnitude shadow prices after the correction process is still equal to the optimal sum, even if we do not constrain it explicitly in 6.25 and 6.27.

We conclude the reporting of results of the correction process by showing the resulting corrected price estimates. Specifically, as described above, we feed the corrected voltage magnitude shadow prices in 5.26 and 5.27 and get updated price estimates, that are closer to the optimal DLMPs. Figure 6-16 overlays the average deviation of the updated price estimates after the correction process to the average deviation of the unassisted price estimates shown in Figure 6-13 above.

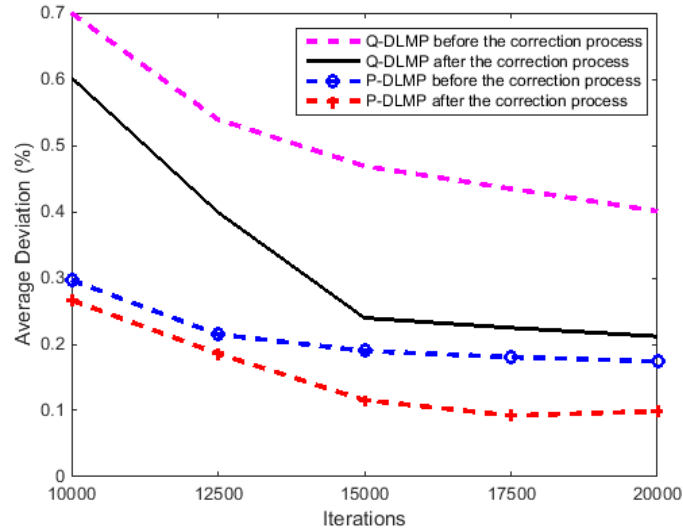


Figure 6-16: Average percent deviation of real and reactive power price estimates from the optimal values before and after the correction process.

Lastly, we present results when using FDA with soft voltage constraints for congested instances. Note that our benchmark results are now different, since they are based on the centralized formulation with soft voltage constraints. We choose the parameters in the voltage barrier function to be such that the voltage magnitudes in the new optimal solution will be as close to the voltages in the original optimal solution with the hard voltage bound inequality constraints.

The two figures below show the superior convergence performance of FDA with soft voltage constraints by means of the maximum and average percent deviation of real power price estimates as compared to the benchmark values obtained from the centralized algorithm with soft voltage constraints.

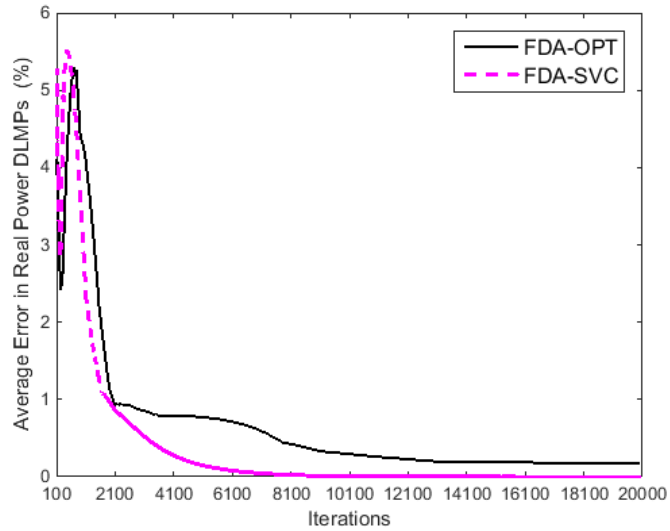


Figure 6-17: Fully Distributed Algorithms, Average Error in Real power DLMPs across iterations (%)

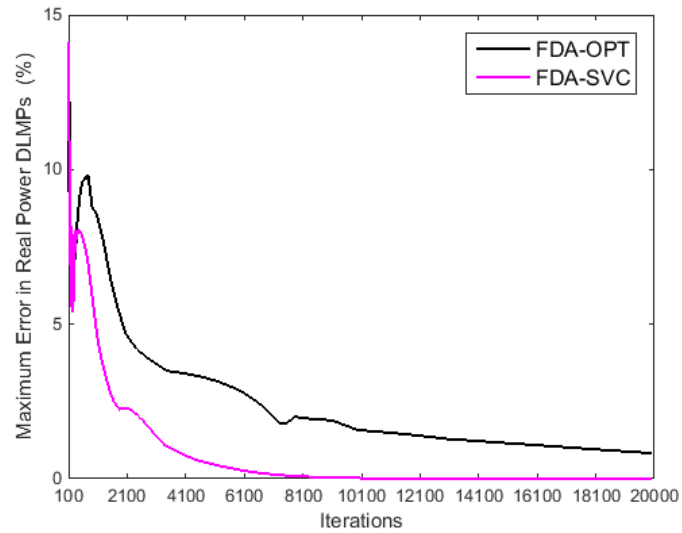


Figure 6-18: Fully Distributed Algorithms, Maximum Error in Real power DLMPs across iterations (%)

The FDA with soft voltage constraints is able to converge fully (accuracy of 0.1% error in the prices) to the centralized benchmark after 7500 iterations. FDA-OPT (FDA with hard voltage bound constraints) is unable to reach this level of accuracy

even after 50000 iterations. Therefore, the computational effort improvement of using soft voltage constraints is at least 6 times.

We repeat our clarification that the deviations of FDA-OPT are based on the benchmark values of C-OPT and the deviations of FDA-SVC are based on the benchmark values of C-SVC.

6.2 Partially Distributed Algorithm (PDA): Distributed DER Scheduling and Centralized Power Flow

This section presents the second distributed algorithm proposed in this thesis, called Partially Distributed Algorithm (PDA). As in FDA, DERs still solve individual cost minimization problems in parallel. The subproblems' objective is the minimization of the DER individual costs plus what the DERs pay for real and reactive power. Contrary to FDA, in PDA, line currents, flows, losses, voltage magnitudes and price estimates are calculated centrally.

6.2.1 Problem Formulation with Hard Voltage Bound Constraints

The FDA subproblems were shown to be equivalent to the subproblems of classic dual decomposition in the sense that they are cost minimization problems for each device or line. This interpretation motivates the Partially Distributed Algorithm (PDA) formulation.

PDA is composed of two steps:

1. DERs self-schedule in parallel, solving cost minimization problems identical to dual decomposition subproblems. In other words, the objective functions of the DER subproblems used in PDA will not include the second-norm-squared augmentation terms that DER and line/ transformer subproblems in FDA included. In PDA, DERs aim at minimizing their individual costs plus what they

pay for real and reactive power based on price estimates they receive from the system operator.

2. The second step includes the update of these price estimates. The system operator receives the DER tentative schedules and uses them to calculate real and reactive flows on lines, voltage magnitudes, and ex-post marginal costs in a centralized fashion, i.e. for all distribution lines and buses together. These quantities can be calculated by the system operator in two equivalent ways:

- (a) Solve a load flow problem to obtain real and reactive power flows and voltage magnitudes and then, insert them into 5.26 and 5.27 to obtain ex-post marginal costs.
- (b) Solve a mock centralized market clearing problem, where DER schedules are fixed to the tentative solution of the individual DER subproblems. The primal solution of this problem is the real and reactive power flows and the voltage magnitudes, while the dual solution is the ex-post marginal costs.

In other words, in PDA the coupling constraints are not relaxed.

The price estimates that the DERs base their scheduling decisions on are based on the ex-post marginal costs that the system operator determined in the previous iteration. If the price estimates of the current iteration are set equal to the ex-post marginal costs of the previous iteration, oscillatory behavior might occur. To this end, more smooth price estimate updates should be implemented. Based on (Caramanis and Foster, 2011), the price estimate of the current iteration is based on the price estimate of the previous iteration, the ex-post marginal costs of the previous iteration as well as a stepsize. This method of price estimate updates has the same functionality as the augmentation terms in the DER and line/ transformer subproblems' objective

functions: oscillation avoidance and convergence robustification. In other words, in both distributed algorithms, oscillations are avoided in different but equivalent ways.

PDA-OPT is described below, using the mock centralized power market with fixed DER injections approach to determine ex-post marginal costs:

PDA-OPT: Partially Distributed Algorithm with Hard voltage bound constraints

1. Initialize $i \leftarrow 1$.
2. For $\alpha \in D, G, E, F$ solve:

$$\underset{P_\alpha(h), Q_\alpha(h)}{\text{minimize}} \sum_h f(P_\alpha(h), Q_\alpha(h)) + \hat{\pi}_b^{P,i}(h) \cdot P_\alpha(h) + \hat{\pi}_b^{Q,i}(h) \cdot Q_\alpha(h) \quad (6.31)$$

$$\text{subject to DER capacity constraints} \quad (6.32)$$

3. The Distribution System Operator calculates the power flow:

minimize

$$\begin{aligned} & \sum_h \pi_\infty^P(h) \cdot P_\infty(h) + \pi_\infty^{OC}(h) \cdot (C_\infty - \sqrt{C_\infty^2 - Q_\infty^2}) \\ & + \sum_{(b,b'),h} f_{b,b'}(P_{b,b'}(h), Q_{b,b'}(h), P_{b',b}(h), Q_{b',b}(h)) \end{aligned} \quad (6.33)$$

subject to equality constraints (5.2)-(5.7) $\rightarrow \pi_b^{P,i}(h), \pi_b^{Q,i}(h)$

and inequality constraints (5.8)

4. Convergence check: if $\max_{b,h}(\hat{\pi}_b^{P,i}(h) - \pi_b^{P,i}(h)) \leq \text{tolerance}$ & $\max_{b,h}(\hat{\pi}_b^{Q,i}(h) - \pi_b^{Q,i}(h)) \leq \text{tolerance}$, break.
5. DLMP estimate update mindful of oscillation avoidance and convergence:
 $\hat{\pi}_b^{P,i+1}(h) = (1 - s(i)) \cdot \hat{\pi}_b^{P,i}(h) + s(i) \cdot \pi_b^{P,i}(h)$ and $\hat{\pi}_b^{Q,i+1}(h) = (1 - s(i)) \cdot$

$$\hat{\pi}_b^{Q,i}(h) + s(i) \cdot \pi_b^{Q,i}(h).$$

6. If tolerance criterion satisfied, terminate. Else, $i \leftarrow i + 1$ and go to 2.

We use $\hat{\pi}_b^{P,i}(h)$ and $\hat{\pi}_b^{Q,i}(h)$ for price estimates, and $\pi_b^{P,i}(h), \pi_b^{Q,i}(h)$ for ex-post marginal costs that appear as the shadow prices of energy balance constraints.

6.2.2 DER Subproblems

We notice that in fact, some subproblems have an even more interesting interpretation than the general cost minimization explanation. Take for example the subproblem of a photovoltaic, that has $f_\alpha(P_\alpha(h), Q_\alpha(h)) = 0$, which is written as:

$$\underset{P_\alpha(h), Q_\alpha(h)}{\text{minimize}} \sum_h \hat{\pi}_b^P(h) \cdot P_\alpha(h) + \hat{\pi}_b^Q(h) \cdot Q_\alpha(h)$$

$$\text{subject to } P_\alpha^2(h) + Q_\alpha^2(h) \leq C_\alpha^2 \rightarrow \kappa_\alpha(h)$$

$$P_\alpha(h), Q_\alpha(h) \leq 0$$

Then the Lagrangian is written as:

$$\mathcal{L} = \sum_h \hat{\pi}_b^P(h) \cdot P_\alpha(h) + \hat{\pi}_b^Q(h) \cdot Q_\alpha(h) + \kappa_\alpha(h) \cdot (P_\alpha^2(h) + Q_\alpha^2(h) - C_\alpha^2)$$

The optimal solution to this subproblem is found by taking the partial derivative of the Lagrangian with respect to, first, $P_\alpha(h)$ and then $Q_\alpha(h)$:

$$0 = \hat{\pi}_b^P(h) + 2 \cdot \kappa_\alpha(h) \cdot P_\alpha(h)$$

and

$$0 = \hat{\pi}_b^Q(h) + 2 \cdot \kappa_\alpha(h) \cdot Q_\alpha(h)$$

that can be combined to:

$$\frac{\hat{\pi}_b^Q(h)}{\hat{\pi}_b^P(h)} = \frac{Q_\alpha(h)}{P_\alpha(h)} \tag{6.34}$$

The ratio of the price estimates that a photovoltaic sees is equal to the ratio of optimal outputs in response to these prices.

Similar results can be extended to a microgenerator subproblem, namely:

$$\underset{P_\alpha(h), Q_\alpha(h)}{\text{minimize}} \sum_h -c_\alpha(h) \cdot P_\alpha(h) + \hat{\pi}_b^P(h) \cdot P_\alpha(h) + \hat{\pi}_b^Q(h) \cdot Q_\alpha(h)$$

$$\text{subject to } P_\alpha^2(h) + Q_\alpha^2(h) \leq C_\alpha^2$$

$$P_\alpha(h), Q_\alpha(h) \leq 0$$

that yields with similar logic:

$$\frac{\hat{\pi}_b^Q(h)}{\hat{\pi}_b^P(h) - c_\alpha} = \frac{Q_\alpha(h)}{P_\alpha(h)} \quad (6.35)$$

These equations can be used as closed-form solutions to the subproblems.

6.2.3 Stepwise Updates

The formulation above implies the use of an adaptive stepsize. As is common in the literature, for our price update we use the following stepsizes $s(i)$:

$$s(i) = \begin{cases} \text{constant, } s(i) = s, \forall i \\ \text{diminishing, } s(i) = \left(\frac{k_{11}}{i}\right)^{k_{12}}, k_{12} \leq 1 \end{cases} \quad (6.36)$$

The choice of a good constant stepsize is not an easy task. Large stepsizes can lead to divergence, while smaller stepsizes can result in slow convergence. This is the reason why we use a diminishing stepsize; it will be large in the beginning to get close to the optimal solution faster and then it will be slow to allow the algorithm to find the optimal solution and not diverge. Our diminishing stepsize satisfies $\lim_{i \rightarrow \infty} s(i) = 0$ and $\sum_i s(i) = \infty$, thereby guaranteeing convergence.

Additionally, to more effectively deal with oscillations, we use stepsize update

rules that are based on the direction of the price changes. This results in stepsizes specific to each hour and bus as well as quantity (real or reactive power) at each iteration. We show the process for real power, but the same can be applied for reactive power.

1. Calculate $\Delta\pi_b^{P,i}(h) = \hat{\pi}_b^{P,i}(h) - \pi_b^{P,i}(h)$

2. Update stepsize based on price trends:

$$s_b^{P,i} = \min\{s_b^{P,1}, s_b^{P,i-1} \cdot (k_{13} \cdot \mathbf{1}_{\Delta\pi_b^{P,i}(h) \cdot \Delta\pi_b^{P,i-1}(h) \geq 0} + k_{14} \cdot \mathbf{1}_{\Delta\pi_b^{P,i}(h) \cdot \Delta\pi_b^{P,i-1}(h) \leq 0})\},$$

where $k_{13} \geq 1$ and $0 \leq k_{14} \leq 1$.

3. Update prices as before using $\hat{\pi}_b^{P,i+1}(h) = \hat{\pi}_b^{P,i}(h) + s_b^{P,i}(h) \cdot \Delta\pi_b^{P,i}(h)$.

6.2.4 PDA modeling Voltage Bound Constraints with a Barrier Function

In section 5.4 we discussed how the hard voltage bound inequality constraints can result in the centralized algorithm being infeasible. Even if the socially optimal solution with hard voltage bound constraints is feasible, i.e. C-OPT is feasible, it is straightforward to see that intermediate steps of PDA-OPT might not be feasible since Step 3, where ex-post marginal costs are calculated, requires the solution of a load flow (or mock OPF) with hard voltage bound constraints. Therefore, voltage barrier functions have an additional use to PDA.

The formulation with voltage barrier functions is based on the corresponding centralized formulation of Chapter 5. The process is detailed below, and only differs from the PDA formulation with hard voltage constraints in Steps 3 and 5. We refer to this algorithm as PDA-SVC, standing for Soft Voltage Constraints.

PDA-SVC: Partially Distributed Algorithm with Soft Voltage Bound Constraints.

1. Initialize $i \leftarrow 1$.
2. For $\alpha \in D, G, E, F$ solve:

$$\underset{P_\alpha(h), Q_\alpha(h)}{\text{minimize}} \sum_h f(P_\alpha(h), Q_\alpha(h)) + \hat{\pi}_b^{P,i}(h) \cdot P_\alpha(h) + \hat{\pi}_b^{Q,i}(h) \cdot Q_\alpha(h) \quad (6.37)$$

$$\text{subject to DER capacity constraints} \quad (6.38)$$

3. The Distribution System Operator calculates the power flow:

$$\begin{aligned} \underset{v_\infty(h)}{\text{minimize}} \sum_h \pi_\infty^P(h) \cdot P_\infty(h) + \pi_\infty^{OC}(h) \cdot (C_\infty - \sqrt{C_\infty^2 - Q_\infty^2}) \\ + \sum_{b,h} k_{6,b} \cdot (\exp(k_{7,b} \cdot (v_b(h) - \bar{v})) + (\exp(k_{8,b} \cdot (v(h) - v_b))) \\ + \sum_{(b,b'),h} f_{b,b'}(P_{b,b'}(h), Q_{b,b'}(h), P_{b',b}(h), Q_{b',b}(h)) \quad (6.39) \end{aligned}$$

subject to equality constraints (5.2)-(5.7) $\rightarrow \pi_b^{P,i}(h), \pi_b^{Q,i}(h)$

4. Convergence check: if $\max_{b,h} (\hat{\pi}_b^{P,i}(h) - \pi_b^{P,i}(h)) \leq \text{tolerance}$ and $\max_b (\hat{\pi}_b^{Q,i}(h) - \pi_b^{Q,i}(h)) \leq \text{tolerance}$, break.
5. DLMP estimate update mindful of oscillation avoidance and convergence:
 $\hat{\pi}_b^{P,i+1}(h) = (1 - s(i)) \cdot \hat{\pi}_b^{P,i}(h) + s(i) \cdot \pi_b^{P,i}(h)$ and $\hat{\pi}_b^{Q,i+1}(h) = (1 - s(i)) \cdot \hat{\pi}_b^{Q,i}(h) + s(i) \cdot \pi_b^{Q,i}(h)$.
6. If tolerance criterion satisfied, terminate. Else, $i \leftarrow i + 1$ and go to 2.

6.2.5 Numerical Results using PDA

For the numerical results of PDA, we use an uncongested instance of the 800-bus network and a congested instance of the 47-bus network.

PDA Results on Uncongested Networks

Convergence of the PDA with either soft or hard voltage constraints to the uncongested instance of the 47 bus network is achieved after a couple of iterations only. Therefore, in this section we proceed to show convergence results of the 800 bus distribution network.

First, we show in Table 6.6 below that the ratios of the price estimates and the ratios of the outputs for photovoltaics indeed are equal. Table 6.6 shows all hours with non-zero irradiation.

Hour	Price Ratio	Output ratio
4am	0.048397	0.048397
5am	0.129386	0.129386
6am	0.162562	0.162562
7am	0.200072	0.200072
8am	0.268259	0.268259
9am	0.282382	0.282382
10am	0.28858	0.28858
11am	0.312838	0.312838
12pm	0.349725	0.349725
1pm	0.381179	0.381179
2pm	0.389191	0.38919
3pm	0.434982	0.434983
4pm	0.539158	0.539158
5pm	0.571462	0.571462
6pm	0.452549	0.452549
7pm	0.416436	0.416436

Table 6.6: Ratio of price estimates (reactive over real) and ratio of outputs (reactive over real) for a photovoltaic subproblem in PDA are equal.

In the PDA with hard voltage constraints, we notice that the prices of buses whose voltage binds might exhibit oscillatory behavior. In particular, we see that in the benchmark results of the 800 bus network, obtained by the solution of C-OPT,

in the neighborhood of a binding bus, there are two other buses that are marginally not binding. PDA results in the binding voltage being assigned periodically to one of three neighboring buses, as Figure 6-19 reveals. Given the effect of voltage binding constraints on DLMPs revealed by (5.26) and (5.27), the voltage oscillations result in real power price deviations. Figure 6-20 shows these price deviations by showing the real power ex-post marginal costs $\hat{\pi}_b^{P,i}(h)$.

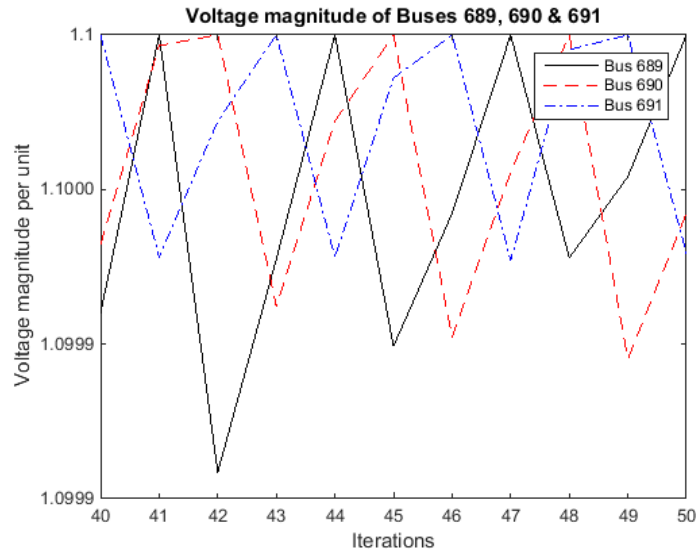


Figure 6-19: Partially Distributed Algorithm with Hard Voltage Constraints, Oscillations of Voltage Magnitude results, Bus 689, 690 and 691, Hour 2pm.

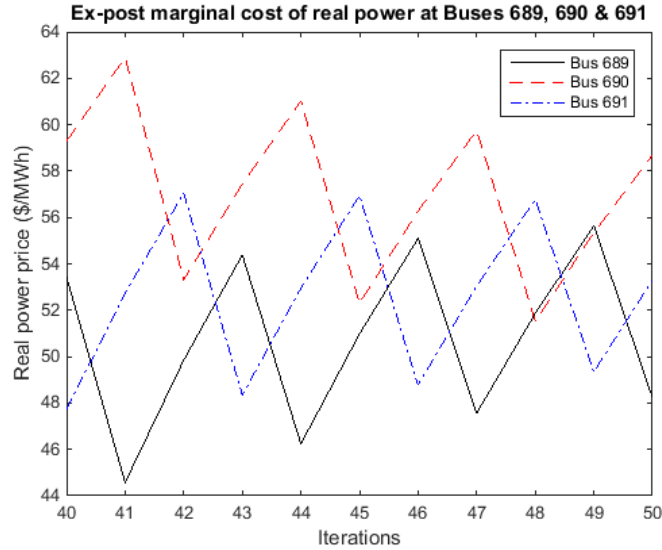


Figure 6-20: Partially Distributed Algorithm with Hard Voltage Constraints, Oscillations of Real power ex-post marginal costs across iterations, Bus 689, 690 and 691, Hour 2pm.

We also note that the sum of the voltage magnitude shadow prices over these three buses is equal to the voltage magnitude shadow price of the true binding bus, as decided by the centralized solution with hard voltage constraints.

With this motivation, we proceed to show results on the 800 bus network using PDA with soft voltage constraints.

The figures below show the maximum (across buses) percent difference between the price estimate and the ex-post marginal costs, i.e. shadow prices of power balance constraints, at the same iteration. The results in these figures refer to the peak hour i.e. the hour in the 24- hour horizon when demand, summed over all buses, is highest. They converge to zero, as does the percent deviation of the ex-post marginal costs to the optimal DLMPs of the centralized solution.

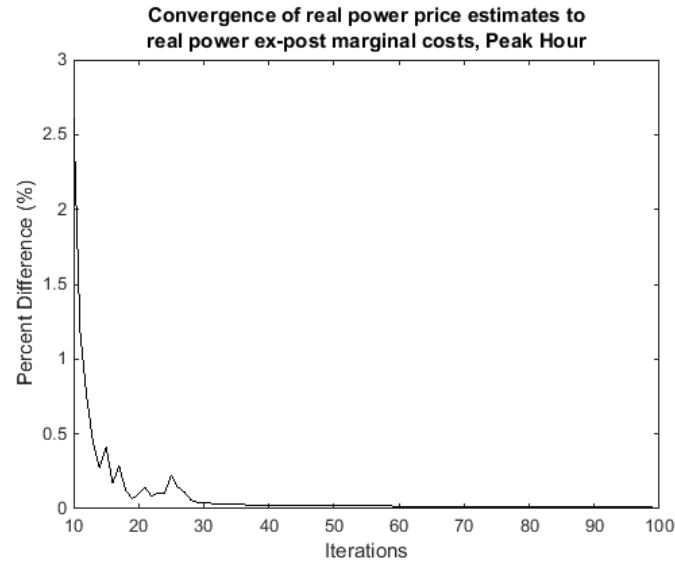


Figure 6-21: Partially Distributed Algorithm with Soft Voltage Bound Constraints, Maximum deviation of Real power price estimates to real power ex-post marginal costs across buses and iterations, Peak Hour.

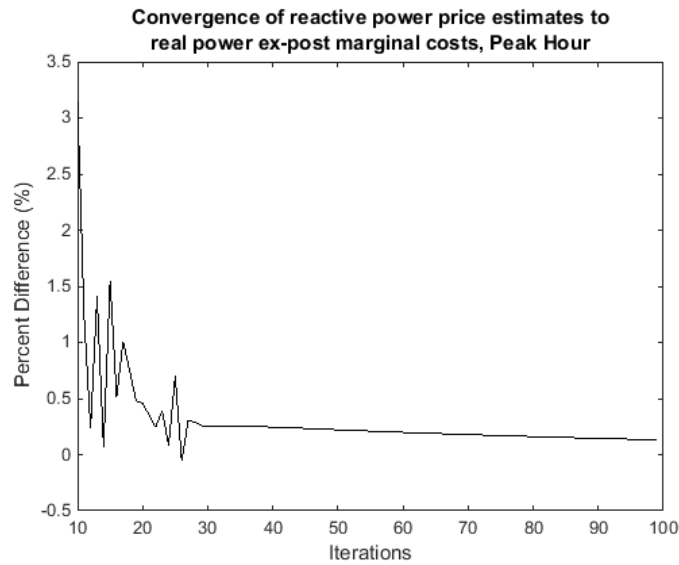


Figure 6-22: Partially Distributed Algorithm with Soft Voltage Bound Constraints, Maximum deviation of Reactive power price estimates to reactive power ex-post marginal costs across buses and iterations, Peak Hour.

The oscillation avoidance achieved by the replacement of hard voltage constraints

with voltage barrier functions provides another benefit of using soft rather than hard voltage magnitude bound constraints.

PDA Results on Congested Networks

First and foremost, we mention the inability of the PDA formulation with hard voltage bound constraints to solve many congested instances on the 47-bus network. Therefore, the results that follow are with the use of the PDA with soft voltage constraints. The figures that follow show the convergence of the average error in the real and reactive power prices, as well as voltage magnitudes. Exact convergence is observed after about 400 iterations only.

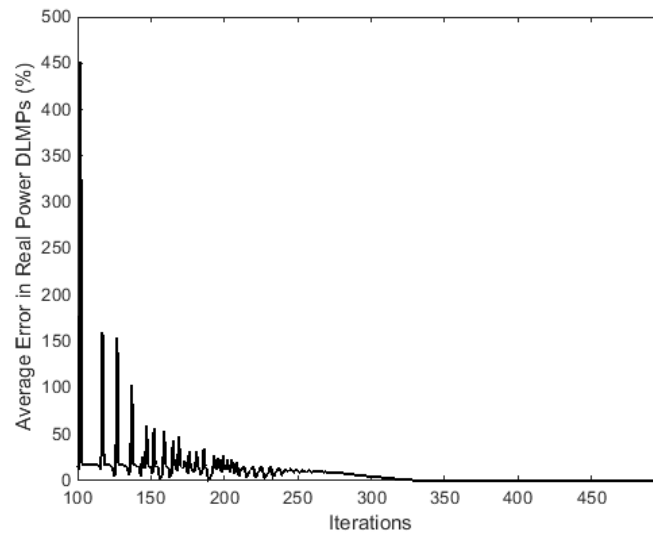


Figure 6-23: Average percent deviation of real power price estimates from the optimal value across all buses and iterations using PDA with SVC.

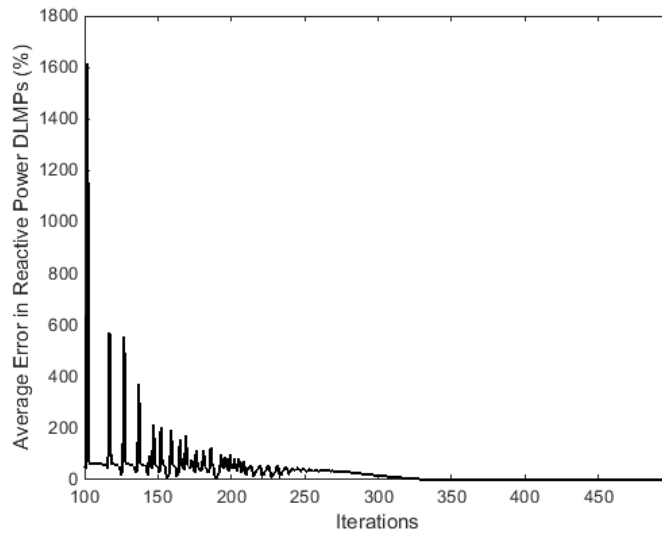


Figure 6-24: Average percent deviation of reactive power price estimates from the optimal value across all buses and iterations using PDA with SVC.

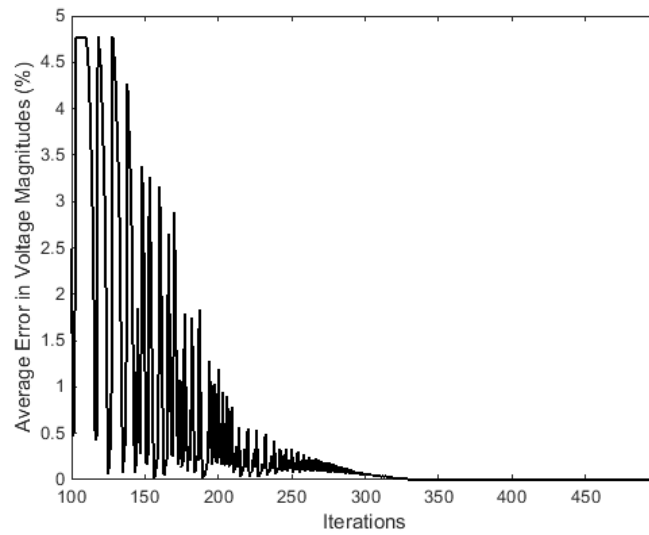


Figure 6-25: Average percent deviation of voltage magnitude iterates from the optimal value across all buses and iterations using PDA with SVC.

The behavior of the convergence curves of the real and reactive prices is a result of the price estimate update that we perform after the solution of the power flow

problem (namely step 5 of PDA-SVC in section 6.2.4 above). The decline in prices is steeper in the first iterations since we use a decreasing stepsize, specifically $s(i) = 10/i$. Convergence is smoother in Figures 6-21 and 6-22 since for our 800 bus simulations we used a stepsize based on the direction of price changes.

6.3 Comparison of FDA and PDA results

In this section, we compare the computational burden of FDA and PDA for congestion conditions, by comparing the number of iterations needed for convergence. One iteration of the FDA algorithm requires the solution of $|A| + |H|$ subproblems, all of which can be executed in parallel. (We assume that the bus level calculations of penalties, prices and imbalances are computationally trivial.) One iteration of PDA consists of the solution of $|A|$ problems, that are parallelizable, plus the centralized load flow that follows.

Figure 6-26 below shows the first 500 iterations of the proposed PDA-SVC, that are actually adequate for absolute convergence to the benchmark, together with the first 500 iterations of the fully distributed algorithms FDA-OPT and FDA-SVC. It can be seen that there is an overall benefit of more than 100 times.

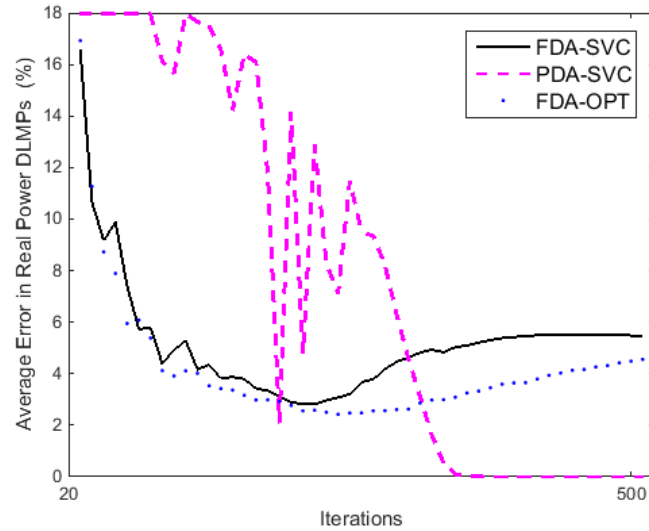


Figure 6-26: Comparison of Average Real power DLMP estimate deviation from the optimal DLMPs during 500 first iterations (%)

Based on our numerical results, we conclude that:

1. Congested instances are much harder to solve than non-congested ones, using either FDA or PDA.
2. PDA-SVC is generally faster than FDA-SVC.
3. FDA-SVC outperforms FDA-OPT.
4. We cannot easily compare FDA-OPT to PDA-OPT, since the latter is prone to infeasibilities of intermediate iterations.

Chapter 7

Reserves

7.1 Reserves in Distribution Power Markets

The increasing integration of renewables is introducing uncertainty to the generation side and mandates increased reserve requirements to deal with the volatility. Given how costly it is to procure these additional reserves from traditional transmission-network connected devices, the literature has proposed the provision of regulation reserves from demand- side connected entities. (Bilgin, 2014) studies the provision of regulation reserves by building loads. (Foster, 2012) discusses the provision of regulation reserves from electric vehicles. In this chapter, we expand this to all non-intermittent DERs like microgeneration and incorporate it in our Day Ahead Distribution Power Market Clearing algorithm.

Before we proceed, we elaborate on a crucial difference between reserves as a transmission power market product and reserves as a distribution power market product. In transmission power markets, where line capacity limits are imposed, the amount of reserves committed in Day ahead and Hour Ahead markets might not be deliverable in real time, if the additional reserve injections result in violations of the line flow capacity constraints. On the other hand, in distribution power markets it is nodal voltage bounds that can make reserves committed in the day ahead or hour ahead markets undeliverable in real time. This happens when the additional reserve injections drive voltages outside the bounds (Caramanis et al., 2016). This difference stems from the different definition of congestion in transmission and dis-

tribution networks. Transmission network congestion, refers to binding line capacity constraints, while distribution network congestion, refers to binding nodal voltage bound constraints, as discussed in Chapter 5.

To address the infeasibilities that might result during the deployment of undeliverable reserves, we account for the "worst case scenario" in distribution power markets that include reserves. Specifically, we include three sets of power flow constraints:

1. Worst case below: $y = -1$, power flow constraints when all resources have to give the maximum amount of promised down reserves. Results in power flow variables $P_{b,b'}^{dn}(h), Q_{b,b'}^{dn}(h), v_b^{dn}(h), l_{b,b'}^{dn}(h)$.
2. Regulation signal $y = 0$, power flow constraints as in Chapter 4. Results in power flow variables $P_{b,b'}(h), Q_{b,b'}(h), v_b(h), l_{b,b'}(h)$.
3. Worst case above: $y = 1$, power flow constraints when all resources have to give the maximum amount of promised up reserves. Results in power flow variables $P_{b,b'}^{up}(h), Q_{b,b'}^{up}(h), v_b^{up}(h), l_{b,b'}^{up}(h)$.

Further, we assume that DERs can slightly adjust their reactive power output based on the value of the regulation signal, so as to deal more efficiently with voltages binding during reserve deployment. Our worst case scenario approach results in three values of the reactive power output $Q_\alpha^{dn}(h), Q_\alpha(h)$ and $Q_\alpha^{up}(h)$. Reactive power outputs for any intermediate value of the regulation signal y can be written as convex combinations of these three values.

7.1.1 Centralized Day-Ahead Distribution Power Market with Reserves

The centralized, day ahead market clearing problem with hard voltage bound constraints and reserve considerations, C-OPT+R, is described below. In addition to costs minimized in the objective function of C-OPT, 5.1, the objective function of

C-OPT+R maximizes the earnings of DERs for reserve provision, remunerated as the amount of reserves reaching the substation (provided reserves adjusted by losses) times the marginal price of reserves at the substation. The latter is assumed to be constant like the substation real power LMP. We also assume that reserves are symmetric and approximate the flow of reserves with $R_{b,b'}(h) = \frac{P_{b,b'}^{up}(h) - P_{b,b'}^{dn}(h)}{2}$. As a result, the flow of reserves at the substation is $R_\infty(h) = \frac{P_\infty^{up}(h) - P_\infty^{dn}(h)}{2}$. This flow of reserves at the substation is upstream, therefore based on our convention $R_\infty(h) \leq 0$. In the formulation that follows, we ignore costs associated with reserve provision from DERs (e.g., additional fuel costs to microgenerators from output modulation to match the regulation signal y).

The mathematical formulation of C-OPT+R is as follows:

$$\begin{aligned} & \text{minimize} && (5.1) + \sum_h \pi_\infty^R(h) \cdot \frac{P_\infty^{up}(h) - P_\infty^{dn}(h)}{2} && (7.1) \\ & P_\alpha(h), R_\alpha(h) \\ & Q_\alpha(h), Q_\alpha^{up}(h), Q_\alpha^{dn}(h) \\ & v_\infty(h), v_\infty^{up}(h), v_\infty^{dn}(h) \end{aligned}$$

+penalties for deviation of $Q_\alpha^{up}(h)$ and $Q_\alpha^{dn}(h)$ from $Q_\alpha(h)$ subject to

$$\begin{cases}
P_\alpha(h) - R_\alpha(h) + \sum_{b',(b,b') \in H_b} P_{b,b'}^{dn}(h) = 0 \rightarrow \pi_b^{P,dn}(h) \\
Q_\alpha^{dn}(h) + \sum_{b',(b,b') \in H_b} Q_{b,b'}^{dn}(h) = 0 \rightarrow \pi_b^{Q,dn}(h) \\
P_{b,b'}^{dn}(h) + P_{b',b}^{dn}(h) = R_{b,b'} \cdot l_{b,b'}^{dn}(h) \\
Q_{b,b'}^{dn}(h) + Q_{b',b}^{dn}(h) = X_{b,b'} \cdot l_{b,b'}^{dn}(h) \\
l_{b,b'}^{dn}(h) = \frac{(P_{b,b'}^{dn}(h))^2 + (Q_{b,b'}^{dn}(h))^2}{v_b^{dn}(h)} \\
v_{b'}^{dn}(h) = v_b^{dn}(h) - 2 \cdot (R_{b,b'} \cdot P_{b,b'}^{dn}(h) + X_{b,b'} \cdot Q_{b,b'}^{dn}(h)) + (R_{b,b'}^2 + X_{b,b'}^2) \cdot l_{b,b'}^{dn}(h) \\
\underline{v}_b \leq v_b^{dn}(h) \leq \bar{v}_b \rightarrow \underline{\mu}_b^{dn}(h), \bar{\mu}_b^{dn}(h) \\
v_\infty^{dn}(h) = v_\infty(h)
\end{cases} \quad (7.2)$$

$$\begin{cases}
P_\alpha(h) + \sum_{b',(b,b') \in H_b} P_{b,b'}(h) = 0 \rightarrow \pi_b^P(h) \\
Q_\alpha(h) + \sum_{b',(b,b') \in H_b} Q_{b,b'}(h) = 0 \rightarrow \pi_b^Q(h) \\
P_{b,b'}(h) + P_{b',b}(h) = R_{b,b'} \cdot l_{b,b'}(h) \\
Q_{b,b'}(h) + Q_{b',b}(h) = X_{b,b'} \cdot l_{b,b'}(h) \\
l_{b,b'}(h) = \frac{P_{b,b'}^2(h) + Q_{b,b'}^2(h)}{v_b(h)} \\
v_{b'}(h) = v_b(h) - 2 \cdot (R_{b,b'} \cdot P_{b,b'}(h) + X_{b,b'} \cdot Q_{b,b'}(h)) + (R_{b,b'}^2 + X_{b,b'}^2) \cdot l_{b,b'}(h) \\
\underline{v}_b \leq v_b(h) \leq \bar{v}_b \rightarrow \underline{\mu}_b(h), \bar{\mu}_b(h)
\end{cases} \quad (7.3)$$

$$\left. \begin{aligned}
& P_\alpha(h) + R_\alpha(h) + \sum_{b',(b,b') \in H_b} P_{b,b'}^{up}(h) = 0 \rightarrow \pi_b^{P,up}(h) \\
& Q_\alpha^{up}(h) + \sum_{b',(b,b') \in H_b} Q_{b,b'}^{up}(h) = 0 \rightarrow \pi_b^{Q,up}(h) \\
& P_{b,b'}^{up}(h) + P_{b',b}^{up}(h) = R_{b,b'} \cdot l_{b,b'}^{up}(h) \\
& Q_{b,b'}^{up}(h) + Q_{b',b}^{up}(h) = X_{b,b'} \cdot l_{b,b'}^{up}(h) \\
& l_{b,b'}^{up}(h) = \frac{(P_{b,b'}^{up}(h))^2 + (Q_{b,b'}^{up}(h))^2}{v_b^{up}(h)} \\
& v_{b'}^{up}(h) = v_b^{up}(h) - 2 \cdot (R_{b,b'} \cdot P_{b,b'}^{up}(h) + X_{b,b'} \cdot Q_{b,b'}^{up}(h)) + (R_{b,b'}^2 + X_{b,b'}^2) \cdot l_{b,b'}^{up}(h) \\
& \underline{v}_b \leq v_b^{up}(h) \leq \bar{v}_b \rightarrow \underline{\mu}_b^{up}(h), \bar{\mu}_b^{up}(h) \\
& v_\infty^{up}(h) = v_\infty(h)
\end{aligned} \right\} \quad (7.4)$$

Constraints 5.9, 5.10, 5.11, 5.13, 5.14, 5.16, 5.17, plus

$$R_\alpha \leq 0 \quad (7.5)$$

$$P_\alpha^2(h) + Q_\alpha^2(h) \leq C_\alpha^2 \quad (7.6)$$

$$(P_\alpha(h) + R_\alpha(h))^2 + (Q_\alpha^{up}(h))^2 \leq C_\alpha^2 \quad (7.7)$$

$$(P_\alpha(h) - R_\alpha(h))^2 + (Q_\alpha^{dn}(h))^2 \leq C_\alpha^2 \quad (7.8)$$

If DER generates real power (eg. microgenerators), $P_\alpha(h) \leq 0$, then:

$$P_\alpha(h) \leq R_\alpha(h) \leq 0, \alpha \in E \quad (7.9)$$

else if DER consumes real power (eg. electric vehicle), $P_\alpha(h) \geq 0$ then:

$$P_\alpha(h) \geq -R_\alpha(h) \geq 0, \alpha \in E \quad (7.10)$$

7.1.2 Distribution Locational Marginal Prices with Reserve Considerations

Having three sets of power flow equations means that we will have three prices for each key value of the regulation signal value for reactive power and for real power. The real power DLMPs for $y = 1$ and $y = -1$ have a limited interpretation apart from their relation to the reserves DLMP. There is a single reserves DLMP for all values of y equal to $\pi_b^R(h) = \pi_b^{P,dn}(h) + \pi_b^{P,up}(h)$.

Following the same process as in Chapter 5, we assume the existence of a costless, infinitesimal generator of one of the following: real power, reserves, reactive power when $y = -1$, reactive power when $y = 0$ and lastly, reactive power when $y = 1$. The unbundling of the prices is as follows:

- Real power marginal price components

$$\pi_b^P(h) = \begin{cases} \pi_\infty^P(h) \cdot \frac{\partial P_\infty(h)}{\partial P_{\dot{g}_\beta(h)}} + \frac{\pi_\infty^{OC}(h) \cdot Q_\infty(h)}{\sqrt{C_\infty^2 - Q_\infty^2(h)}} \cdot \frac{\partial Q_\infty(h)}{\partial P_{\dot{g}_\beta(h)}} + \\ \sum_{h_1 \geq h, (b,b') \in tr} C_{b,b'}^{tr} \cdot \frac{\partial \Gamma_{b,b'}(S_{b,b'}(h_1))}{\partial P_{\dot{g}_\beta(h)}} + \sum_b \mu_b(h) \cdot \frac{\partial v_b(h)}{\partial P_{\dot{g}_\beta(h)}} - \\ \sum_{(b,\alpha), \alpha \in F_b} \kappa_\alpha(h) \cdot 1_{v_b(h) < 1} \cdot C_\alpha \cdot \frac{\partial v_b(h)}{\partial P_{\dot{g}_\beta(h)}} \end{cases} .$$

- Reactive Power price marginal price components when $y = 0$

$$\pi_\beta^Q(h) = \begin{cases} \pi_\infty^P(h) \cdot \frac{\partial P_\infty(h)}{\partial Q_{\dot{g}_\beta(h)}} + \frac{\pi_\infty^{OC}(h) \cdot Q_\infty(h)}{\sqrt{C_\infty^2 - Q_\infty^2(h)}} \cdot \frac{\partial Q_\infty(h)}{\partial Q_{\dot{g}_\beta(h)}} + \\ \sum_{h_1 \geq h, (b,b') \in tr} C_{b,b'}^{tr} \cdot \frac{\partial \Gamma_{b,b'}(S_{b,b'}(h_1))}{\partial Q_{\dot{g}_\beta(h)}} + \sum_b \mu_b(h) \cdot \frac{\partial v_b(h)}{\partial Q_{\dot{g}_\beta(h)}} - \\ \sum_{(b,\alpha), \alpha \in F_b} \kappa_\alpha(h) \cdot 1_{v_b(h) < 1} \cdot C_\alpha \cdot \frac{\partial v_b(h)}{\partial Q_{\dot{g}_\beta(h)}} \end{cases} .$$

- Reactive power marginal price components when $y = -1$

$$\pi_b^{Q,dn}(h) = -\frac{\pi_\infty^R(h)}{2} \cdot \frac{\partial P_\infty^{dn}(h)}{\partial Q_{\dot{g}_\beta^{dn}(h)}} + \sum_b \mu_b^{dn}(h) \cdot \frac{\partial v_b^{dn}(h)}{\partial Q_{\dot{g}_\beta^{dn}(h)}} .$$

- Reactive power marginal price components when $y = 1$

$$\pi_b^{Q,up}(h) = \frac{\pi_\infty^R(h)}{2} \cdot \frac{\partial P_\infty^{up}(h)}{\partial Q_{\dot{g}_\beta^{up}(h)}} + \sum_b \mu_b^{up}(h) \cdot \frac{\partial v_b^{up}(h)}{\partial Q_{\dot{g}_\beta^{up}(h)}} .$$

- Reserves marginal price components

$$\pi_b^R(h) = \pi_\infty^R(h) \frac{\partial R_\infty(h)}{\partial R_{\hat{g}_\beta(h)}} + \sum_b \mu_b^{up}(h) \cdot \frac{\partial v_b^{up}(h)}{\partial R_{\hat{g}_\beta(h)}} + \sum_b \mu_b^{dn}(h) \cdot \frac{\partial v_b^{dn}(h)}{\partial R_{\hat{g}_\beta(h)}}, \text{ where } R_\infty = \frac{P_\infty^{up} - P_\infty^{dn}}{2} \leq 0.$$

7.1.3 Fully Distributed Algorithm with Reserves

In this section we repeat the Fully Distributed Algorithm of Chapter 6, with the addition of reserves. The derivation is similar to the derivation of the original FDA without reserves shown in Chapter 6.

FDA-OPT+R: Fully Distributed Algorithm with Hard voltage bound constraints and reserve considerations

1. Initialize $i \leftarrow 1$.
2. For $\alpha \in D, G, E, F$ solve:

$$\begin{array}{l} \text{minimize} \\ P_\alpha(h), R_\alpha(h), \\ Q_\alpha(h), Q_\alpha^y(h), \\ y \in up, dn \end{array} \sum_h \left\{ \begin{array}{l} f_a(P_a(h), Q_a(h)) \\ + \hat{\pi}_b^{P,i+1}(h) \cdot P_a(h) + \frac{\rho_P}{2} \cdot \|P_a(h) - P_a^i(h) + \hat{P}_b^i(h)\|_2^2 \\ + {}_y\hat{\pi}_b^{P,i+1}(h) \cdot P_a^y(h) + \frac{\rho_P^y}{2} \cdot \|P_a^y(h) - P_a^{y,i}(h) + \hat{P}_b^{y,i}(h)\|_2^2 \\ + \hat{\pi}_b^{Q,i+1}(h) \cdot Q_a(h) + \frac{\rho_Q}{2} \cdot \|Q_a(h) - Q_a^i(h) + \hat{Q}_b^i(h)\|_2^2 \\ + {}_y\hat{\pi}_b^{Q,i+1}(h) \cdot Q_a^y(h) + \frac{\rho_Q^y}{2} \cdot \|Q_a^y(h) - Q_a^{y,i}(h) + \hat{Q}_b^{y,i}(h)\|_2^2 \\ + \text{penalties for deviation of } Q_a^{up}(h) \text{ and } Q_a^{dn}(h) \text{ from } Q_a(h) \end{array} \right. \quad (7.11)$$

subject to DER capacity constraints and $P_a^{up}(h) = P_a(h) + R_a(h)$ and $P_a^{dn}(h) = P_a(h) - R_a(h)$.

3. For $(b, b') \in H$ solve:

$$\begin{aligned}
& \text{minimize} \sum_h \left\{ \begin{aligned}
& f_{b,b'}(P_{b,b'}(h), Q_{b,b'}(h), P_{b',b}(h), Q_{b',b}(h)) \\
& + \hat{\pi}_{b,b'}^{P,i}(h) \cdot P_{b,b'}(h) + \hat{\pi}_{b,b'}^{Q,i}(h) \cdot Q_{b,b'}(h) \\
& + \frac{\rho_P}{2} \cdot \|P_{b,b'}(h) - P_{b,b'}^i(h) + \hat{P}_b^i(h)\|_2^2 \\
& + \frac{\rho_Q}{2} \cdot \|Q_{b,b'}(h) - Q_{b,b'}^i(h) + \hat{Q}_b^i(h)\|_2^2 \\
& + \zeta_{b,b'}^i(h) \cdot v_{b,b'}(h) + \frac{\rho_v}{2} \cdot \|v_{b,b'}(h) - \hat{v}_b^i(h)\|_2^2 \\
& + {}_y\hat{\pi}_{b,b'}^{P,i}(h) \cdot P_{b,b'}^y(h) + {}_y\hat{\pi}_{b,b'}^{Q,i}(h) \cdot Q_{b,b'}^y(h) \\
& + \frac{\rho_P^y}{2} \cdot \|P_{b,b'}^y(h) - P_{b,b'}^{y,i}(h) + \hat{P}_b^{y,i}(h)\|_2^2 \\
& + \frac{\rho_Q^y}{2} \cdot \|Q_{b,b'}^y(h) - Q_{b,b'}^{y,i}(h) + \hat{Q}_b^{y,i}(h)\|_2^2 \\
& + {}_y\zeta_{b,b'}^i(h) \cdot v_{b,b'}^y(h) + \frac{\rho_v^y}{2} \cdot \|v_{b,b'}^y(h) - \hat{v}_b^{y,i}(h)\|_2^2 \\
& + \hat{\pi}_{b',b}^{P,i}(h) \cdot P_{b',b}(h) + \hat{\pi}_{b',b}^{Q,i}(h) \cdot Q_{b',b}(h) \\
& + \frac{\rho_P}{2} \cdot \|P_{b',b}(h) - P_{b',b}^i(h) + \hat{P}_{b'}^i(h)\|_2^2 \\
& + \frac{\rho_Q}{2} \cdot \|Q_{b',b}(h) - Q_{b',b}^i(h) + \hat{Q}_{b'}^i(h)\|_2^2 \\
& + \zeta_{b',b}^i(h) \cdot v_{b',b}(h) + \frac{\rho_v}{2} \cdot \|v_{b',b}(h) - \hat{v}_{b'}^i(h)\|_2^2 \\
& + {}_y\hat{\pi}_{b',b}^{P,i}(h) \cdot P_{b',b}^y(h) + {}_y\hat{\pi}_{b',b}^{Q,i}(h) \cdot Q_{b',b}^y(h) \\
& + \frac{\rho_P^y}{2} \cdot \|P_{b',b}^y(h) - P_{b',b}^{y,i}(h) + \hat{P}_{b'}^{y,i}(h)\|_2^2 \\
& + \frac{\rho_Q^y}{2} \cdot \|Q_{b',b}^y(h) - Q_{b',b}^{y,i}(h) + \hat{Q}_{b'}^{y,i}(h)\|_2^2 \\
& + {}_y\zeta_{b',b}^i(h) \cdot v_{b',b}^y(h) + \frac{\rho_v^y}{2} \cdot \|v_{b',b}^y(h) - \hat{v}_{b'}^{y,i}(h)\|_2^2
\end{aligned} \right. \\
& P_{b,b'}(h), Q_{b,b'}(h), v_{b,b'}(h), \\
& P_{b,b'}^y(h), Q_{b,b'}^y(h), v_{b,b'}^y(h) \\
& P_{b',b}(h), Q_{b',b}(h), v_{b',b}(h), \\
& P_{b',b}^y(h), Q_{b',b}^y(h), v_{b',b}^y(h), \\
& y \in up, dn
\end{aligned} \tag{7.12}$$

subject to line constraints (6.2), (6.3), (5.2), (5.6) and (5.7)

4. For all buses update:

$$\hat{\pi}_b^{P,i+1}(h) = \hat{\pi}_b^{P,i}(h) + \rho_P \cdot \hat{P}_b^{i+1}(h)$$

$$\begin{aligned}
{}_y \hat{\pi}_b^{P,i+1}(h) &= {}_y \hat{\pi}_b^{P,i}(h) + \rho_P \cdot \hat{P}_b^{y,i+1}(h) \\
\hat{\pi}_b^{Q,i+1}(h) &= \hat{\pi}_b^{Q,i}(h) + \rho_Q \cdot \hat{Q}_b^{i+1}(h) \\
{}_y \hat{\pi}_b^{Q,i+1}(h) &= {}_y \hat{\pi}_b^{Q,i}(h) + \rho_Q \cdot \hat{Q}_b^{y,i+1}(h) \\
\zeta_{b,b'}^{i+1}(h) &= \zeta_{b,b'}^i(h) + \rho_v \cdot (v_{b,b'}^{i+1}(h) - \hat{v}_b^{i+1}(h)) \\
{}_y \zeta_{b,b'}^{i+1}(h) &= {}_y \zeta_{b,b'}^i(h) + \rho_v \cdot (v_{b,b'}^{y,i+1}(h) - {}_y \hat{v}_b^{i+1}(h)) \\
v_b^{i+1}(h) &= \frac{\sum_{b',(b,b') \in H_b} v_{b,b'}^{i+1}(h)}{|H_b|} \\
\mu_b^{i+1}(h) &= \sum_{b',(b,b') \in H_b} \mu_{b,b'}^{i+1}(h) \\
v_b^{up,i+1}(h) &= \frac{\sum_{b',(b,b') \in H_b} v_{b,b'}^{up,i+1}(h)}{|H_b|} \\
\mu_b^{up,i+1}(h) &= \sum_{b',(b,b') \in H_b} \mu_{b,b'}^{up,i+1}(h) \\
v_b^{dn,i+1}(h) &= \frac{\sum_{b',(b,b') \in H_b} v_{b,b'}^{dn,i+1}(h)}{|H_b|} \\
\mu_b^{dn,i+1}(h) &= \sum_{b',(b,b') \in H_b} \mu_{b,b'}^{dn,i+1}(h)
\end{aligned}$$

5. If tolerance criterion satisfied, terminate.

Else, $i \leftarrow i + 1$ and go to 2.

The subproblems retain the same interpretation as the subproblems of FDA without reserves: they are cost minimization problems where additional market-based (price times quantity) costs for reserves are now considered.

7.1.4 Partially Distributed Algorithm with Reserves

This section elaborates on the Partially Distributed Algorithm with reserve considerations, which follows:

PDA-OPT+R: Partially Distributed Algorithm with Hard voltage bound constraints and reserve considerations

1. Initialize $i \leftarrow 1$.

2. For $a \in D, G, E, F$ solve:

$$\underset{P_\alpha(h), Q_\alpha(h), Q_\alpha^y(h), R_\alpha(h), y \in \text{up, dn}}{\text{minimize}} \sum_h \begin{cases} f_a(P_a(h), Q_a(h)) \\ + P_a(h) \cdot \hat{\pi}_b^{P,i}(h) + R_a(h) \cdot \hat{\pi}_b^{R,i}(h) \\ + Q_a(h) \cdot \hat{\pi}_b^{Q,i}(h) + Q_a^y(h) \cdot y \cdot \hat{\pi}_b^{Q,i}(h) \\ + \text{penalties for deviation of } Q_a^y(h) \text{ from } Q_a(h) \end{cases} \quad (7.13)$$

subject to DER capacity constraints.

3. The Distribution System Operator calculates the power flow:

minimize

$$\begin{aligned} \sum_h \pi_\infty^P(h) \cdot P_\infty(h) + \pi_\infty^{OC}(h) \cdot (C_\infty - \sqrt{C_\infty^2 - Q_\infty^2}) + \pi_\infty^R(h) \cdot \frac{P_\infty^{\text{up}} - P_\infty^{\text{dn}}}{2} \\ + \sum_{(b,b'),h} f_{b,b'}(P_{b,b'}(h), Q_{b,b'}(h), P_{b',b}(h), Q_{b',b}(h)) \end{aligned} \quad (7.14)$$

$$\text{subject to Power flow constraints (5.2)-(5.8)} \rightarrow \pi_b^{P,i}(h), \pi_b^{Q,i}(h) \quad (7.15)$$

$$7.2 \text{ and } 7.4 \rightarrow y \pi_b^{P,i}(h), y \pi_b^{Q,i}(h) \quad (7.16)$$

4. Convergence check: if $\max_{b,h}(\hat{\pi}_b^{P,i}(h) - \pi_b^{P,i}(h)) \leq \text{tolerance}$, $\max_{b,h}(\hat{\pi}_b^{Q,i}(h) - \pi_b^{Q,i}(h)) \leq \text{tolerance}$, $\max_{b,h}(y \hat{\pi}_b^{Q,i}(h) - y \pi_b^{Q,i}(h)) \leq \text{tolerance}$, $\max_{b,h}(\hat{\pi}_b^{R,i}(h) - \pi_b^{R,i}(h)) \leq \text{tolerance}$, break.

5. DLMP estimate update mindful of oscillation avoidance and convergence:

$$\begin{aligned} \pi_b^{R,i}(h) &=_{\text{up}} \pi_b^{P,i}(h) +_{\text{dn}} \pi_b^{P,i}(h) \\ \hat{\pi}_b^{R,i}(h) &= (1 - s(i)) \cdot \hat{\pi}_b^{R,i}(h) + s(i) \cdot \pi_b^{R,i}(h) \\ \hat{\pi}_b^{P,i+1}(h) &= (1 - s(i)) \cdot \hat{\pi}_b^{P,i}(h) + s(i) \cdot \pi_b^{P,i}(h) \\ \hat{\pi}_b^{Q,i+1}(h) &= (1 - s(i)) \cdot \hat{\pi}_b^{Q,i}(h) + s(i) \cdot \pi_b^{Q,i}(h). \end{aligned}$$

$${}_y\hat{\pi}_b^{Q,i+1}(h) = (1 - s(i)) \cdot {}_y\hat{\pi}_b^{Q,i}(h) + s(i) \cdot {}_y\pi_b^{Q,i}(h).$$

6. If tolerance criterion satisfied, terminate. Else, $i \leftarrow i + 1$ and go to 2.

7.2 Numerical Results

We proceed with results on the 47 bus network, using the centralized Day ahead algorithm C-OPT+R. The following three figures show the hourly evolution of real power DLMPs, reserves DLMPs and reactive power DLMPs respectively.

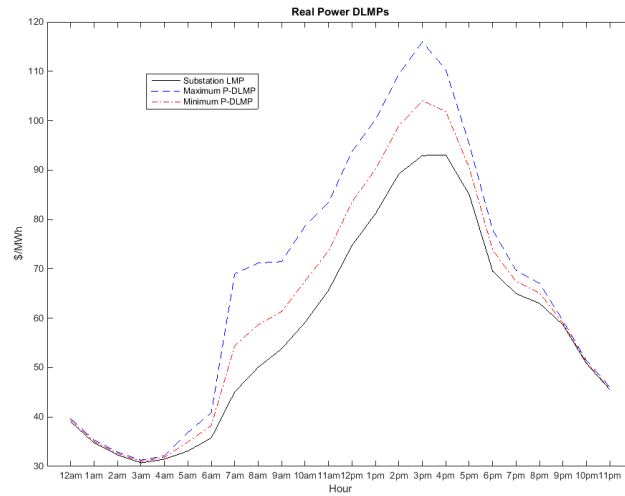


Figure 7.1: Hourly minimum, maximum and substation value of real power DLMP.

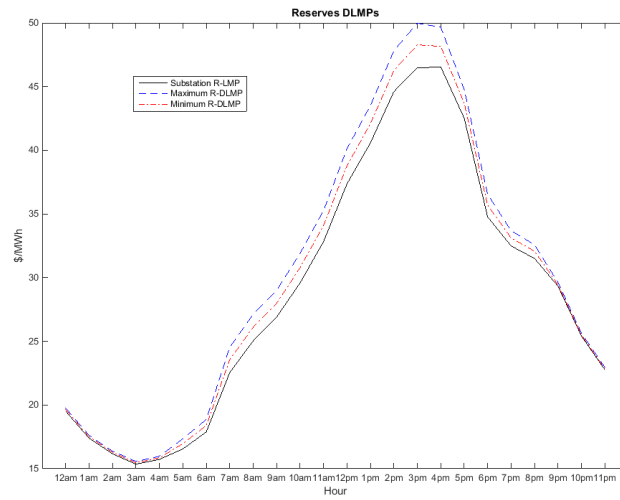


Figure 7.2: Hourly minimum, maximum and substation value of reserve DLMP.

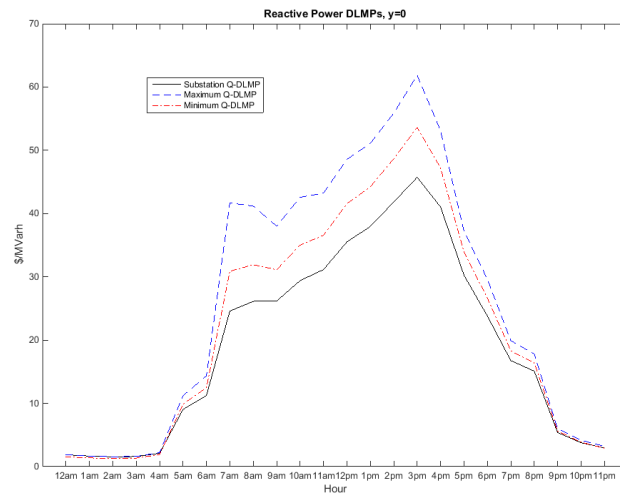


Figure 7.3: Hourly minimum, maximum and substation value of reactive power DLMP, $y=0$.

We notice that the minimum marginal price across all distribution buses is higher than the substation price for all products (real power, reactive power and reserves). This indicates that distribution demand is higher than DER injections and distribution flows are still downstream. When DERs injections are higher than the local bus

demand, then DLMPs can be lower than the substation LMP and the flows can be upstream. This is the case for the 800- bus network results presented in Chapter 5. If we increase DG capacity, we notice that the minimum value of the reserve DLMPs indeed becomes lower than the substation reserve LMP. This happens for the hours that there is export of real power from the distribution network to the transmission network, i.e. upstream flow at the substation at $y=0$. We proceed to show the real power flow on the substation line for the case of small DGs and larger DGs.

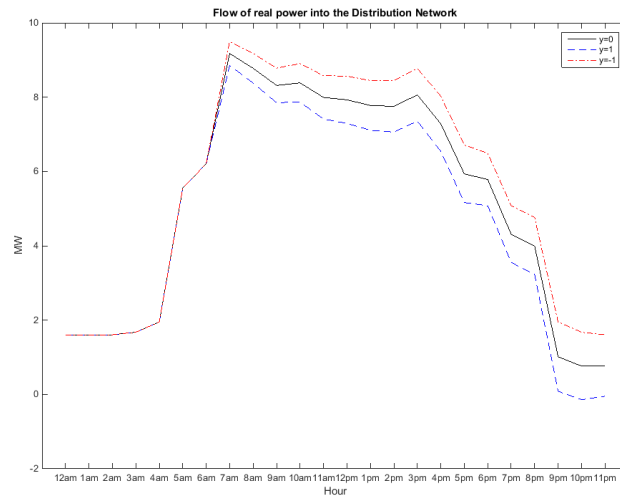


Figure 7-4: Flow of real power into the distribution network with small DGs present for the three key values of the regulation signal.

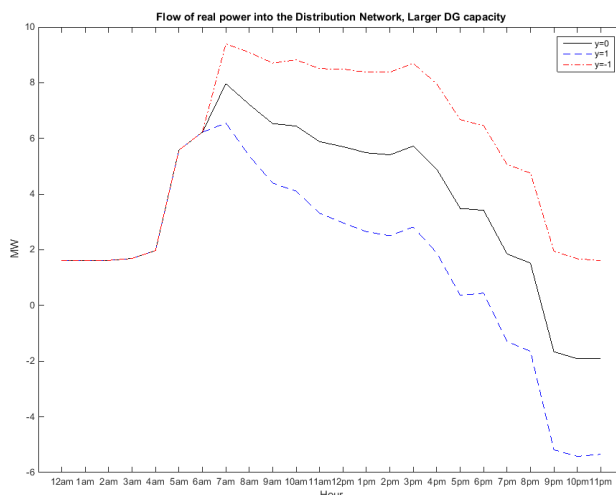


Figure 7-5: Flow of real power into the distribution network with larger DGs present for the three key values of the regulation signal.

During the hours of 10pm and 11pm, in the presence of small DGs, we only have net export of real power when the regulation signal is $y = 1$. As the preceding graphs show, DLMPs are always higher than LMPs in this case. On the other hand, for the hours of 10pm and 11pm, in the presence of larger DGs, we have net export of real power when the regulation signal is $y = 0$ and when the regulation signal is $y = 1$. This is indicated by the negative real power flows for $y = 0$ and $y = 1$ reported in Figure 7.5 above. In this case, DLMPs are lower than LMPs for the hours that net export is observed while $y = 0$.

The following three graphs show the unbundling of the marginal prices of real power, reactive power and reserves to their respective components at a selected distribution bus. We notice that the transformer loss of life is a significant contributor to the marginal prices. Also, the symmetry in providing up and down reserves is reflected in the components of the reserve DLMP: the $y = 1$ component makes up about half of the reserve DLMP, while the $y = -1$ component is the other half. The peak hour refers to the hour of the 24- hour horizon that has the highest demand,

summed over all buses.

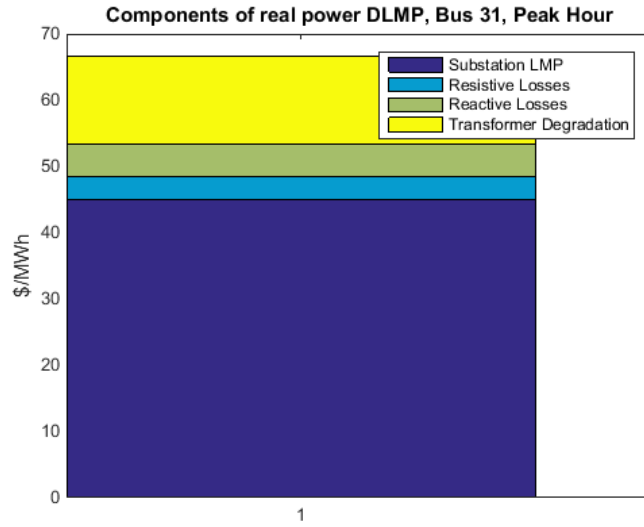


Figure 7·6: Components of the real power DLMP at Bus 31 during the peak hour.

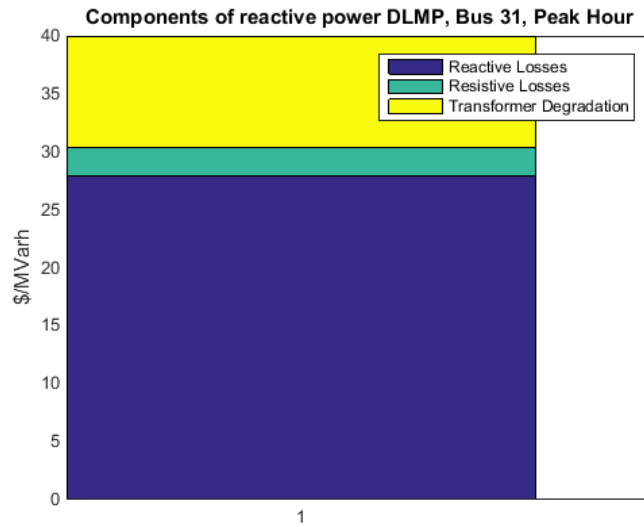


Figure 7·7: Components of the reactive power DLMP at Bus 31 during the peak hour, for $y=0$.

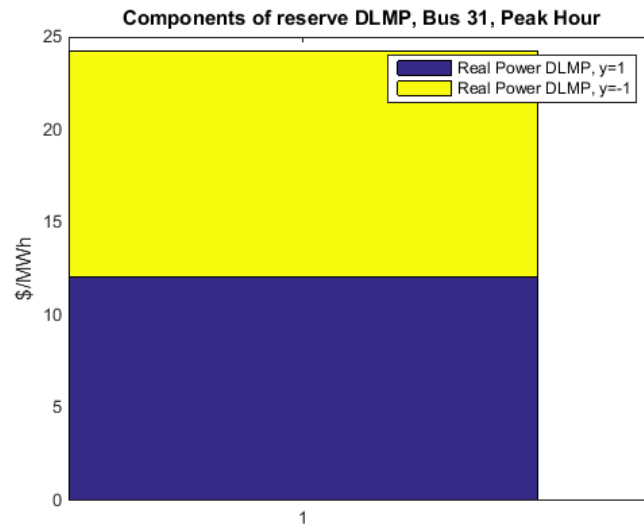


Figure 7-8: Components of the reserves DLMP at Bus 31 during the peak hour.

Chapter 8

Concluding Remarks and Future Work

8.1 Contributions

This work proposes the novel concept of marginal-cost based, distribution power markets. It is the first attempt at calculating dynamic spatiotemporal marginal costs at the distribution network. This thesis provides a complete spectrum of theoretical foundation and implementation, starting from the market formulation and leading up to computationally efficient formulations. The first part of the work has to do with the market formulation: defining the relevant distribution power market products, costs and constraints. We formulate a centralized distribution power market whose products are:

1. Real power
2. Reactive power
3. Reserves

The salient distribution network costs include real and reactive power losses, transformer degradation, voltage sensitive loads, and utilities of loads. With regard to the constraint set, we model full non-convex AC load flow constraints, nodal power balance constraints, nodal voltage magnitude bounds and intertemporal DER dynamics and capabilities. The primal solution of the centralized distribution power market clearing algorithm is the optimal allocation of the DER capacity among these three

products, as well as the power flows and voltage magnitudes. The dual solution includes the Distribution Locational Marginal Prices (DLMPs) of each product at each bus and hour. DLMPs reflect marginal costs.

The exact relations between real and reactive power, in both the load flow equations and the market participants' capabilities, are often ignored by the literature for simplicity, but are taken into account in this thesis. This detailed modeling showcases the complexity of marginal-cost analysis/network pricing with multiple, correlated products and price-contributing network dynamics.

While one of our goals and contributions is to provide realistic and detailed models of costs and market participants, our market algorithm formulation remains accommodating to any other types of DER (eg. data centers (Chen et al., 2015)).

We apply first order optimality conditions to the centralized algorithm to derive valuable relationships between the DLMPs of real power, reactive power and reserves at distribution buses with:

1. other dual variables, like the shadow prices of the voltage magnitude bounds
2. sensitivities of line flows and voltage magnitudes
3. prices at the substation bus, where distribution and transmission interface.

These relationships define the components of DLMPs and as such are called DLMP unbundling equations.

Another crucial result is the definition of congestion in distribution networks. Congestion is a well-known and much studied transmission network issue. In transmission networks, congestion occurs when transmission line capacity constraints are binding, whereas in distribution networks, congestion is a nodal problem and appears when buses' voltage magnitudes constraints are binding above or below. From a market perspective, congestion is undesirable in wholesale markets since it can increase

operational costs when cheap resources are underutilized because all lines out of them are congested. Distribution network congestion works in similar ways to affect distribution prices and DER schedules. For example, our simulations have revealed that photovoltaics, whose variable costs are zero, are providing below their capacity when connected to a bus whose voltage is binding above.

We also provide an analysis of the benefits of the proposed granular marginal-cost based prices relative to today’s flat prices. We conclude that compared to flat prices, spatiotemporal prices would yield significant cost benefits to price elastic, as well as price inelastic market participants alike. Moreover, our results indicate that spatially varying prices are the only way to appropriately incentivize DERs on how to optimally provide reactive power.

The non-convex AC load flow constraints together with the intertemporal DER dynamics and capabilities make centralized market clearing algorithms non-scalable for real size distribution networks, motivating the second part of this thesis that provides equivalent distributed algorithms for distribution power market clearing. The proposed methods harness new developments in algorithms, computation and technology.

First, we apply augmented Lagrangian logic to our centralized market formulation and use the Alternating Direction Method of Multipliers (ADMM) to obtain a fully distributed algorithm (FDA). The relaxation of nodal equality constraints (like power balance constraints and voltage related constraints) allows for the splitting of the problem into simpler DER and distribution line/ transformer specific subproblems. The DER subproblems are shown to be individual cost minimization problems of personal costs (e.g., uncharged battery costs for electric vehicles) plus market based costs (nodal price estimate times quantity). Line subproblems are also cost minimization problems, if we consider the line as an entity minimizing the cost of buying (real

or reactive power or reserves) from its one end and selling it at the other end. These subproblems are coordinated through nodal price estimates that promote and eventually enforce nodal equality constraints. Upon convergence, nodal balances hold and marginal prices are discovered. We further the literature around proximal message passing and ADMM methods, by *(i)* providing a new application to a much more complex initial problem and *(ii)* using local updates to the multipliers of the augmentation terms and local convergence state signaling to reduce communication time and costs.

Moreover, we provide a novel partially distributed formulation (PDA). In it, DERs self-schedule again through cost minimization subproblems, based on nodal price estimates. These price estimates are calculated centrally by a system operator either through the solution of a load flow and the use of the DLMP unbundling equations or equivalently through a mock centralized market clearing problem, where DER schedules are fixed. The dual solution of this mock centralized market clearing problem provides the price estimates.

All in all, the main difference between partially and fully distributed algorithms is whether coupling constraints are relaxed or not. With regard to similarities, both fully and partially distributed algorithms rely on massive DER (and line for FDA) subproblem parallelization, rendering them scalable to real-size distribution networks embracing numerous DERs.

Finally, extending our finding that binding voltage bound constraints express distribution network congestion, we studied clearing voltage congested instances with distributed algorithms. We applied several enhancements like:

- We use the abovementioned DLMP unbundling equations to decrease the error of intermediate price estimates.
- We model hard voltage constraints with voltage-related barrier functions that

lead to significantly increased convergence speed.

The solution of FDA with binding voltage constraints is challenging because binding voltage constraints (*i*) impose an additional constraint on voltage decisions and can make voltage consensus hard to reach and (*ii*) they affect the DLMPs, i.e. they contribute to the prices.

We expect that our methods and conclusions can be used for other applications of reaching consensus on constrained variables, when these constraints bind at the optimal solution.

Distribution power markets will be the stepping stone for a wide range of benefits that will include not only distribution network efficiencies, but also synergies with renewables. On the distribution side, dynamic locational prices will incentivize the efficient distributed provision of real power, reactive power and reserves from DERs. This will itself lead to lower losses as well as assist voltage and frequency control. Those network benefits extend to economic benefits, since they will allow the distribution system operator to defer infrastructure investments. Another advancement of the adoption of distribution power markets is that the aforementioned dynamic locational prices will not only appropriately guide existing DERs, but also serve as incentives for investments in new types of DERs, new technologies and new products. Lastly, the synergies between DERs and renewables will allow for the increase of the renewable penetration safety limit, promoting lower emissions.

Related areas of research Finally, we point out current work in different areas that align with this thesis. First, work in the area of cyber-attacks, recently growing in popularity as the internet-based applications grow. (Caramanis et al., 2016) discusses how power markets can fall victim to cyber-attacks. Centralized and distributed formulations can face feasibility and convergence issues if the physical layer is attacked (eg. set point of tap transformers). Distributed market algorithms are also prone to

attacks to the bus calculations. (Caramanis et al., 2016) mentions the ability to detect and isolate the attacked buses without changes to our market formulation. Indeed, initial numerical results indicate that external changes to price estimates or nodal imbalances are 'absorbed' by the quadratic augmentation terms of ADMM within a couple of iterations. Thus, we expect that in order to take effect, changes should be numerically coordinated and across many buses.

Our market formulation also ties in with work in the area of microgrids and islanding.

The detailed modeling and tractable algorithms developed in this thesis provide answers to which quantities should be measured, how they should be calculated and how variables relate to one another. It does not include analysis of how this market should and could be practically implemented. A detailed analysis of this aspect can be found in (Tabors et al., 2016) and (Tabors et al., 2017). These papers propose the introduction of an economic platform. DERs will join the platform and submit bids to receive/ provide service and will be matched for service reception/ provision through the platform. This platform, owned and provided by the distribution system operator, is consistent with our market structure and furthers its benefits by exploiting the effects of network economics.

Current applications of dynamic distribution pricing We conclude this section by noting that the concept of dynamic distribution pricing has become more and more popular with academics as well as system operators, regulators and utilities. While techniques like DER aggregation, direct load control and cost averaging are becoming outdated, dynamic distribution pricing is starting to slowly but steadily become the clear means for achieving distribution network efficiency. Australia is currently evaluating such measures (Brown and Faruqui, 2014), while recent orders of the New York State Energy Research and Development Authority's (NYSERDA)

Reforming the Energy Vision (REV) aim at pricing described as "consumer-centered approach that harnesses technology and markets" (Tabors et al., 2016).

8.2 Future Work

Modeling This thesis included traditional transformer models to show the effect of their degradation costs to marginal cost based distribution prices. Future work could be directed towards the modeling of tap-changing transformers that would provide the system operator with an additional degree of freedom. An important type of tap-changing transformers for distribution networks is voltage regulators, as mentioned in Chapter 3. However, modeling of tap-changing transformers will dictate the inclusion of shunt elements to the modeling. The shunt elements of tap transformers are shunt capacitors, whose capacity depends on the tap setting. Modeling these shunt capacitances might end up being a challenging task. (Christakou et al., 2015) mentions that the presence of shunt capacitors in an OPF problem can lead to various computational issues. First, the OPF problem cannot be convexified as in (Li et al., 2012a). Second, (Christakou et al., 2015) also mentions that ADMM can fail to converge and exhibit oscillatory behavior.

Moreover, this thesis assumed a balanced distribution network and as such concentrated on a single phase model. A more realistic model would be a multiphase model that would be able to capture the physics of non-balanced distribution networks. The OPF problem for unbalanced distribution networks has been investigated by the literature. We mention recent work by (Dall’Anese et al., 2012) and (Peng and Low, 2015) as representative. Both papers include considerations for the evolution of the feeder from three phases to two phases to one phase. The phases are of course not independent, therefore a multiphase market-based OPF should examine the need for distinct prices at each bus’ phase and the inter-relationships of these prices.

Power Markets We consider this thesis to be foundational to the implementation of distribution power markets. As these markets evolve and become mature, we expect to see well-known transmission power market issues appearing in distribution power markets. One of them is market power. The potential of DERs to exercise market power by withholding capacity should be examined. This might be a harder task compared to transmission resource market power, given the existence of multiple, correlated products as well as the higher volatility of reactive power prices, compared to real power prices (Ntakou and Caramanis, 2015).

The second issue is that of distribution network topology control. Distribution networks are created with meshed capabilities but are operated radially. Distribution system operators routinely switch loads to different distribution transformers (secondary side) for reliability reasons. Line switching for reliability purposes is also performed in transmission networks. Recent research (Foster, 2012) and (Goldis, 2015) has shown that transmission line switching can also serve economic purposes. Therefore, we propose distribution network topology control for cost reduction as a promising future research direction.

In this thesis, DLMPs are calculated relative to fixed substation prices. As seen in Chapter 5, the resulting DLMPs can be significantly higher or lower than the substation prices. This motivates future work towards quantifying the effect of distribution network injections and withdrawals on transmission nodal prices. This is equivalent to the simultaneous clearing of both distribution and transmission markets. (Caramanis et al., 2016) envisions and lays down the formulation of such a unified market. At a higher level, we can describe the process as iterating between transmission and distribution market clearing. The transmission market clearing assumes fixed DER injections and withdrawals to determine marginal prices at all transmission buses. Those prices are then used as in Chapters 4 to 7 for the calculation

of marginal prices at all distribution buses. The two-step process will repeat until convergence. While we managed to obtain some numerical results with a simplified transmission network and a fully detailed distribution network, the effect of distribution injections and withdrawals on transmission prices is suppressed because we have a single feeder. Were we to model multiple distribution feeders, the effect on transmission prices would be revealed.

Tractable Algorithms Because the centralized market clearing formulation does not scale, this thesis has provided two distributed market clearing formulations: a fully distributed one and a partially distributed one. While computational experience simulating the same network instance with different methods allowed us to compare distributed methods to each other, future work should also look into the drivers of the convergence rate of each formulation. (Peng and Low, 2015) narrows these driving factors down to two for the case of distribution OPF problems solved with ADMM: the network size and the network diameter (the distance between the two furthest buses). The latter is shown to have higher effect on the number of iterations needed for convergence.

In the same direction, computational experience can be extended through additional simulations with alternate software. AIMMS was used for the entirety of the simulations in this thesis. While GAMS is almost identical, CVX might be promising. Granted, CVX requires that the problem be convex, so the relaxations in (Li et al., 2012a) need to be utilized.

The fully distributed algorithm proposed in this thesis is based on ADMM therefore, based on theoretical conditions for convergence (Boyd et al., 2011) and (Kraning et al., 2014), it employs a common clock for iteration synchronization. This ensures that:

- A DER will not re-solve unless it receives an updated price estimate from its

connection bus.

- A distribution line or transformer will not re-solve unless it receives updated price estimates from both its receiving bus and its sending bus.
- A bus will not update its price estimates unless all devices in the distribution network have solved and sent their connection buses updated tentative schedules.

Therefore, the rate of iterations is limited by the slowest subproblem solution.

Recent work (Li et al., 2014), (Zhang and Kwok, 2014), (Wei and Ozdaglar, 2013) and (Li and Marden, 2012) focuses on asynchronous updates. In our case, this would allow buses to update price estimates after receiving at least one schedule update. DERs and lines can still re-solve only after receiving updated price estimates from their connection bus(es), but since the latter will no longer be limited by the slowest proximal subproblem, DER subproblems will be solved more frequently. An interesting research direction is to examine whether such asynchrony is suitable for as complex problems as the proposed power market.

Our fully distributed formulation belongs to the sphere of (augmented) Lagrangian methods, much like most of the distributed algorithms so far used for power markets' and power systems' applications. Opting for methods that exhibit speedier convergence, a promising direction is the use of second order Newton-like methods. The basic challenge in these methods is that each iteration requires the inversion of a matrix in a distributed fashion.

Appendix A

Description of Simulated Distribution Networks

A.1 800 bus Distribution Network

The network is adapted from a prototypical feeder (Feeder 9) from the library of distribution networks developed by the Pacific Northwest National Labs (PNNL). Of the 800 buses, 202 are residential load points (buses 599-800) and another 72 are commercial load points (buses 325-396). Commercial buses are at 480V, while residential buses are at 120V. There is a medium to low voltage transformer in front of each load. For residential loads, an additional low voltage line after the transformer is added. Therefore, lines ending at buses 325-598 are transformers.

The maximum commercial demand at the peak hour is 0.589MW and the total commercial demand at the peak hour is 5.1MW. The maximum residential demand at the peak hour is 0.4MW and the total residential demand at the peak hour is 11.3MW.

Figure A.1 shows an aggregated topology of the network. Residential loads not depicted as well as all commercial loads are aggregated for space limitation reasons under bus 127. All 800 bus are treated as individual (non-aggregated) in all simulations.

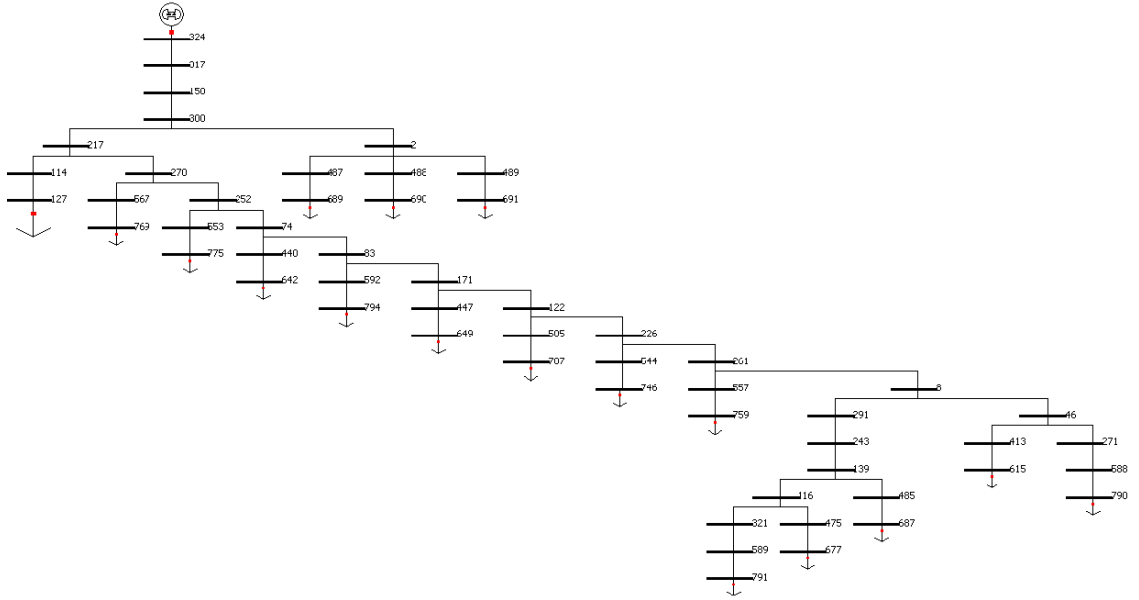


Figure A.1: Topology of the 800-bus distribution network.

With respect to DERs, we spread photovoltaic installations of relevant sizes across both residential and commercial buses. Commercial PVs are collocated with commercial loads. Out of 72 commercial load buses, 25 have photovoltaic installations: one of 500kW, one of 300kW and the remaining 23 are of 40kW capacity. All residential load buses have an 8kW PV attached. This results in commercial PV capacity totaling 1.72MW and the residential PV capacity 1.6MW.

As for electric vehicles, most residential loads (150 out of 202) are assumed to have an electric vehicle. The charging rate is at 3.3kW and the initial uncharged battery is at 24kWh, while the capacity of the EV charger is set to 6.6kW.

We also assume that commercial loads can have two parts: a fixed load part and a price responsive part, in the form of smart thermostats.

Since our feeder is described by PNNL as being in the cold climate zone, we use Albany, NY area data for the time varying inputs (solar irradiation, outside temperature, hourly evolution of residential and commercial loads). We pick a day with high LMPs, specifically July 2, 2014.

The following figures show the hourly evolution of the substation real power LMP, the solar irradiation, the hourly demand as percentage of the peak hour demand and the evolution of the outside temperature, respectively.

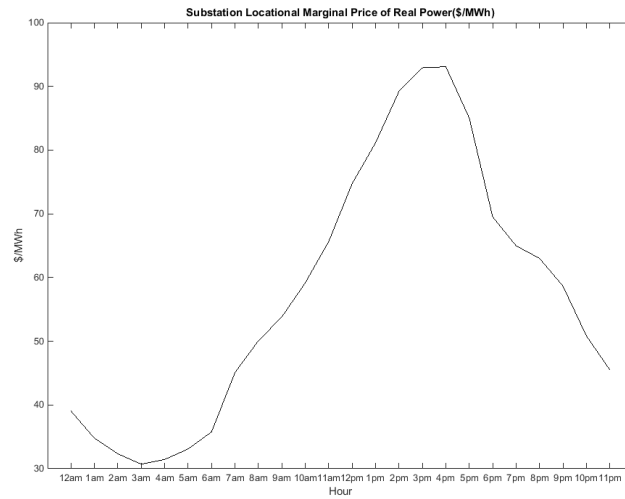


Figure A-2: Hourly values of the substation real power LMP in \$/MWh.

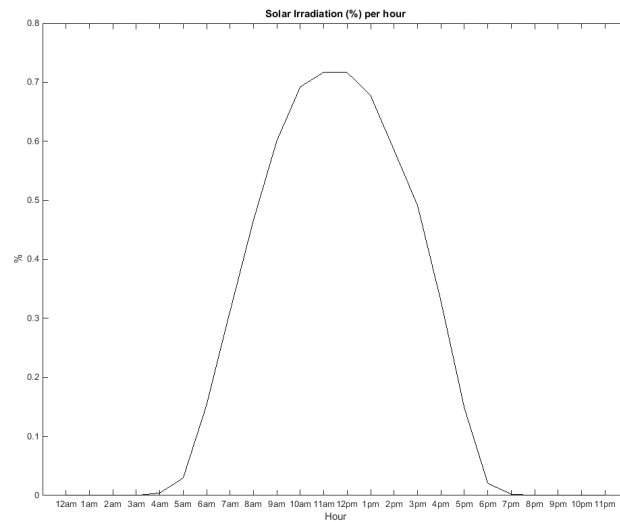


Figure A-3: Hourly values of the solar irradiation as a percentage.

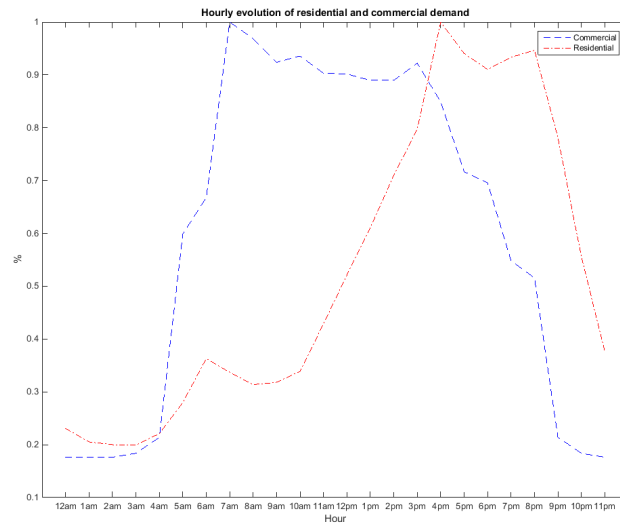


Figure A-4: Hourly evolution of the residential and commercial demand as a percentage of the peak demand.

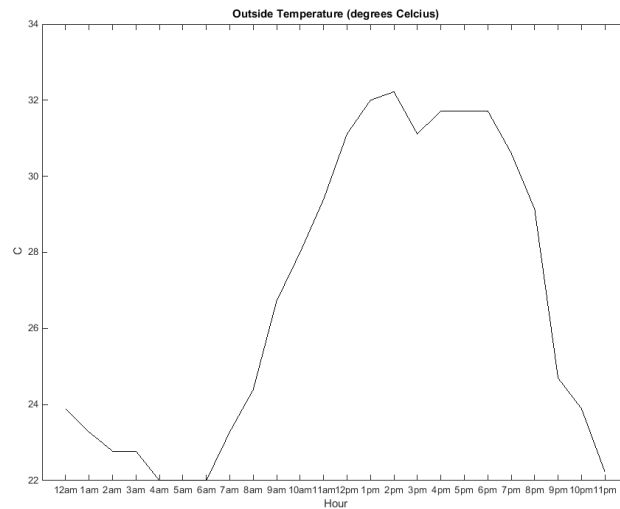


Figure A-5: Hourly evolution of the outside temperature in degrees Celcius.

Voltage bounds are set to $\pm 10\%$.

Finally, we calculate the per hour cost of the distribution transformers present in the network, starting from the cost of a 50kVA transformer assumed at 4000\$,

complete of purchase and installation costs. Using an annulization rate of 15% we estimate the total hourly cost of a transformer of rated capacity $S_{b,b'}^N$ as $c_{b,b'}^{tr}(h) = \frac{0.15 \cdot 4000}{8760} \cdot \left(\frac{S_{b,b'}^N}{50}\right)^{0.8}$.

Section 5.5.1 We use the hottest spot temperature hourly evolution equation 3.2 and $w = 0$ for constraint 5.10.

Section 5.5.2 We use the hottest spot temperature evolution equation 3.2 and $w = 1, \check{v} = 0.96$ for constraint 5.10.

Section 6.2.5 We use the hottest spot temperature hourly evolution equation 3.3 and $w = 0$ for constraint 5.10.

A.2 47 bus Distribution Network

The 47-bus network is based on Southern California Edison data and was originally published in (Farivar et al., 2011). Input data for the network, like network topology, line characteristics, load apparent demand and location, photovoltaics and capacitor capacity and location, are kept the same.

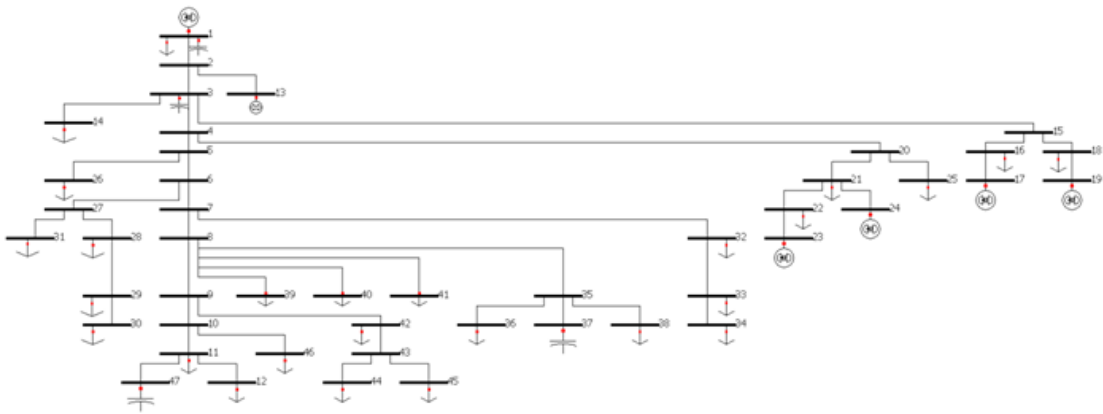


Figure A.6: Topology of the 47-bus distribution network.

Additionally, we use $\pi_\infty^P = \pi_\infty^{OC} = 50 \frac{\$}{kWh}$ in the objective function costs.

Uncongested instance We infer real and reactive demand from the apparent demand data by assuming that loads have a constant power factor of 0.8 and are inflexible.

The table below shows the location and size of photovoltaics and capacitors.

PV	Bus	Capacity (MW)
1	13	1.5
2	17	0.4
3	19	1.5
4	23	1
5	24	2

Table A.1: Location and capacity of photovoltaics in the 47 bus network.

PV	Bus	Capacity (MW)
1	1	6
2	3	1.2
3	37	1.8
4	47	1.8

Table A.2: Location and capacity of shunt capacitors in the 47 bus network.

Voltage bounds are set to $\pm 10\%$.

Congested instance In order to induce congestion, we remove photovoltaics and capacitors from the network, as well as tighten the allowable voltage bounds to $\pm 5\%$ while setting the substation voltage to 1 per unit.

In this instance, loads might not be met. We infer the maximum real demand from the apparent demand data by assuming that loads have a constant power factor of 0.8. For improved convergence and without loss of generality, we mitigate solution degeneracy by assuming load utilities are of the form $u_\alpha(P_\alpha) = -A_\alpha \cdot P_\alpha + B_\alpha \cdot P_\alpha^2$, $A_\alpha \geq 0$, $B_\alpha \geq 0$, $\forall \alpha \in D$.

A.3 47 bus Distribution Network with Reserves

Finally, for our market clearing simulation instances considerate of reserves we alter the 47 bus network described above by adding:

1. Distribution Transformers
2. Electric Vehicles
3. Replacing PVs with DGs.

The following lines are now considered to be transformer lines, i.e. they have a rated capacity and a cost showing the loss of their life with respect to loading relative to that capacity, as seen in Chapters 5 and 3.

Transformer	Line Number	Bus From	Bus To
1	1	1	2
2	5	3	14
3	9	5	26
4	13	7	32
5	15	8	40
5	16	8	39
7	17	8	41
8	21	9	42
9	22	10	11
10	23	10	46
11	31	20	25
12	35	27	31
13	36	27	28
14	41	35	36
15	43	35	38

Table A.3: Location of distribution transformers in the 47 bus network used for simulations including reserves.

To be complete, the following table shows the location and capacity of DG.

DG	Bus	Capacity (MW)
1	13	0.4
2	17	0.4
3	19	0.4
4	23	0.4
5	24	0.4

Table A.4: Location and capacity of DGs in the 47 bus network used for simulations including reserves.

DGs are considered to have a marginal cost of $c_a(h) = 60\$/MWh$. All the electric vehicles have the same parameters as the electric vehicles connected to the 800 bus network: charging rate of 3.3kW, uncharged battery of 24kWh and battery charger of 6.6kW. The following table shows the location of the electric vehicles in the 47 bus network.

Electric Vehicle	Bus
1	12
2	15
3	25
4	26
5	30
6	31
7	34
8	36
9	38
10	39
11	40
12	41
13	44
14	45
15	46

Table A.5: Location and size of electric vehicles in the 47 bus network used for simulations including reserves.

We use the same real power LMP at the substation as the 800 bus network above (see Figure A.2) and a reserve LMP at the substation equal to half the substation real power LMP. The following figure reports the reserve LMP values.

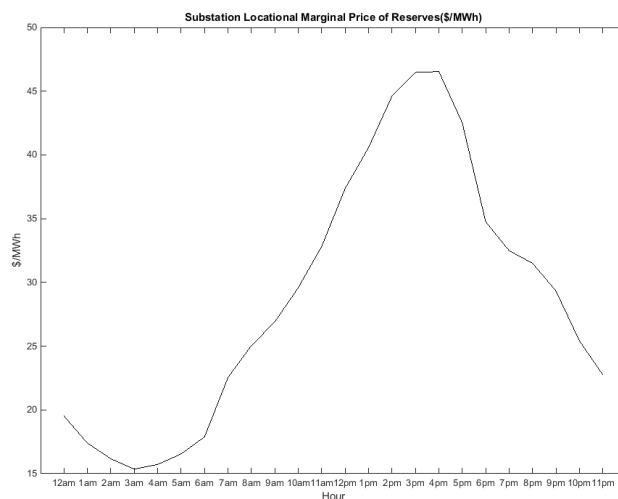


Figure A-7: Hourly values of the substation reserve LMP in \$/MWh.

A.4 253 bus Distribution Network

The 253-bus network topology is shown in Figure A-8 below.

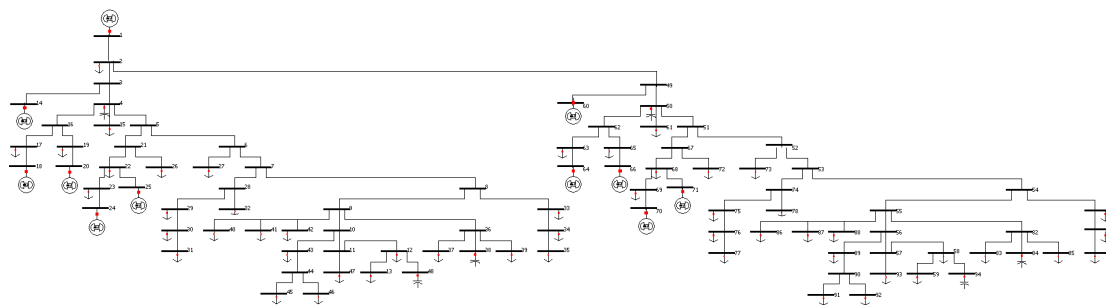


Figure A-8: Topology of the 253-bus distribution network.

The left-hand side of the feeder (buses 2-48) is identical to the 47-bus network shown in (Farivar et al., 2011). The right-hand side of the feeder (buses 49-253) is a duplicate of that feeder, where some loads were substituted by several residential loads. This is done for loads of buses 63, 73, 75-79, 81, 87, 89 and 92, yielding 253 buses overall.

We use $\pi_{\infty}^P = \pi_{\infty}^{OC} = 50 \frac{\$}{kWh}$. Voltage bounds are set to $\pm 10\%$. Loads and line resistance and reactance are identical to (Ntakou, 2014).

The location and capacity of photovoltaics and shunt capacitors are shown below.

PV	Capacity (MW)	Bus
1	1.5	14
2	0.4	18
3	1.5	20
4	1	24
5	2	25
6	1.5	60
7	0.4	64
8	1.5	66
9	1	70
10	2	71

Table A.6: Location and capacity of photovoltaics in the 253 bus distribution network.

Capacitor	Capacity	Bus
1	1.2	4
2	1.8	38
3	1.8	48
4	1.2	50
5	1.8	84
6	1.8	94

Table A.7: Location and capacity of shunt capacitors in the 253 bus distribution network.

References

- Baran, M. E. and Wu, F. F. (1989). Optimal capacitor placement on radial distribution systems. *IEEE Transactions on Power Delivery*, 4(1):725–734.
- Bertsekas, D. P. and Tsitsiklis, J. N. (1989). *Parallel and Distributed Computation: Numerical Methods*. Prentice-Hall, Inc., Upper Saddle River, NJ, USA.
- Bilgin, E. (2014). *Participation of distributed loads in power markets that co-optimize energy and reserves*. dissertation, Boston University.
- Boyd, S., Parikh, N., Chu, E., Peleato, B., and Eckstein, J. (2011). Distributed optimization and statistical learning via the alternating direction method of multipliers. *Foundations & Trends in Machine Learning*, 3(1):1–122.
- Brown, T. and Faruqui, A. (2014). Structure of electricity distribution network tariffs: Recovery of residual costs. <https://www.hks.harvard.edu/hepg/Papers/2014>.
- Caramanis, M., Ntakou, E., Hogan, W. W., Chakraborty, A., and Schoene, J. (2016). Co-optimization of power and reserves in dynamic t amp;d power markets with nondispatchable renewable generation and distributed energy resources. *Proceedings of the IEEE*, 104(4):807–836.
- Caramanis, M. C. and Foster, J. M. (2011). Uniform and complex bids for demand response and wind generation scheduling in multi-period linked transmission and distribution markets. In *2011 50th IEEE Conference on Decision and Control and European Control Conference*, pages 4340–4347.
- Chakrabarti, S., Kraning, M., Chu, E., Baldick, R., and Boyd, S. (2014). Security constrained optimal power flow via proximal message passing. In *2014 Clemson University Power Systems Conference*, pages 1–8.
- Chen, H., Zhang, B., Caramanis, M. C., and Coskun, A. K. (2015). Data center optimal regulation service reserve provision with explicit modeling of quality of service dynamics. In *2015 54th IEEE Conference on Decision and Control (CDC)*, pages 7207–7213.
- Chiang, H. D. and Baran, M. E. (1990). On the existence and uniqueness of load flow solution for radial distribution power networks. *IEEE Transactions on Circuits and Systems*, 37(3):410–416.

- Christakou, K., Tomozei, D., Boudec, J. L., and Paolone, M. (2015). AC OPF in radial distribution networks - parts I, II. <http://arxiv.org/abs/1503.06809>.
- Dall’Anese, E., Giannakis, G. B., and Wollenberg, B. F. (2012). Economic dispatch in unbalanced distribution networks via semidefinite relaxation. <http://arxiv.org/abs/1207.0048v2>.
- Dimitrovski, A. and Tomsovic, K. (2004). Slack bus treatment in load flow solutions with uncertain nodal powers. In *2004 International Conference on Probabilistic Methods Applied to Power Systems*, pages 532–537.
- Ela, E., Milligan, M., and Kirby, B. (2011). Operating reserves and variable generation. <http://www.nrel.gov/docs/fy11osti/51978.pdf>.
- Eremia, M. and Bulac, C. (2013). *Voltage Stability*, pages 657–736. John Wiley & Sons, Inc.
- Fairley, P. (2010). An easy smart-grid upgrade saves power [update]. *IEEE Spectrum*, 47(10):13–14.
- Farivar, M., Clarke, C. R., Low, S. H., and Chandy, K. M. (2011). Inverter var control for distribution systems with renewables. In *2011 IEEE International Conference on Smart Grid Communications (SmartGridComm)*, pages 457–462.
- Farivar, M. and Low, S. H. (2013). Branch flow model: Relaxations and convexification; part i. *IEEE Transactions on Power Systems*, 28(3):2554–2564.
- Faruqui, A. (2012). California’s search for a better rate design. http://www.cfee.net/_documents/Faruqui.pdf.
- Flores-Espino, F. (2015). Compensation for distributed solar: A survey of options to preserve stakeholder value. In *National Renewable Energy Laboratory Technical Report*.
- Foster, J. M. (2012). *Control systems in power markets: Demand response, transmission topology control, and renewable integration*. dissertation, Boston University.
- Goldis, E. (2015). *Topology control algorithms in power systems*. dissertation, Boston University.
- IEEE (1996). Ieee guide for loading mineral-oil-immersed transformers. *IEEE Std C57.91-1995*, pages i–.
- Joo, J. Y. and Ilic, M. D. (2013). Multi-layered optimization of demand resources using lagrange dual decomposition. *IEEE Transactions on Smart Grid*, 4(4):2081–2088.

- Kraning, M., Chu, E., Lavaei, J., and Boyd, S. (2014). Dynamic network energy management via proximal message passing. *Foundations & Trends in Optimization*, 1(2):73–126.
- Lavaei, J. and Low, S. H. (2012). Zero duality gap in optimal power flow problem. *IEEE Transactions on Power Systems*, 27(1):92–107.
- Li, N., Chen, L., and Low, S. H. (2012a). Exact convex relaxation of opf for radial networks using branch flow model. In *2012 IEEE Third International Conference on Smart Grid Communications (SmartGridComm)*, pages 7–12.
- Li, N., Gan, L., Chen, L., and Low, S. H. (2012b). An optimization-based demand response in radial distribution networks. In *2012 IEEE Globecom Workshops*, pages 1474–1479.
- Li, N. and Marden, J. R. (2012). Designing games for distributed optimization with a time varying communication graph. In *2012 IEEE 51st IEEE Conference on Decision and Control (CDC)*, pages 7764–7769.
- Li, N., Qu, G., and Dahleh, M. (2014). Real-time decentralized voltage control in distribution networks. In *2014 52nd Annual Allerton Conference on Communication, Control, and Computing (Allerton)*, pages 582–588.
- Liu, H., Tesfatsion, L., and Chowdhury, A. A. (2009). Locational marginal pricing basics for restructured wholesale power markets. In *2009 IEEE Power Energy Society General Meeting*, pages 1–8.
- MIT Energy Initiative (2015). Mit electric power system basics, appendix B. <http://www.uvm.edu/~phines/classes/ee217/2015-fall>.
- Molzahn, D. K. (2013). *Application of Semidefinite Optimization Techniques to Problems in Electric Power Systems*. dissertation, University of Wisconsin-Madison Department of Electrical and Computer Engineering.
- North American Electric Reliability Corporation (2008). Glossary of terms used in reliability standards. http://www.nerc.com/files/glossary_of_terms.pdf.
- Ntakou, E. (2014). Spatiotemporal marginal-cost-based retail electricity markets: Efficiency, structure and feasibility. <http://bu.edu/pcms/caramanis/ElliDistr.pdf>.
- Ntakou, E. and Caramanis, M. (2014). Distribution network electricity market clearing: Parallelized pmp algorithms with minimal coordination. In *53rd IEEE Conference on Decision and Control*, pages 1687–1694.

- Ntakou, E. and Caramanis, M. (2015). Distribution network spatiotemporal marginal cost of reactive power. In *2015 IEEE Power Energy Society General Meeting*, pages 1–5.
- Ntakou, E. and Caramanis, M. (2016). Enhanced convergence rate of inequality constraint shadow prices in pmp algorithm cleared distribution power markets. In *2016 American Control Conference (ACC)*, pages 1433–1439.
- Pacific Northwest National Laboratory (2010). Evaluation of conservation voltage reduction (cvr) on a national level. http://www.pnl.gov/main/publications/external/technical_reports/PNNL-19596.pdf.
- Peng, Q. and Low, S. H. (2015). Distributed algorithm for optimal power flow on an unbalanced radial network. In *2015 54th IEEE Conference on Decision and Control (CDC)*, pages 6915–6920.
- Schweppe, F., Caramanis, M., Tabors, R., and Bohn, R. (1988). *Spot Pricing of Electricity*. Kluwer Academic Publishers, Norwell, MA, USA.
- Shahidehpour, M., Yamin, H., and Li, Z. (2002). *Market Operations in Electric Power Systems*. Wiley Interscience.
- She, X., Burgos, R., Wang, G., Wang, F., and Huang, A. Q. (2012). Review of solid state transformer in the distribution system: From components to field application. In *2012 IEEE Energy Conversion Congress and Exposition (ECCE)*, pages 4077–4084.
- Sivanagaraju, S. (2009). *Power System Operation and Control*. Pearson Education India.
- Tabors, R., Caramanis, M., Ntakou, E., Parker, G., VanAlstyne, M., Centolella, P., and Hornby, R. (2017). Distributed energy resources: New markets and new products. In *2017 Hawaii International Conference on System Sciences (HICSS)*.
- Tabors, R., Parker, G., Centolella, P., and Caramanis, M. (2016). White paper on developing competitive electricity markets and pricing structures. <https://www.hks.harvard.edu/hepg/Papers/2016>.
- US Department of Energy (2011). Energy efficiency in distribution systems: Impact analysis approach. https://www.smartgrid.gov/files/Distribution_System_Energy_Efficiency_17Nov11.pdf.
- Wainwright, M. J., Jaakkola, T. S., and Willsky, A. S. (2003). Tree-based reparameterization framework for analysis of sum-product and related algorithms. *IEEE Transactions on Information Theory*, 49(5):1120–1146.

- Wang, X.-F., Song, Y., and Irving, M. (2009). *Modern Power Systems Analysis*. Springer.
- Wei, E. and Ozdaglar, A. (2013). On the $o(1/k)$ convergence of asynchronous distributed alternating direction method of multipliers. <https://arxiv.org/abs/1307.8254>.
- Zhang, R. and Kwok, J. (2014). Asynchronous distributed admm for consensus optimization. In Jebara, T. and Xing, E. P., editors, *Proceedings of the 31st International Conference on Machine Learning (ICML-14)*, pages 1701–1709. Journal on Machine Learning Research (JMLR) Workshop and Conference Proceedings.
- Zimmerman, R. (1995). Comprehensive distribution power flow: Modeling, formulation, solution algorithms and analysis. <http://www.pserc.cornell.edu/ray/pubs/PhDThesis.pdf>.

CURRICULUM VITAE

Elli Ntakou

entakou@bu.edu

Education

Boston University Jan. 2013- Jan. 2017
Doctor of Philosophy in Systems Engineering
Dissertation title: Distribution Power Markets: Detailed Modeling
and Tractable Algorithms.

Boston University Sept. 2011- Jan. 2013
Master of Science in Systems Engineering
Concentration in Operations Research

National Technical University of Athens Sept. 2006- Aug. 2011
Diploma in Electrical and Computer Engineering (summa cum laude)
Major: Power Systems, Minor: Electronics
Thesis title: Economic and Environmental Benefits of Microgrids with
Increased Renewable Penetration

Publications

E. Ntakou and M. Caramanis, "Discovery of Dynamic Locational Prices on Power Distribution Networks: Efficient and Robust Distributed Algorithms in the Presence of Binding Voltage Constraints," 2017 American Control Conference (ACC), submitted.

R. Tabors, M. Caramanis, **E. Ntakou**, G. Parker, M. VanAlstyne, P. Centolella and R. Hornby, "Distributed Energy Resources: New Markets and New products", accepted to the 2017 Hawaii International Conference on System Sciences.

E. Ntakou and M. Caramanis, "Enhanced convergence rate of inequality constraint shadow prices in PMP algorithm cleared distribution power markets," 2016 American Control Conference (ACC), Boston, MA, 2016, pp. 1433-1439.

M. Caramanis, **E. Ntakou**, W. W. Hogan, A. Chakraborty and J. Schoene, "Co-Optimization of Power and Reserves in Dynamic T&D Power Markets With Nondispatchable Renewable Generation and Distributed Energy Resources," in Proceedings of the IEEE, vol. 104, no. 4, pp. 807-836, April 2016.

E. Ntakou and M. Caramanis, "Distribution network spatiotemporal marginal cost of reactive power," 2015 IEEE Power & Energy Society General Meeting, Denver, CO, 2015, pp. 1-5.

E. Ntakou and M. Caramanis, "Distribution network electricity market clearing: Parallelized PMP algorithms with minimal coordination," 53rd IEEE Conference on Decision and Control, Los Angeles, CA, 2014, pp. 1687-1694.

E. Ntakou and M. Caramanis, "Price discovery in dynamic power markets with low-voltage distribution-network participants," 2014 IEEE PES T&D Conference and Exposition, Chicago, IL, 2014, pp. 1-5.

M. Caramanis, I. C. Paschalidis, C. Cassandras, E. Bilgin and **E. Ntakou**, "Provision of regulation service reserves by flexible distributed loads," 2012 IEEE 51st IEEE Conference on Decision and Control (CDC), Maui, HI, 2012, pp. 3694-3700.

P. A. Ruiz, A. Rudkevich, M. C. Caramanis, E. Goldis, **E. Ntakou** and C. R. Philbrick, "Reduced MIP formulation for transmission topology control," 2012 50th Annual Allerton Conference on Communication, Control, and Computing (Allerton), Monticello, IL, 2012, pp. 1073-1079.

Awards

Honorable Mention, Boston University Research Symposium, April 2016
 Student Travel Awards, Boston University Systems Engineering, June 2016, August 2015, September 2014

Grigoris Farakos award, awarded by the National Technical University of Athens to the top 3 students in the graduating class with energy major of both electrical and mechanical engineering departments.

Subsidy award by the Greek government for the top 20% of the entering class of each University.

Organizational Skills

Organizer, CISE Graduate Student Workshop, January 2015

Student Host, Weekly CISE Seminars, 2012-2016

Head of the committee organizing the graduating class' trip to the USA, National Technical University of Athens, Fall 2010.

Other Skills

Programming Languages: R, C, C++

Engineering Software: Excel, Matlab, GAMS, AIMMS, PowerWorld

Languages: Greek (native), English (full bilingual proficiency), French.